

1998

Effect of carbon overcoat on corrosion of thin film magnetic media

Valérie Vivarès
San Jose State University

Follow this and additional works at: https://scholarworks.sjsu.edu/etd_theses

Recommended Citation

Vivarès, Valérie, "Effect of carbon overcoat on corrosion of thin film magnetic media" (1998). *Master's Theses*. 1721.

DOI: <https://doi.org/10.31979/etd.3ymj-62t4>

https://scholarworks.sjsu.edu/etd_theses/1721

This Thesis is brought to you for free and open access by the Master's Theses and Graduate Research at SJSU ScholarWorks. It has been accepted for inclusion in Master's Theses by an authorized administrator of SJSU ScholarWorks. For more information, please contact scholarworks@sjsu.edu.

INFORMATION TO USERS

This manuscript has been reproduced from the microfilm master. UMI films the text directly from the original or copy submitted. Thus, some thesis and dissertation copies are in typewriter face, while others may be from any type of computer printer.

The quality of this reproduction is dependent upon the quality of the copy submitted. Broken or indistinct print, colored or poor quality illustrations and photographs, print bleedthrough, substandard margins, and improper alignment can adversely affect reproduction.

In the unlikely event that the author did not send UMI a complete manuscript and there are missing pages, these will be noted. Also, if unauthorized copyright material had to be removed, a note will indicate the deletion.

Oversize materials (e.g., maps, drawings, charts) are reproduced by sectioning the original, beginning at the upper left-hand corner and continuing from left to right in equal sections with small overlaps. Each original is also photographed in one exposure and is included in reduced form at the back of the book.

Photographs included in the original manuscript have been reproduced xerographically in this copy. Higher quality 6" x 9" black and white photographic prints are available for any photographs or illustrations appearing in this copy for an additional charge. Contact UMI directly to order.

UMI

**A Bell & Howell Information Company
300 North Zeeb Road, Ann Arbor MI 48106-1346 USA
313/761-4700 800/521-0600**

Effect of Carbon Overcoat on Corrosion

of

Thin Film Magnetic Media

A thesis presented to
The Faculty of the Department
of
Materials Engineering
San Jose State University

In partial fulfillment
of the
Requirements for the
Degree of Master of Science

By
Valérie Vivarès

August 1998

UMI Number: 1391544

**Copyright 1998 by
Vivares, Valerie**

All rights reserved.

**UMI Microform 1391544
Copyright 1998, by UMI Company. All rights reserved.**

**This microform edition is protected against unauthorized
copying under Title 17, United States Code.**

UMI
**300 North Zeeb Road
Ann Arbor, MI 48103**

© 1998
Valérie Vivarès
ALL RIGHTS RESERVED

Abstract

Effect of Carbon Overcoat on Corrosion of Thin Film Magnetic Media

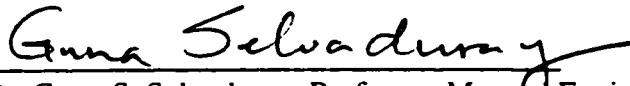
By Valérie Vivarès

Corrosion in thin film magnetic media represents a problem resulting in a potential loss of data for users of hard drives. Typically, the purpose of the carbon overcoat is to reduce wear of the magnetic layer, and possibly to limit corrosion.

The objective of this investigation was to determine the effect the carbon overcoat has on the corrosion behavior of the magnetic layer. Carbon overcoats of different hydrogen and nitrogen content were sputtered on, and the effect of this compositional difference was determined by measuring the corrosion current. Two electrolytes were used: chloride solutions at 0 and 7.5 ppm concentrations. The carbon films were characterized for thickness, k-value, and mechanical wear resistance.

The results indicate that disks with carbon overcoat have better corrosion resistance than disks without overcoat. Disks overcoated with nitrogenated carbon overcoats were found to have better corrosion resistance when they were compared to those with hydrogenated carbon overcoats.

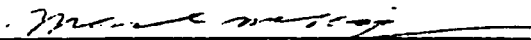
APPROVED FOR THE DEPARTMENT OF MATERIALS ENGINEERING



Dr. Guna S. Selvaduray, Professor, Material Engineering Department
San Jose State University

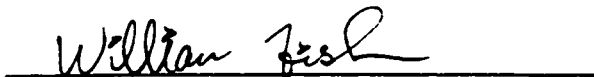


Dr. Avtar Singh, Professor, Electrical Engineering Department
San Jose State University



Mr. Manuel Mekhjian, Manager, Materials Technology,
United Defense, Corporate Technology Center

APPROVED FOR THE UNIVERSITY



Acknowledgements

The author wishes to thank her advisor, Dr. Guna Selvaduray, Professor, Department of Materials Engineering, San Jose State University, for his guidance and perseverance in seeing this project to its completion. The author would like to express her appreciation for Manuel Mekhjian, Manager of Materials and technology with United Defense Corporate Technology Center, for his guidance with corrosion issues, and his input on the research results. The author would like to thank the help of Dr. Avtar Singh for the careful editing of this manuscript. The author also would like to acknowledge the help of Andy Hormola, currently with Komag, for his technical input and comments. The author would also like to thank Eric Li, Consultant, for his help interpreting the result of the characterization of the carbon overcoat. Many thanks to Nasser Lama, currently with Kobe Precision, for his support. The author also wishes to express her appreciation for Keith Goodson, Vice president for Media Development at Western Digital, for providing the early impetus for undertaking this study. A special thanks to Ratnesh Saxena for his constant support during the writing of this manuscript.

Table of contents

Abstract.....	ii
Acknowledgements.....	iv
List of Figures	vii
List of Tables	viii
Chapter 1 . Introduction.	1
Chapter 2 . Thin film magnetic media and corrosion background	3
2.1 Thin film magnetic media	3
2.2 Brief overview of corrosion.....	4
2.2.1 Basis for corrosion	4
2.2.2 Electrochemical Kinetics of corrosion	6
Chapter 3 . Effect of the carbon overcoat on corrosion of magnetic media.....	12
3.1 Environmental chamber exposure / Qualitative experimental methods	12
3.2 Electrochemical methods.....	16
Chapter 4 . Effect of overcoat on corrosion current and research objective.....	25
Chapter 5 . Research methodology.....	26
5.1 Disks and Solution Preparation	26
5.1.1 Preparation of disks.....	26
5.1.2 Solution Preparation.....	27
5.2 Equipment	27
5.3 Test Matrix.....	29

5.4 Procedure	29
6.1 Materials characterization	30
6.2 Taffel plots	31
6.3 Corrosion current	33
6.4 Polarization resistance	36
Chapter 7 . Corrosion mechanisms in thin film magnetic media: interpretation of results	39
7.1 Taffel plots	39
7.2 Current density and polarization resistance	40
Chapter 8 . Conclusions	43
Chapter 9 . Recommendations for future research	44
9.1 Wetting angle of water and carbon overcoat.....	44
9.2 Carbon overcoat porosity measurements	44
Chapter 10 . References.....	45
Appendix A.....	46

List of Figures

Figure 1: Areal Densities reached per year, based on IBM's Laboratory demonstrations and production product.	2
Figure 2: Head and disk Schematic	4
Figure 3: Three required elements for corrosion to occur	6
Figure 4: Schematic Taffel Plot	10
Figure 5: Schematic diagram of corrosion mechanism for porous overcoat with a) high electrical conductivity b) low electrical conductivity.	21
Figure 6: Schematic of Disk Partitioning	27
Figure 7: EG&G Flat cell schematic	28
Figure 8: Typical results for: a) No carbon overcoat; b) Carbon overcoated samples in DI water, c) Carbon overcoated Samples in 7.5ppm HCl	33
Figure 9: Corrosion Current density for all samples; error bars represent data scattering	35
Figure 10: Corrosion Current density for Overcoated samples	36
Figure 11: Polarization resistance for all samples; error bars represent data scattering	39
Figure 12: Hydrophilic (a), and hydrophobic (b) carbon overcoat-solution contact comparison	43

List of Tables

Table 1: Experimental Matrix	29
Table 2 : Carbon overcoat characteristics	31
Table 3: Solution characteristics	31

Chapter 1. Introduction.

Personal computers are in almost every home. In each of them, there is a hard drive to store data. Based on current technology, magnetic storage offers the best compromise in terms of speed, reliability, capacity and price. Today, it is possible to purchase a 2 Gbit drive for about \$0.05/Mbit. In such a drive, the areal density (number of bits per square inch of magnetic media) can be up to 1 Gbit/in². IBM and Fujitsu have already developed areal densities of up to 5 Gbit/in², thus confirming the on-going progress of the magnetic disk drive industry. Progress on head characteristics, communication channels and media are responsible for a good part of the impressive increase in areal density of up to 65% per year, as shown in Figure 1.

With such high areal densities, each bit is stored in an increasingly small amount of space; therefore, the magnetic defects on the media have to be extremely small. Corrosion can create a patch of surface where the magnetic surface is damaged and is not able to store magnetic information. Such a patch of surface constitutes a defect that can grow as corrosion progresses. Defects apparent before the drive is shipped to the customer can sometimes be overcome by using an appropriate configuration to arrange the data. Unfortunately, if the defects appear after the drive is in use, or if the defect grows with time, the end user can experience loss of data. Such “growing” defects can result in a major reliability issue. With increasing areal densities the control and minimization of corrosion becomes more important.

In Chapter 2, pertinent background information, including a brief overview of corrosion, and of thin-film magnetic media is presented. Chapter 3 is a review of past research on corrosion of thin film magnetic media. The research hypothesis and objectives are in Chapter 4. In Chapter 5, the research protocol is described, followed by the results and discussion of the results in Chapter 6 and Chapter 7, respectively. Chapter 8 and Chapter 9 contain the conclusions and recommended future research.

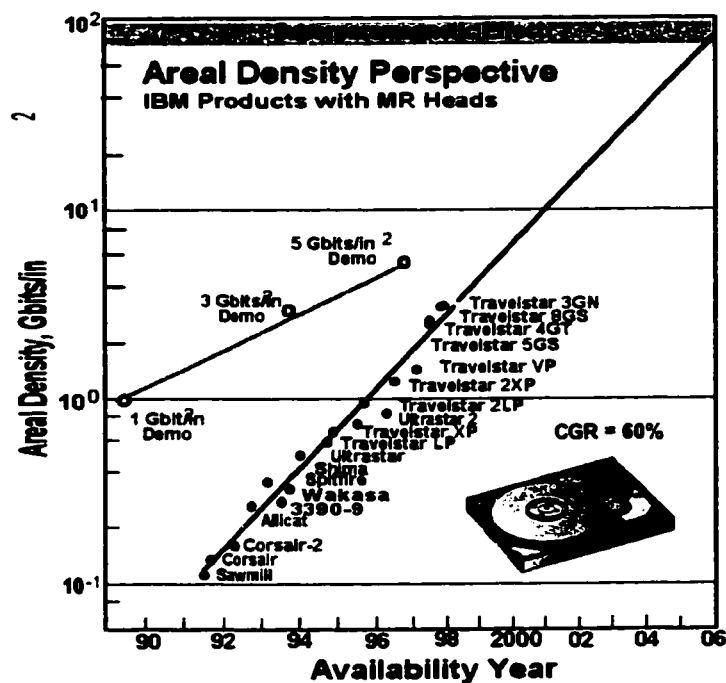


Figure 1: Areal Densities reached per year, based on IBM's Laboratory demonstrations and production product.⁽¹⁾

Chapter 2. Thin film magnetic media and corrosion background

This chapter is a presentation of the background knowledge necessary for full comprehension of the study. The first part is a description of thin film magnetic media, followed by a brief overview of corrosion mechanisms.

2.1 Thin film magnetic media

Thin film magnetic disks are composed of a set of layers, each being present for a specific reason. A cross-section of a thin film magnetic disk and head is shown in Figure 2. The substrate is an aluminum alloy or glass. The aluminum substrate is machined to the proper dimensions and then electroplated with a nickel-phosphorous (Ni-P) alloy. The Ni-P layer provides a hardened non magnetic surface as a base for the other layers. The disk is then polished with different grain sizes to form the final substrate.

Texturing is then done on the disk to obtain the desirable surface roughness. The disk is textured for at least two reasons: to enhance stiction characteristics of the head on the finished media and to orient the magnetic layer longitudinally.

After texturing, a chrome-based undercoat is sputtered on to enhance adhesion of the magnetic media, which is sputtered on subsequently. The final sputtered layer is a carbon overcoat which reduces wear of the media in the assembled hard drive. The carbon overcoat can be of at least two types: nitrogenated or hydrogenated. Nitrogenated carbon is used to improve the bonding of the lubricant to the surface of the disk. Hydrogenated carbon usually offers better protection against wear.

A Lubricant layer is added, often by a dip and slow pull process, to improve head flight characteristics.

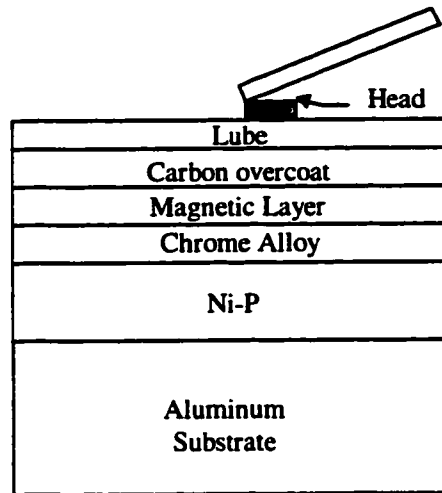


Figure 2: Head and disk Schematic

2.2 Brief overview of corrosion^[2]

This section contains a brief review of the mechanisms and kinetics of corrosion that are relevant to this study.

2.2.1 Basis for corrosion

Corrosion is the result of chemical reaction between a metal or a metal alloy and its environment. In thin film magnetic media, the alloy of interest is the magnetic alloy which is composed primarily of cobalt, chromium and tantalum. Other additives are present in the alloy in various concentrations but past research has shown cobalt compounds at the surface of the disk to be a telltale sign of corrosion.^[3]

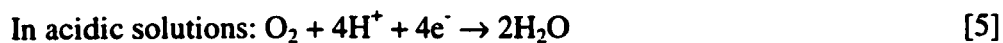
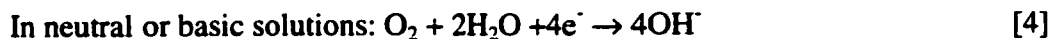
Corrosion is electrochemical in nature. In general, metallic corrosion is the oxidation of the metal in aqueous solution. The oxidation of metallic cobalt in a chloride containing environment can be represented by the following overall reaction:



This overall reaction can be separated into an oxidation, or anodic, reaction and a reduction, or cathodic, reaction:



Most of the anodic reactions are of the form described above. Cathodic reactions can be of different types, but are often the reduction of oxygen in neutral or acidic solutions, as shown below:



Oxidation reactions are present at all times; they can be advantageous as in the case of the oxidation of aluminum, which forms a protective layer, or deleterious as in the case of the oxidation of iron under atmospheric conditions, forming rust. The rate at which oxidation occurs determines the corrosion resistance of the material to the environment. In some cases, corrosion can be prevented entirely by stopping one of the three necessary conditions for corrosion, which are illustrated in Figure 3. The driving

force is thermodynamic in nature. The ion and electron paths are the paths by which the ions reach the reaction surface and the electrons complete the electrochemical cell, respectively.

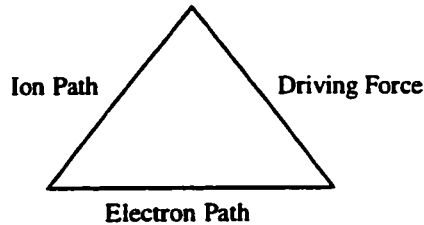


Figure 3: Three required elements for corrosion to occur

In the event when design cannot prevent corrosion entirely, the kinetics of corrosion are the designer's main concern.

2.2.2 Electrochemical Kinetics of corrosion

In thin film disks, design is driven by performance in the drive. This design creates several driving forces for corrosion: galvanic corrosion between the magnetic layer and the carbon overcoat, galvanic corrosion between the Ni-P layer and the magnetic layer, and cell corrosion via the pores of the carbon overcoat. Since corrosion cannot be prevented in these cases, the kinetics of the corrosion becomes the main concern. In this section, the kinetics involved in corrosion are discussed. The physical laws governing the reaction rate are presented in Section 2.2.2.1, followed by a brief review of polarization and passivation.

2.2.2.1 Rate of reaction

The rate of production or consumption of electrons can accurately measure the rate at which a reaction occurs. Electron flow can be measured as current (I) in amps. Faraday's law gives the proportionality between the mass reacted and the current measured, I .

$$m = \frac{a}{n} \cdot \frac{It}{F} \quad [6]$$

where F is Faraday's constant, n is the number of equivalent weights exchanged, a the atomic weight, and t the time in seconds.

At equilibrium, the forward reaction rate (r_f) is equal to the reverse reaction rate (r_r).

$$r_f = r_r = \frac{i_0 a}{nF} \quad [7]$$

where i_0 is the exchange current density and has to be measured, i_0 is a kinetic constant for the reaction but depends strongly on the surface geometry.

The current density at equilibrium is a measurable quantity that defines the rate of corrosion in a system. Plotting the equilibrium current density as a function of the potential in an active system (a Taffel plot), allows one to gather information regarding the mechanism of corrosion in the system by studying the polarization curves. A discussion of polarization mechanisms follows in Section 2.2.2.2.

2.2.2.2 Polarization

The availability of electrons at the surface of a metal determines the rate of the reaction. An excess of electrons at the surface of the metal represents cathodic polarization. Anodic polarization is the deficiency of electrons at the surface of the metal, and a driving force for corrosion.

In aqueous solutions the potential at the surface of the metal reaches a steady state potential, called E_{corr} , which depends on the ability and rate at which electrons can be exchanged at the surface by the anodic and cathodic reactions. As the potential at the surface increases above E_{corr} the anodic reaction takes place and corrosion occurs at a finite rate. Anodic polarization then occurs.

Polarization is the difference of potential between the equilibrium electrode potential and the potential resulting from the reaction. Cathodic polarization is present when the electrons are building up at the surface and the surface potential becomes lower than the equilibrium potential. Polarization can be classified into two main categories: activation polarization and concentration polarization.

Activation polarization occurs when the reaction rate (represented by the exchange current) is limited by the reaction itself. Thermodynamics then limits the reaction rate. In that case the overpotential, η , is related to the reaction rate (i) by:

$$\eta = \beta \log \frac{i}{i_0} \quad [8]$$

The overpotential is related to E_{corr} as shown below:

$$\eta = E - E_{corr} \quad [9]$$

where E is the applied potential.

The relationship between the overpotential and the logarithm of the current density ($\log i$) is linear. Also, the anodic Taffel constant (β_a) is positive since the overpotential is positive ($E > E_{corr}$) and the cathodic Taffel constant (β_c) is negative since the overpotential is negative ($E < E_{corr}$).

Concentration polarization occurs when the concentration of the reduced ions limits the reaction rate. In this case, the solution forms a boundary layer in which the ions are depleted and the reaction is driven by the availability of the ions. The overpotential is then related to the current density by:

$$\eta_{conc} = \frac{2.3RT}{nF} \log \left[1 - \frac{i_c}{i_L} \right] \quad [10]$$

where i_L is the minimal current density at which the system shows this behavior.

This limiting current depends on the concentration of the solution, the diffusivity of the species, and the agitation of the solution. For thin film magnetic media, concentration polarization could indicate the lack of availability of reacting ions or electrons at the surface of the magnetic media. This could be due to the presence of the carbon overcoat. The total polarization is the sum of concentration and activation polarization. In many systems, at potentials around E_{corr} , the main polarization mechanism is activation polarization; further away from E_{corr} the dominant mechanism is

concentration polarization. A typical Taffel plot showing these two behaviors is presented in Figure 4.

The Polarization resistance (R_p) is proportional to the inverse of the corrosion current density (i_{corr}) according to the Stern-Geary equation

$$i_{corr} = \left[\frac{\beta_a \beta_c}{2.303(\beta_a + \beta_c)} \right] \frac{1}{R_p} \quad [11]$$

Polarization resistance is the slope of the polarization curve at the origin (E_{corr}) and is independent of the degree of linearity of the curve. The reaction potential E_{corr} , current i_0 , and polarization resistance R_p are constants for a given system.

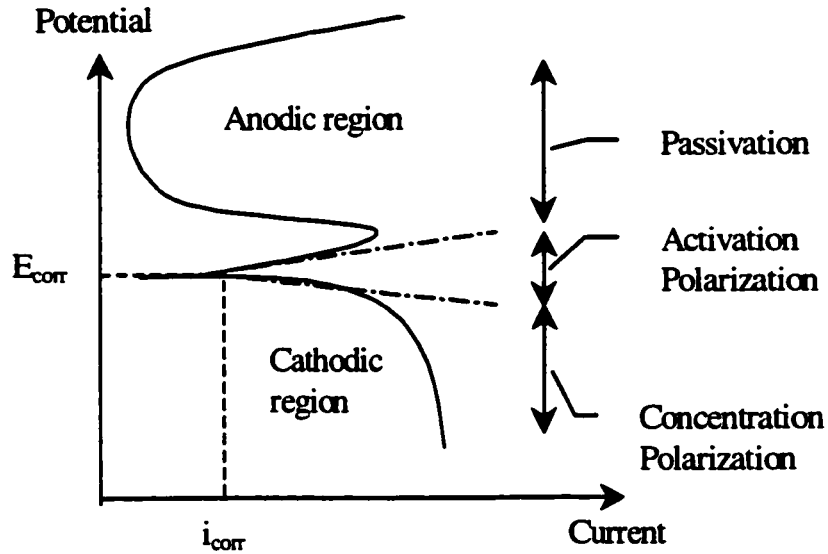


Figure 4: Schematic Taffel Plot

Some metals, such as aluminum and cobalt also exhibit passivation, which is described in the Section 2.2.2.3.

2.2.2.3 Passivation

Some metals form a protective oxide that acts as a barrier for the anodic reaction. In this case, when the potential rises above E_{corr} , the corrosion rate first increases. However, when a certain potential is reached, the corrosion current decreases to reach very low rates. Active-passive metals can be active in some environments and passive in others.

The study of Taffel plots for thin film magnetic media would not only allow the determination of expected corrosion rates, but would also provide information on the corrosion mechanisms and the effect of carbon overcoats on the corrosion resistance.

Chapter 3. Effect of the carbon overcoat on corrosion of magnetic media

Initially magnetic media was composed of metal particulates. As demand for higher areal density increased thin-film magnetic media, which are easily manufacturable and customizable, were developed. However, the magnetic film is less chemically stable than the older metal particulate media. ^[3] For this reason a number of studies were dedicated to understanding the mechanism of corrosion of this type of media, with particular emphasis on the effect of carbon overcoats. Intuitively, the carbon overcoat, if perfect, should isolate the magnetic media from the environment and protect it from corrosion. Experimentally, corrosion products composed of cobalt hydroxides have been found on the surface of disks. ^[4] These results suggest that water is absorbed by imperfections in the surface. Water oxidizes the cobalt and the cobalt hydroxides migrate to the surface. Another hypothesis is the existence of galvanic coupling between cobalt and the carbon. Both hypotheses were formulated using two main experimental approaches: exposure to controlled environments, and electrochemical methods. In this chapter the different experimental approaches, and the results obtained from previous studies are discussed.

3.1 Environmental chamber exposure / Qualitative experimental methods

Environmental chamber exposure and disk testing is often used in industry to validate disk reliability. Merchant et al. ^[5] studied the effect of environmental exposure of annealed and non-annealed, overcoated and non-overcoated, disks to a gaseous corrosive environment (10ppb Cl₂, 120ppb H₂S and 200ppb NO₂, at 30°C and 75% relative

humidity (RH)). The magnetic media was either a cobalt-chrome alloy or cobalt-chrome-tantalum alloy. The extent of corrosion was monitored by measuring the change of light scattering with time. The induction time was defined as the time when the reflectivity of the media showed a marked increase of more than $0.1 \mu\text{W}$. This limit was correlated with the time at which the disk would most likely cause a head crash. Scanning Electron Microscope (SEM) observation of non-overcoated disks after environmental exposure showed that, for aluminum substrates, corrosion products gather preferentially along the texture lines. Electron micrographs of the texture lines also indicated an increased porosity of the film. The corrosion products were mainly nickel and chlorine. Annealed disks, with and without overcoat, showed a longer induction time compared to the non-annealed samples, and also showed no nickel in the corrosion products. The overcoated samples showed a shorter induction time compared to non-overcoated samples. A longer induction time, of about 37 hours, was obtained for the annealed non-overcoated samples as opposed to 9 hours for non-annealed overcoated samples and 13 hours for non-annealed non-overcoated samples. On the samples without carbon overcoat Auger depth profiling suggested the presence of an oxide layer passivating the surface.

In two studies ^[3,4] environmental chamber exposure was used in conjunction with electrochemical measurements in order to correlate the methods, and also to characterize the porosity of the overcoat.

Novotny and Staud ^[4] experimented on coated and uncoated media. The magnetic layer was a cobalt alloy with various amounts of chromium, nickel, phosphorous,

platinum, etc. Films were sputtered on AlMg/Ni-P substrates or silicon wafers. Environmental tests were conducted in wet and dry conditions. In dry conditions the higher temperature was 300°C and in wet conditions the maximum temperature and relative humidity were 90°C and 90%, respectively. Experiments using corrosive gasses (2 ppbw Cl₂, 300 ppbw SO₂, 40 ppbw H₂S, and 500 ppbw NO₂) were done at 25°C and 70% RH. Other exposure conditions were ambient environment with a temperature of 22°C and relative humidity of 40-50%. The samples were analyzed using X-ray Photoemission Spectroscopy (XPS), Auger Electron Spectroscopy (AES), and Secondary Ion Mass Spectroscopy (SIMM). XPS analysis of the non-overcoated samples, after exposure to ambient environment, showed a mixture of chromium and cobalt oxides and hydroxides on the surface. The analysis at higher temperature showed preferential oxidation of cobalt and nickel. Overcoated samples showed no cobalt on the surface prior to exposure. After exposure cobalt and nickel (when nickel was present in the magnetic layer) hydroxides were found on the surface. AES depth profiles showed that cobalt and oxygen levels were high at the surface, minimal in the carbon layer and rose again when the carbon-magnetic layer interface was reached. Samples exposed to 200°C in dry air showed no migration of cobalt or nickel to the surface. The amount of cobalt and nickel present on the surface increases with increased humidity and decreased pH of the gases. These results indicate that cobalt migrates to the surface not due to thermal diffusion but probably due to thermodynamic forces. The presence of cobalt at the surface is in disagreement with the results from Merchant,^[5] who did not find any

evidence of cobalt on the surface and concluded that the reacting surface was probably the Ni-P/magnetic interface layer. Novotny and Staud^[4] complemented this environmental exposure with electrochemical measurements which are described in Section 3.2.1.1. Also, the concentration of chromium and cobalt oxides on the surface was investigated, using AES depth profiling, and correlated to the electrochemical results.

Environmental exposure was also used by Brusic et al^[3] to characterize the carbon overcoat porosity. Electrochemical methods were used to test samples for corrosion; environmental exposure (10ppb Cl₂, 70% RH and 25°C) was used to demonstrate the existence of pores in the carbon overcoat. The samples were composed of electroless Ni-P and magnetic alloy plated on the aluminum substrate; the carbon overcoat was then sputtered on with argon. The magnetic media was pure cobalt or a cobalt-phosphorus alloy. Some samples were not overcoated with carbon. SEM/Electron Discharge Spectroscopy (EDS) analysis was done on the surface corrosion products after exposure. For overcoated samples, the analysis showed that the carbon overcoat was incomplete, with numerous sites where the underlayer was exposed. This “pore decoration” allowed the author to count the number of pores per unit surface area and obtain an approximation of the porosity of the carbon overcoat. Corrosion products were found to be composed of cobalt oxides and chlorine and were located preferentially along surface scratches or other discontinuities. Again, the presence of cobalt is in contradiction with the study by Merchant,^[5] but, it is in agreement with the study by Novotny.^[4] Brusic also measured the thickness of corrosion products for the coated and uncoated samples. The uncoated

Merchant,^[5] but, it is in agreement with the study by Novotny.^[4] Brusic also measured the thickness of corrosion products for the coated and uncoated samples. The uncoated sample showed uniform corrosion of about 3 nm thickness, detected by ellipsometry measurements. The overcoated samples showed localized corrosion products as thick as 1 μm and as large as several μm .

The pore decoration technique would seem useful to characterize the porosity of the overcoat, but it depends on the uniformity of the pore distribution on the surface. Therefore, the results should be used as an indication more than a means of definitive characterization.

The electrochemical measurements done by Brusic et al.^[3] are described in Section 3.2.1.1.

3.2 Electrochemical methods

Two main types of polarization measurements have been used to study thin film magnetic media: linear polarization and impedance measurements. The studies carried out by Brusic,^[3] Novotny^[4] and Sides^[6] are explained in detail in Section 3.2.1.1 on linear polarization measurements. Section 3.2.1.2 contains the description of impedance measurements by Sides^[6] and Walmsley.^[7]

3.2.1.1 Linear polarization studies

Most polarization studies were done using a standard three-electrode setup, using standard water based electrolytes. Brusic et al.,^[3] however, used a water droplet setup to

electrolyte. This setup was intended to replicate atmospheric conditions.

Potentiodynamic curves were plotted after stabilization of the cell for about 15-20 min.

The objective of this study was to define the role of the carbon overcoat in the corrosion process and evaluate ways to minimize corrosion. The AlMg/Ni-P/magnetic layer/carbon overcoat samples were described in Section 3.1. The magnetic media was pure cobalt or a cobalt-phosphorus alloy. The carbon layer was sputtered on using argon. Some other samples were also made with only the carbon layer on the Si or AlMg substrate. The reference electrode was mercurous sulfate, and the counter electrode was a platinum mesh. The setup was designed to mimic atmospheric conditions. The cell was composed of the working electrode (exposed surface 0.32cm^2), covered by a filter paper, followed by the counter electrode, followed again with another filter paper and finally, the reference electrode. 20 μL of solution was used to wet the filter paper. Several solutions were used, including DI water (pH 7.2) and NaOH/ $\text{Na}_2\text{B}_4\text{O}_7$ (pH 11). This setup allowed the investigators to limit the effect of the ohmic resistance of the electrolyte. Electrochemical measurements showed that overcoated and non-overcoated magnetic layers have similar corrosion currents, between 1.1 and 6.9 nA/cm^2 .

The corrosion potential of an overcoated sample and a sample with only a carbon layer showed significant differences. This allowed the author to hypothesize that the corrosion behavior could be explained by galvanic interaction between the magnetic layer and the carbon overcoat. Galvanic interaction requires that two, active and dissimilar materials must be in contact with each other, while they are being exposed to the same

environment. The differences in potential between them must also be more than 0.5 V. Since the carbon is conductive and the carbon and the cobalt alloy have a difference in potential of more than 0.5 V, galvanic corrosion can occur, given that both layers are exposed to the same environment. The last condition for galvanic corrosion is fulfilled if the carbon is porous and the magnetic layer is exposed to the environment. That condition has been proved by the environmental exposure study described in Section 3.1. Brusic et al.^[3] also evaluated the ratio between the area covered by the carbon and the area where the magnetic layer was “visible” through the overcoat. They evaluated this ratio to be approximately 14:1 for a textured disk. Since the area ratio is so high, the corrosion rate in those galvanic cells has to be several orders of magnitude higher than the average corrosion rate. Brusic et al.^[3] then proceeded to isolate the magnetic media from the conductive carbon overcoat using a dielectric. They obtained a lower corrosion current density for relatively thick dielectric layers and relatively smoother surfaces. They concluded that the main driving force for corrosion in thin film disks is galvanic coupling between the magnetic layer and the carbon overcoat.

Novotny and Staud ^[4] also carried out electrochemical measurements to complement their environmental exposure study. The samples described in Section 3.1 were tested by DC polarization and potentiodynamic scanning techniques. The working electrodes were pie-shaped coupons cut from hard drives or silicon wafers with sputtered films. The area exposed was 1.35cm². All potentials were measured using a standard calomel electrode. No detailed description of the cell was given, including the volume of

solution used. The electrolyte, 0.1 N Na₂SO₄ (pH=7), was deaerated using a nitrogen purge. H₂SO₄ or NaOH was added to the solution to vary the pH. The potential was varied from -10 to +10 mV against E_{corr}. The cell was allowed to reach equilibrium for 15-20 min before starting the scan at the rate of 0.1 mV/s. Several scans were taken for each condition, and the average taken as the actual corrosion current. Polarization resistance was also measured using a scan from -200 to +800 mV against corrosion potential, with a scan rate of 1 mV/s.

The corrosion current, for non-overcoated samples, ranged from 0.1 to 0.8 $\mu\text{A}/\text{cm}^2$, depending on the amount of chromium in the magnetic layer. The corrosion potentials ranged from -400 to -600 mV vs. Standard Calomel Electrode (SCE). The corrosion current was also dependent on the pH; a higher concentration of protons and lower pH, translates to a higher corrosion current which varied from 0.8 to 0.4 $\mu\text{A}/\text{cm}^2$ for pH varying from 1 to 11, respectively.

Overcoated samples showed lower or similar corrosion current when compared to non-overcoated samples, with currents varying from 0.5 to 0.03 $\mu\text{A}/\text{cm}^2$ for samples with overcoats B, C, and D in a solution of pH = 1. Unfortunately, no description of the three different types of carbon overcoats (B, C and D) was given by the author. Sample A was the non-overcoated sample.

The author correlated the chromium oxide concentration at the surface after the environmental exposure with the inverse of the corrosion current. The integrated

chromium oxide concentration over the surface was found to vary according to the inverse of the corrosion current raised to a power $1/x$, x being unknown; an increase of corrosion current equates to a decrease in chromium oxide concentration. The author also correlated the surface concentration of cobalt and nickel with the corrosion current density and found a linear relationship. The difference in corrosion current for the various overcoats was said to be dependent on the conductivity of the carbon overcoat film (porosity being assumed to be similar for all films). For a non-conductive carbon, both the anodic reaction and cathodic reaction have to occur at the magnetic layer/electrolyte interface. Therefore, oxygen has to be available at the magnetic layer surface and the pores have to be larger. For a conductive overcoat, only the anodic reaction has to occur at the magnetic layer/solution interface. The cathodic reaction can occur at the carbon layer/solution interface. According to this reasoning, at equal porosity, a non-conductive overcoat would offer better corrosion protection to the magnetic layer. This hypothesis is supported by the measurement of the resistivity of the best carbon overcoat tested and the worst, around $5 \Omega\text{cm}$ and $10^5 \Omega\text{cm}$, respectively. Porosity was not measured and the characterization of the composition of the carbon overcoat was not reported in the article. The two corrosion mechanisms, for a conductive carbon overcoat and a non-conductive carbon overcoat, are illustrated in Figure 5.

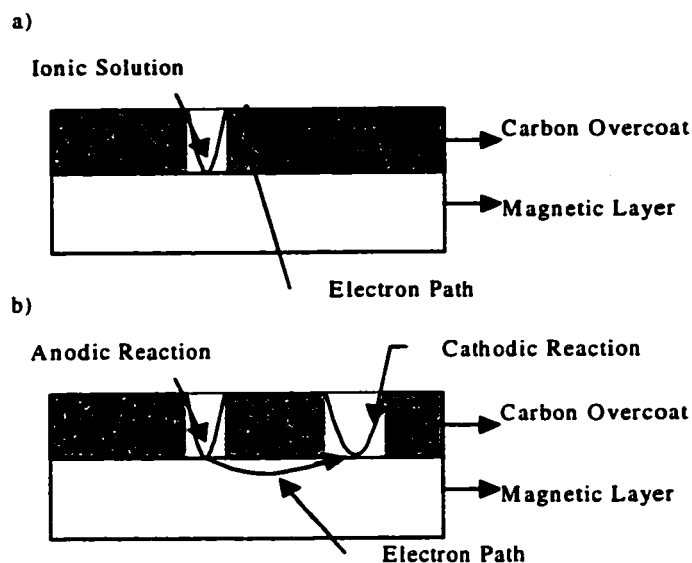


Figure 5: Schematic diagram of corrosion mechanism for porous overcoat with a) high electrical conductivity b) low electrical conductivity.^[4]

Sides^[6] carried out a dual study of potentiodynamic linear sweep measurement and impedance. The samples were sputtered, using a DC magnetron sputter system, with a magnetic layer of the same composition but under differing conditions which were designed to test the effect on corrosion characteristics. The electrolyte was 30g of KCl dissolved in one liter of DI water (pH 5.5). The reference electrode was Ag/AgCl, but the counter electrode was not identified. The potential was swept from -50 mV to 250 mV against the corrosion potential at a scan rate of 0.5 mV/s . The comparison of the average faradaic resistance was mostly inconclusive since the results were quite scattered. Overcoated samples showed a resistance larger than the resistance for non-overcoated samples by about an order of magnitude ($50\text{ k}\Omega/\text{cm}^2$ to about $350\text{ k}\Omega/\text{cm}^2$). This result is in agreement with the results from Novotny^[4] and Brusic^[3] but in disagreement with the

results from Merchant^[5] who found carbon overcoats detrimental for corrosion resistance. Sides determined that the carbon overcoat sputtering condition showed no significant effect. Sides^[6] also carried out impedance measurements in order to determine the actual corrosion mechanism in this system. These experiments are described in Section 3.2.1.2.

3.2.1.2 Impedance studies

Sides^[6] measured the impedance and phase shift for frequencies varying from 0.01 Hz to 25,000 Hz. The samples, setup, and solution were the same as described in Section 3.2.1.1. Amplitude and phase were plotted against frequency. The amplitude was directly proportional to frequency in the mid-range of frequency indicating that the system behaved as a capacitor. The phase angle for most samples was between 25°C and 80°C, which indicated that the film was mainly porous and permeable. This was in agreement with previous studies from Brusic^[3] and Novotny.^[4] However, the phase angle did not change consistently with corrosion susceptibility. The capacitance was lower for higher faradaic resistance, which is characteristic of a relatively non-porous carbon. The author suggests that the impedance study did not produce any results that were not already obtained by linear polarization.

Walmsley et al.^[7] studied complete disk structures using AC impedance. The objective of the study was to determine the corrosion mechanism in the complete disk structure. The disk structure consisted of an AlMg substrate, with a nickel-phosphorous underlayer, a 3000 Å chromium layer, a 300-1000 Å cobalt alloy layer, a 100 Å chromium layer, and a 400 Å carbon overcoat. The working electrode had an area of

1cm², the counter electrode was platinum, and the reference electrode was a standard calomel electrode. The electrolytes employed were 0.4N NaCl, 0.4N K₂SO₄, 0.1N KCl/HCl, and 0.1N H₂SO₄. The electrolytes were de-aerated by nitrogen purging for 10 min prior to exposure. The system was allowed to reach equilibrium for 10 s prior to the experiment. (Note that most other studies allowed the system to reach equilibrium for about 15-20 min before starting the experiment.) A DC potential, equal to the open circuit potential, was first applied and an AC current of small amplitude was then superimposed. The superimposed frequencies were logarithmically distributed from 50mHz to 100mHz. The experiment was repeated after 10 min, and Nyquist plots were made. The plots corresponded to the graphs obtained for mass transport controlled systems. The corrosion currents were found to be decreasing with an increasing concentration of chromium in the cobalt alloy. The corrosion currents for electrolytes that are more aggressive were higher than for less aggressive electrolytes. This behavior was found to be true for sulfates or chloride containing electrolytes. Magnetic recording tests were also conducted to correlate to the electrochemical results. The results correlated qualitatively, with a higher corrosion current resulting in lower performance in magnetic recording.

In summary, studies on corrosion of thin film magnetic media showed that the active layer is the magnetic alloy, with the presence of cobalt and nickel at the surface (if nickel is present in the magnetic alloy). Only one study^[5] showed no presence of cobalt at

the surface. This appears counter intuitive since cobalt is an active metal present in the magnetic media.

The studies involving environmental exposure and electrochemical measurements showed good qualitative and quantitative correlation.

The effect of the carbon overcoat is still poorly understood, but its presence seems to increase corrosion resistance in most cases. This appears to be a reasonable result since the carbon overcoat should limit two of the three main mechanisms of corrosion: ion and electron transport. However, no study was carried out on nitrogenated carbon. In the study by Sides^[6] the sputtering conditions of the carbon overcoat were varied, but not the sputtering medium, which was argon. Novotny^[4] does not explain the differences in the carbon overcoat he tested, therefore yielding little information to compare amorphous, hydrogenated and nitrogenated carbon in terms of corrosion resistance.

Chapter 4. Effect of overcoat on corrosion current and research objective

The carbon overcoat plays an important role in protecting the magnetic media. Protection of wear from the head is usually the main concern, but corrosion protection is also a concern. Among the types of overcoats used in industry, two are receiving special interest: hydrogenated and nitrogenated amorphous carbon.

If the carbon overcoat was non-porous and the magnetic layer was not exposed to an aqueous interface, corrosion would not occur. Unfortunately, carbon overcoats are porous and can absorb water. Increasing porosity of the overcoat increases the area of the magnetic layer in contact with the environment. Therefore, a more porous overcoat would be expected to offer lower corrosion resistance to the film.

Hydrogenated and nitrogenated amorphous carbon overcoats have widely different mechanical characteristics and therefore can be expected to have different porosity.

The main objective of this study was to determine the effect of carbon overcoat composition on the corrosion characteristics of the magnetic layer. A secondary objective was to determine the effect of the presence of chloride ions on the corrosion characteristics of the magnetic layer. The corrosion current density and polarization resistance were measured in aerated DI water and 7.5 ppm HCl concentration aerated DI water.

Chapter 5. Research methodology

The materials, equipment, test matrix and procedure employed in the course of this investigation are described in this chapter.

5.1 Disks and Solution Preparation

5.1.1 Preparation of disks

Aluminum/Ni-P substrates were sputtered with the chromium, magnetic and carbon layer using an Intervac MDP 250 DCTM system. The magnetic layer was an alloy of cobalt, chrome and tantalum. The sputtering conditions during the deposition of the chrome and magnetic layer were the same for all samples. During carbon overcoat deposition, the gas composition was varied as follows: (a) pure argon, (b) 30% methane balance argon, (c) 20% nitrogen balance argon, and (d) 30% nitrogen balance argon.

Five different disk categories were thus created: no carbon overcoat, argon-carbon overcoat (no intentional hydrogen), hydrogenated-carbon overcoat, nitrogenated-carbon overcoat (nominal 20% nitrogen no intentional hydrogen), and nitrogenated-carbon overcoat (nominal 30% nitrogen, no intentional hydrogen). The samples were then stored in vacuum-sealed cassettes until testing.

Each disk was partitioned, as shown in Figure 6, into six sections using tape or scribe marks. Three alternating sections were used for electrochemical measurements. The other three sections were left untested so that there would be fresh surfaces in case the measurements had to be repeated.

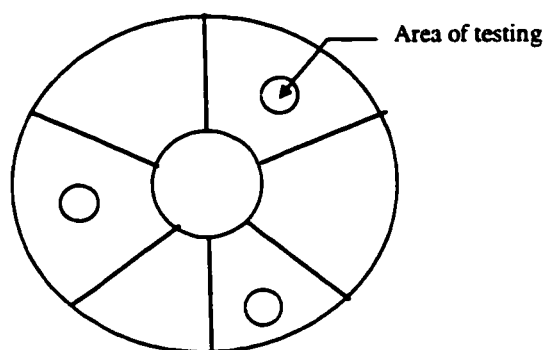


Figure 6: Schematic of Disk Partitioning

5.1.2 Solution Preparation

5.1.2.1 Oxygenated DI water

High purity de-ionized water was contained in a glass jar with a narrow opening, and a pump was installed to bubble air through the water for at least 12 hours before testing. In this manner, the solution was saturated with oxygen.

5.1.2.2 7.5 ppmw HCl solution

High purity DI water was mixed with concentrated HCl in order to obtain a concentration of 7.5 ppmw HCl. Air was then bubbled through the solution for an excess of 12 hours to saturate the solution with oxygen.

5.2 Equipment

An EG&G flat cell was used to expose the samples to the solutions. The active area was 1cm^2 with a solution volume of 500 ml. The working electrode was the disk itself. The counter electrode was a platinum mesh. The reference electrode was silver-silver chloride. A schematic diagram of the flat cell is shown in Figure 7.

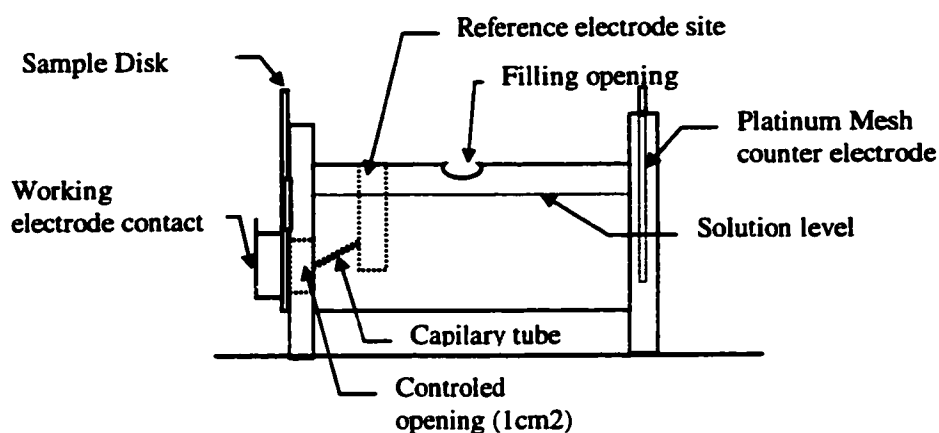


Figure 7: EG&G Flat cell schematic

The potential was varied using an EG&G Potentiostat Model 273, which was linked to a standard personal computer. The software used was EG&G Softcorr v 1.0 and v2.1.

The oxygen content, pH and temperature of the solutions were measured using a YSI Model 57 Dissolved O₂ Meter.

The wear resistance of the various carbon overcoats was measured using a Selket HD1000A. The Selket test characterizes how much the reflectivity of the surface varies with the time the abrasive tape is in contact with the surface. A lower Selket value indicates a higher wear resistance. The k-value and overcoat thickness were measured using an ellipsometer. The k-value is an optical parameter that correlate with the inverse of the hydrogen content of the film^[9].

5.3 Test Matrix

Each disk type was tested in aerated DI water and 7.5 ppm HCl solutions. Three measurements were taken for each condition. Table 1 contains a summary of the experimental matrix. For each condition, a Taffel plot was created, thus permitting determination of E_{corr} and I_{corr} .

Table 1: Experimental Matrix

Solution	Carbon overcoat	No Carbon	Argon Carbon	Hydrogenated carbon	Nitrogenated carbon
O ₂ saturated DI water		✓	✓	✓	✓
O ₂ saturated 7.5ppmw HCl		✓	✓	✓	✓

5.4 Procedure

The corrosion potential and corrosion current were determined from potentiodynamic measurements. Taffel plots were plotted and the corrosion potential and current were inferred by non-linear least square fitting of the Stern-Geary Equation. The potential was stepped from -250 mV from the open circuit potential to +250 mV at a scan rate of 0.5mV/s.

The sample was positioned and clamped in the sample holder of the flat cell, after which the solution was poured through the top opening. The reference electrode was then positioned in the reference electrode holder. The cell was left for 15 min in order to

Chapter 6. Material characterization and electrochemical results

The results of the sample and sample characterization are presented first, followed by the results of the electrochemical measurements.

6.1 Materials characterization

The disk characterization measurements are presented Table 2. The Selket values are consistent with the general knowledge that nitrogenated carbon is more graphitic, and therefore less wear resistant, than hydrogenated carbon, which is more diamond like. Argon carbon was similar to hydrogenated carbon in terms of these measurements. The k-values were expected to be approximately 0.6 for argon carbon and 0.8 for nitrogenated overcoats^[8]. However, the measured k values are somewhat different than the expected values. In particular, the k-value for argon carbon is significantly lower than expected, and it is thought that this is due to the presence of residual hydrogen in the sputtering chamber since the same chamber had been previously used for sputtering hydrogenated carbon. While the k-values for nitrogenated carbon are also lower than expected, the drop in values isn't as dramatic. Nevertheless, the nitrogenated carbon overcoat still has k-values higher than those for hydrogenated carbon overcoats. The solution characterization measurements are presented Table 3. As expected, the conductivity of the 7.5 ppmw HCl O₂ saturated solution was higher, by about 10 times, than O₂ saturated DI water. The pH of the HCl solution was one point lower than the pH of the DI water, which accounts for part of the conductivity difference. The dissolved oxygen content was the same for both solutions.

Table 2 : Carbon overcoat characteristics

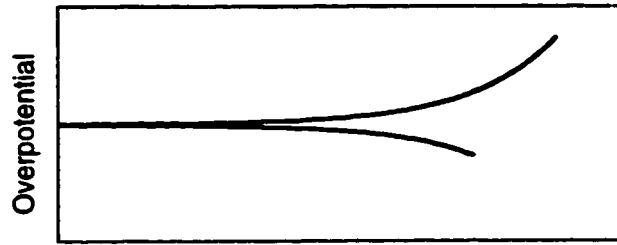
Carbon type	No	Argon Carbon	Hydrogenated Carbon	Nitrogenated carbon (20%)	Nitrogenated Carbon (30%)
Sputtering gas	None	Argon 100%	20% Methane balance Argon	20% Nitrogen balance Argon	30% Nitrogen balance Argon
Thickness	0	~110Å	~120Å	~130Å	~120Å
K value	N/A	~0.240	~0.200	~0.500	~0.600
Selket value	N/A	13	14	21	24

Table 3: Solution characteristics

Solution	DI water	7.5ppmw HCl
Conductivity	6.1 $\mu\Omega^{-1}$	63 $\mu\Omega^{-1}$
O ₂ Content	8.1mg/l	8.3mg/l
pH	4.3	3.2
Temperature	22°C	22°C

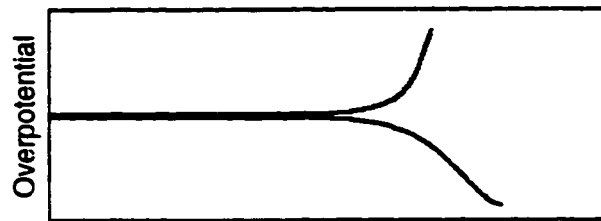
6.2 Taffel plots

The Taffel plots generated during this study are contained in Appendix A. The three typical plots types found during this study are presented in Figure 8. All Taffel plots for non-overcoated samples, in DI water or 7.5 ppm HCl, were similar in terms of the shape of the plot. For overcoated samples, the plots were similar in shape for all samples in DI water, and for samples in 7.5ppm HCl.



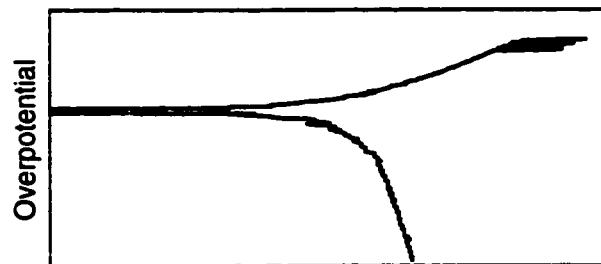
Current density (log scale)

a) No Carbon Overcoat



Current Density (log scale)

b) Carbon Overcoat, DI Water



Current density (log scale)

c) Carbon Overcoat, 7.5 ppm HCl

Figure 8: Typical results for: a) No carbon overcoat; b) Carbon overcoated samples in DI water, c) Carbon overcoated Samples in 7.5ppm HCl

The shapes of the anodic reaction are slightly different for each of these three cases. In the samples without carbon overcoats the anodic current density increased continuously and never stabilized at a given value. This is indicative that not only was passivation not attained but also that no steady state was reached.

For the samples with carbon overcoats, in DI water, the anodic current density tended to stabilize at higher voltages, suggesting that a steady state current was reached. This is an indication that the dominant process at higher voltages was concentration polarization. For overcoated samples, in HCl, the anodic current does not reach a steady state and there was no apparent concentration polarization.

6.3 Corrosion current

The corrosion currents reported in this section represent the average value of three measurements. The average corrosion currents for the different conditions are plotted in Figure 9 and Figure 10.

The samples with no carbon overcoat showed the highest corrosion current density, with about 450 nA/cm^2 in DI water and 4300 nA/cm^2 in 7.5 ppm HCl. The overcoated samples had a much lower corrosion current density, with the values being less than 50 nA/cm^2 for both DI water and HCl solution.

The lowest corrosion current was obtained for the two nitrogenated carbon overcoats, with average values of 5 and 9 nA/cm^2 in DI water (20% nitrogen and 30% nitrogen respectively) and 23 nA/cm^2 in HCl solution. The highest average corrosion

current, for overcoated samples, was found for argon carbon with 36 nA/cm² in DI water and 13 nA/cm² in HCl solution. The corrosion current density average for hydrogenated carbon was 17 nA/cm² in DI water and 32 nA/cm² in HCl.

All samples, with the exception of argon-carbon, had a lower corrosion current density in DI water than in diluted HCl.

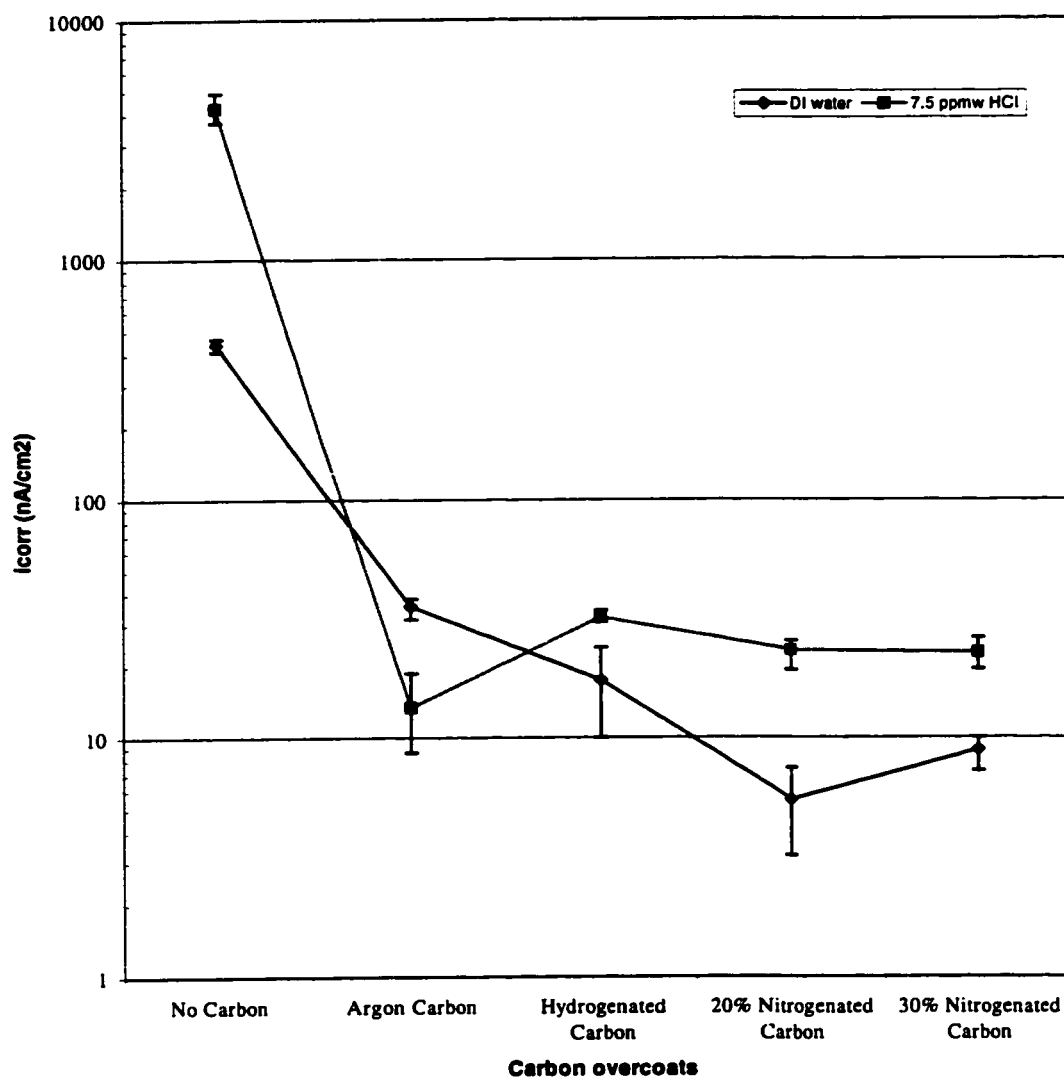


Figure 9: Corrosion Current density for all samples; error bars represent data scattering

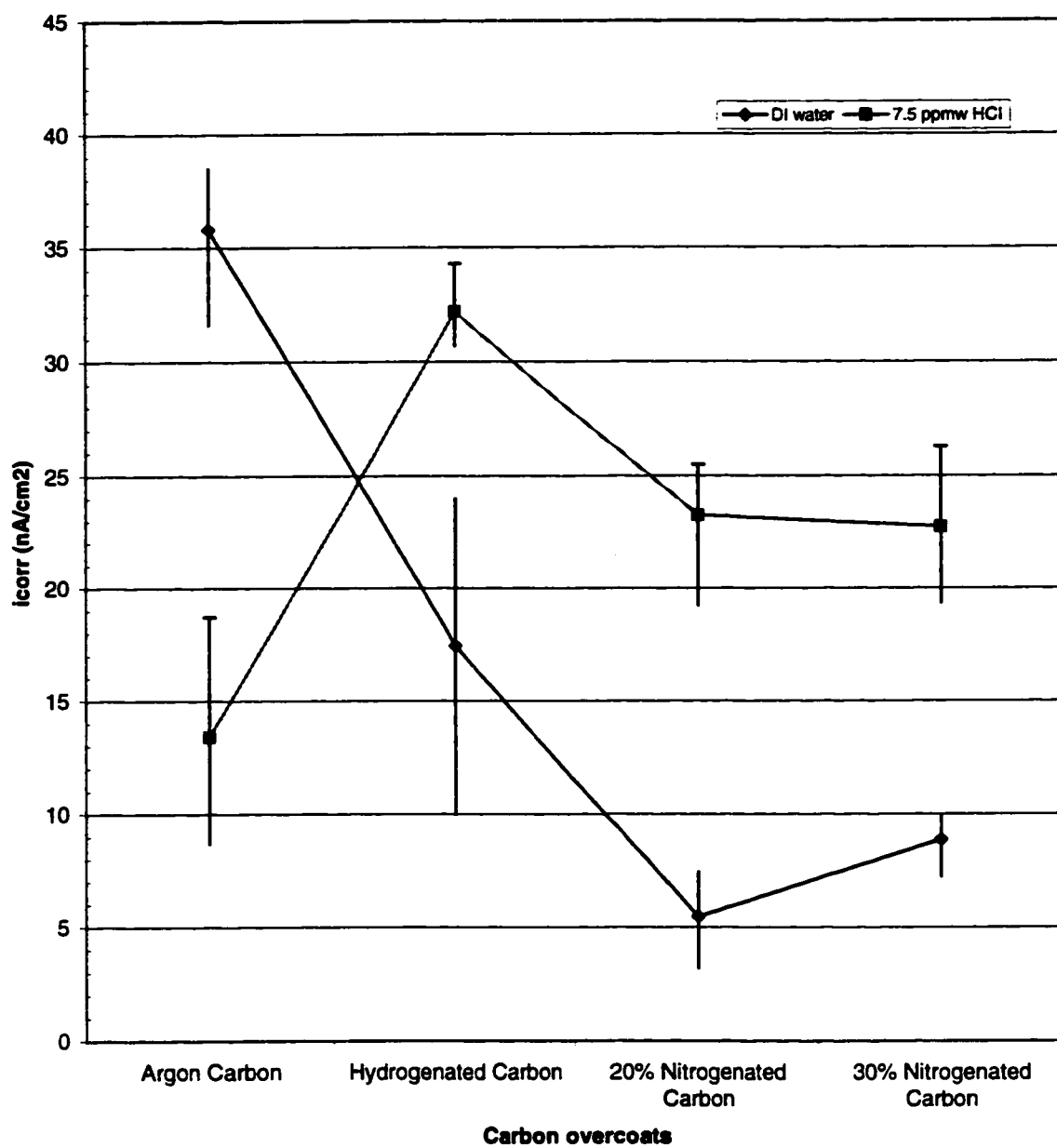


Figure 10: Corrosion Current density for Overcoated samples

First of all, the results indicate that the presence of a carbon overcoat reduces the corrosion current. The effect is quite dramatic, with corrosion current for the samples with overcoats being less than 1/10 of that of the samples without overcoats. This trend was found for both aerated DI water and aerated HCl solution.

When the hydrogenated and nitrogenated carbon overcoats are compared, the latter were found to have lower corrosion currents than the former. While this trend is significant for DI water, the trend for the HCl solution is less significant.

The data for argon-carbon overcoats is somewhat anomalous. While the trend for DI water is the same as that stated above, the trend for the HCl solution is not the same. Possible reasons for this anomalous behavior are discussed in Chapter 7.

6.4 Polarization resistance

The polarization resistances around E_{corr} results are presented in Figure 11. The samples without carbon overcoat had an average polarization resistance of about 22 k Ω for the HCl solution and about 330 k Ω for DI water.

For overcoated samples, the polarization resistance goes up to several M Ω . The highest polarization resistance was found for 30% nitrogenated carbon in DI water with an average value of 8.2 M Ω . In diluted HCl, the polarization resistance drops to 2.6 M Ω . 20% carbon showed a polarization resistance of 6.5 M Ω and 2.6 M Ω for DI water and diluted HCl, respectively. The lowest polarization resistance, for overcoated samples, was found for argon carbon with 3.1 M Ω in DI water, and 3.7 M Ω in diluted HCl.

Hydrogenated carbon had a polarization resistance of 5.1 M Ω in DI water and 1.5 M Ω in diluted HCl. Most samples had higher polarization resistance in DI water than in diluted HCl, with the exception of argon carbon.

The polarization resistance measurements are consistent with the corrosion current measurements, with the argon-carbon overcoated samples showing anomalous behavior.

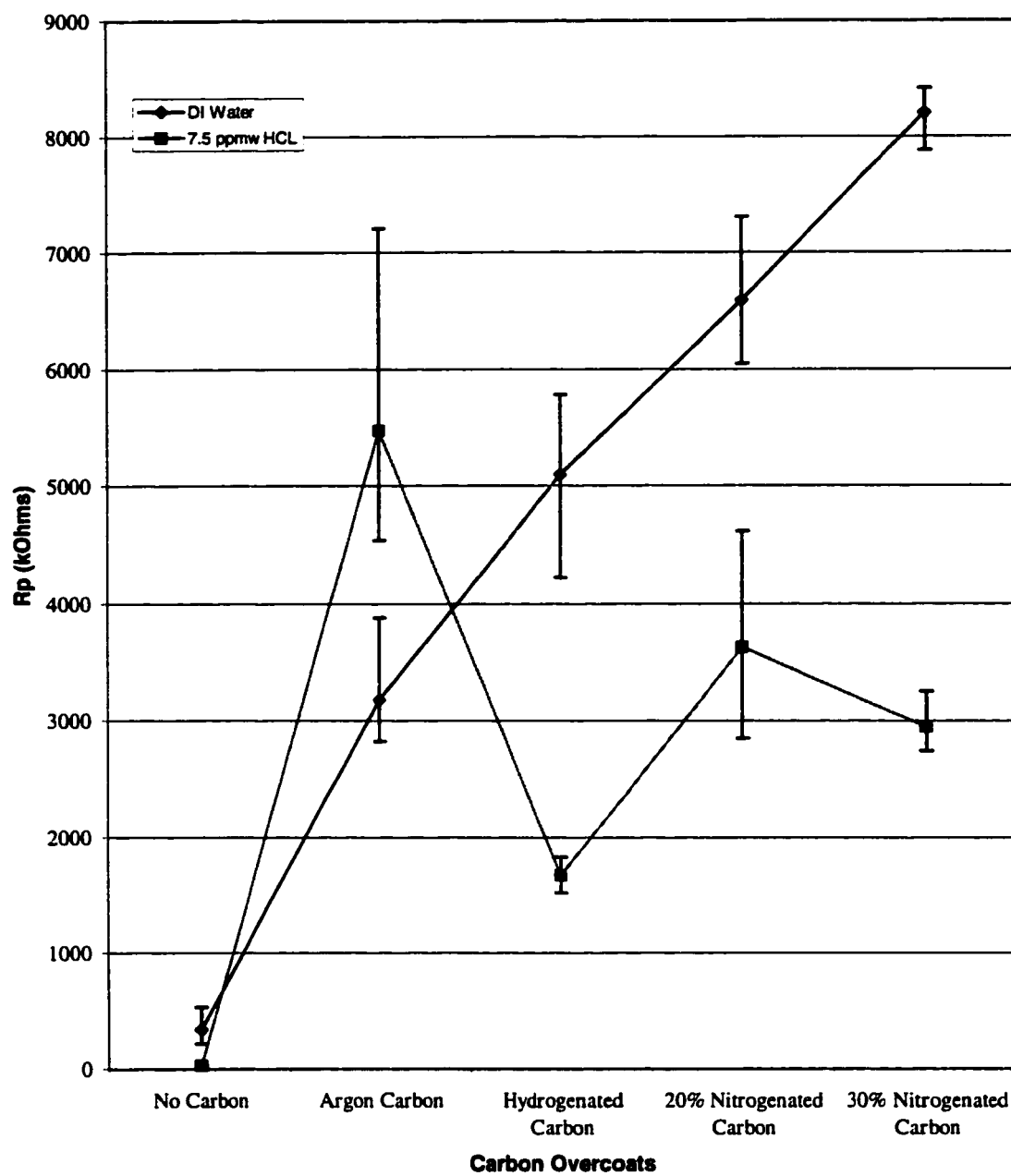


Figure 11: Polarization resistance for all samples; error bars represent data scattering

Chapter 7. Corrosion mechanisms in thin film magnetic media: interpretation of results

In this chapter, the results obtained in this study are discussed, starting with a brief explanation of the Taffel plots and then followed by an explanation of the electrochemical results.

7.1 Taffel plots

As seen in Figure 8, the Taffel plots for non-overcoated samples show no concentration polarization and no passivation. This means that the cobalt alloy does not passivate and that the ion and electron paths are not the controlling factors.

For samples with carbon overcoats in DI water, the Taffel plots show anodic concentration polarization. This was valid for any of the carbon overcoats and it means that the controlling factor for the reaction rate was either the electron path or the ion path. In this case, it was probably due to the restriction in ion path due to the build-up of corrosion products on the surface. This hypothesis is supported by the fact that the Taffel plots of overcoated samples in dilute HCl solution shows no concentration polarization. The corrosion products were probably soluble in the HCl solution but not in DI water since cations generally have much higher solubilities in chloride-containing solutions. This theory is consistent with the fact that in most cases the corrosion current was lower in DI water than that in 7.5 ppm HCl.

7.2 Current density and polarization resistance

The main parameter extractable from the Taffel plot is the corrosion current density which indicates the relative corrosion resistance of the system.

For samples without overcoats, the corrosion currents were higher than for overcoated samples. This result is consistent with intuition: since less surface area is in contact with the solution we can expect to obtain a lower current density for the samples with carbon overcoat. These results are in accordance with the results of Sides,^[6] Novotny^[4] and Brusic^[3] but in disagreement with the study by Merchant.^[5]

The polarization resistance measurements are consistent with the corrosion current measurement. This is compatible with the Stern-Geary Equation. Since the two measurements use different computational methods, good correlation is an indication of the validity of the mathematical model. Polarization resistance results are in fair agreement with Sides^[6] who reports a polarization resistance increase by about an order of magnitude between non-overcoated and overcoated samples. Sides^[6] measured a polarization resistance of about 50 k Ω for non-overcoated samples and 350 k Ω for overcoated samples. The polarization resistance measured during this research was on the order of several hundred k Ω for non-overcoated samples and several M Ω for overcoated samples. The differences in the actual values of the resistance between the two studies can be attributed to differences in the cobalt alloy composition, texture roughness, carbon overcoat composition and sputtering conditions.

Both, polarization resistance and corrosion current for the argon carbon sample, show confusing results. The corrosion current density was actually higher in DI water than in dilute HCl. This result is counter-intuitive since corrosion rates are usually higher in chlorinated solutions than in DI water, as has also been demonstrated by the results obtained for the hydrogenated and nitrogenated carbon overcoat disks. This is due to the higher solubility of corrosion products in chlorinated solutions than in DI water and the higher concentration of protons in lower pH solutions. If the argon-carbon samples had followed the trend of the other samples, the corrosion current density would have been in the range of 100 nA/cm^2 . This would be a large corrosion current density since most of the surface was covered by the argon-carbon overcoat. It is possible that during the time the system was allowed to equilibrate the magnetic layer was completely consumed by corrosion and that the results plotted were actually the corrosion current density of the chromium undercoat.

The corrosion current results for overcoated samples show nitrogenated samples to have better corrosion resistance than hydrogenated samples. According to the abrasion test hydrogenated carbon was the overcoat with the highest wear resistance, as was shown in Table 2. Intuitively, this overcoat should be the less porous and the corrosion current lower than argon carbon and nitrogenated carbon. The results for these specific carbon overcoats appear counter intuitive. Also, hydrogenated carbon is relatively more insulating than nitrogenated carbon,^[9] and therefore, according to Novotny's^[4] theory illustrated in Figure 5, hydrogenated carbon should have better corrosion resistance.

However, hydrogenated carbon is also more hydrophilic than nitrogenated carbon.^[9] Since the carbon layer is hydrophilic, the solution can penetrate deeper into pores and form an interface with the magnetic layer. In hydrophobic overcoats the pore needs to be larger in order for the solution to enter and be in contact with the magnetic layer. If the magnetic layer is not in contact with the solution, no ions can migrate from the magnetic layer to the solution and little to no corrosion occurs in that pore. This mechanism is illustrated in Figure 12.

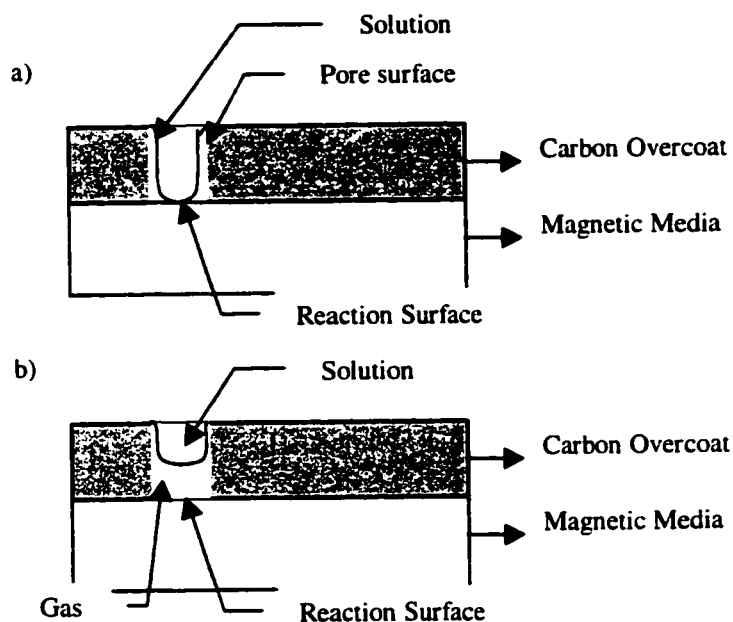


Figure 12: Hydrophilic (a), and hydrophobic (b) carbon overcoat-solution contact comparison

Chapter 8. Conclusions

The presence of carbon overcoats was found to enhance the corrosion resistance of the magnetic media by reducing the area exposed to the solution.

For the overcoated samples, nitrogenated carbon has better corrosion resistance than all other films tested in terms of corrosion current. This could be due to the relatively low affinity of this carbon film for water.

Chapter 9. Recommendations for future research

The following studies are recommended to improve the understanding of the effect of the carbon overcoat on corrosion of thin film magnetic media.

9.1 Wetting angle of water and carbon overcoat

Measure contact angle and corrosion current for various carbon and correlate the results. A lower contact angle, between the solution and the carbon overcoat, should lead to a lower corrosion resistance of the overcoated magnetic media. A higher contact angle should lead to a higher corrosion resistance.

9.2 Carbon overcoat porosity measurements

Measure carbon overcoat porosity in terms of pore size and number of pores and correlate to corrosion current or polarization resistance.

Chapter 10. References

1. Grochowski, E. and J.G. Belleson, "MR Head technology evolves into next generation GMR/SPIN valve heads", IDEMA Insight, Volume X, Number 6, Nov-Dec 1997, p1.
2. Jones, D., Principles and Prevention of Corrosion, Chapter 1-3, MacMillan Publishing, New York, 1992
3. Brusic, V., M. Russak, R. Staud, G. Frankel, A. Selius, and D. DiMilia "Corrosion of thin film magnetic disk: Galvanic effect of the carbon overcoat", Journal of Electrochemical Society, Vol. 136, No 1, Jan 1989. pp 42-46.
4. Novotny, V. and N. Staud. "Correlation between environmental and electrochemical corrosion of thin film magnetic recording media", Journal of Electrochemical Society, Electrochemical Science and Technology, Dec 1988. pp 2931-2938
5. Merchant, K., M. Smallen, R. Fisher, and S. Smith, "Physical Factors Affecting the corrosion resistance of CoCr thin-film media", Journal of Applied Physics 67 (9), 1 May 1990, pp 4707-4709
6. Sides, Paul, J., "The dependence of the corrosion behavior of rigid disk magnetic recording media on the deposition conditions of the underlayer, magnetic layer, and carbon overcoat", Journal of Electrochemical Society, Vol. 139, No 5, May 1992, pp 1352-1357.
7. Walmsley, R. G., B. R. Natarajan, and D. Wong, "Applying AC impedance electrochemical methods to corrosion testing cobalt alloy media", IEEE Transactions on Magnetics, Vol. 24, No 6, Nov: 1988, pp 3000-3002
8. Li, E. , Consultant, Personal communication on 6/08/98
9. Chia, R., W., E. Li, S. Sugi, G.G. Li, H. Zhu, A. R. Forouhi, and I. Bloomer, "Optical characterization of nitrogenated carbon overcoat", ICMCT, Fall 97 Conference paper.
10. Veerasamy, V. S. and M. Weiler, "Water adsorption level on a-C:H and a-C:N films", Unpublished report, Akashic Memories Corporation, 06/97.

Appendix A

Model 352/252 Corrosion Analysis Software, v. 0.00

Filename: C:\M352\data\0C1.T

TA TAFEL

Date Run: UNKNOWN

File Status: NORMAL

Time Run: UNKNOWN

Cond. Time	CT	pass	s	Initial Pot.	IP	-50.00E-3	V oc
Cond. Pot.	CP	pass	V	Final Pot.	FP	250.0E-3	V oc
Initial Delay	ID	pass	s				
Scan Rate	SR	200.0E-3	mV/s	Curr. Range	CR	Auto	
Scan Incr.	SI	1.000	mV	Step Time	ST	5.000	s
No. of Points	NP	300					
Line Sync.	LS	no		GI Time Const.	TC	off	
Rise Time	RT	high stability		IR Mode	IR	none	
Working Elec.	WE	Solid		Filter	FL	5.3Hz	
Sample Area	AR	1.000	cm ²	Ref. Elec.	RE	AgCl	197.0E-3V
Density	DE	0.0000	g/ml	Equip. Mt.	EW	0.0000	g
Open Circuit	OC	270.0E-3	V	AUX A/D	AU	no	

Comment: No Carbon Overcoat. DI water O2 saturated

Rp CALCULATIONS:

Corrosion Rate = N.A.

Rp = 527.8 KOHms

E(I=0) = 299.8 mV

Beta Anodic = 1.100

Begin = 221.0 mV

Correlation = -1000.0E-3

Icorr(R) = 449.4 nA/cm²

Beta Cathodic = 1.016 V/decade

End = 517.0 mV

TAFEL CALCULATIONS:

Corrosion Rate = N.A.

E(I=0) = 299.3 mV

Beta Anodic = 1.100

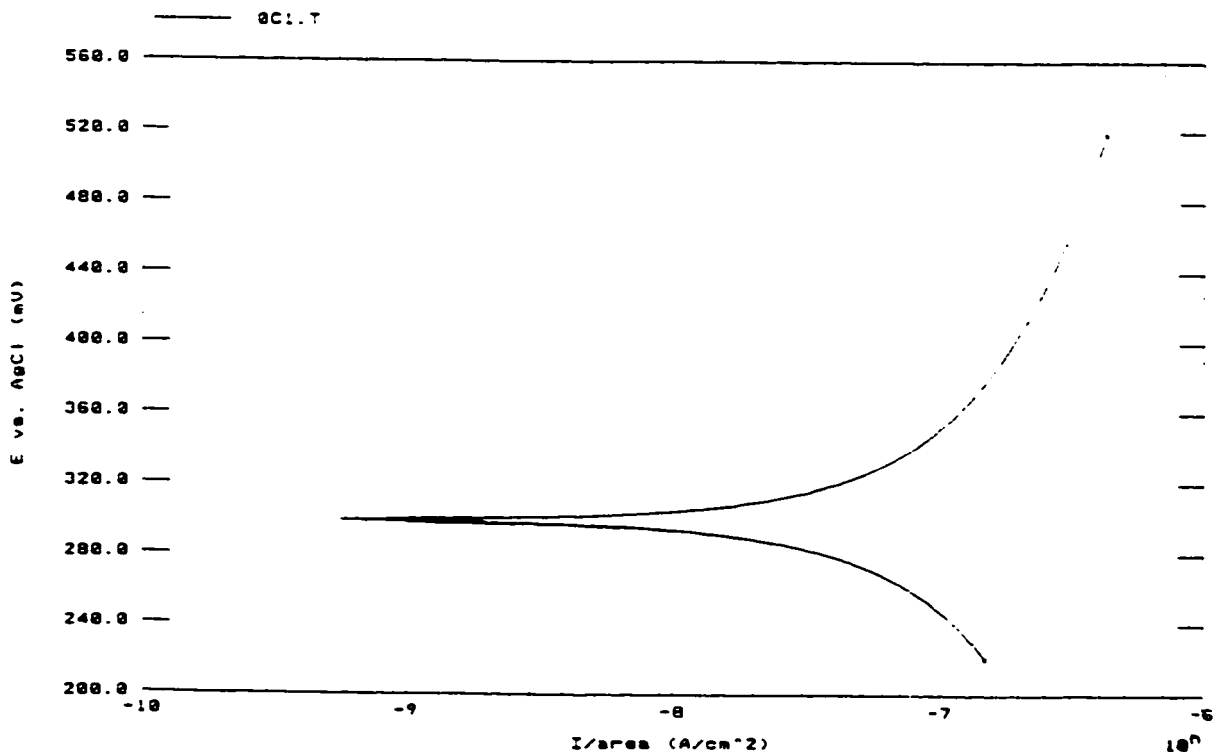
Begin = 221.0 mV

Chi² = 6.06E-002

Icorr = 450.0 nA/cm²

Beta Cathodic = 1.016 V/decade

End = 519.0 mV



Model 352/252 Corrosion Analysis Software, v. 0.00

Filename: c:\a352\data\NoCD12

TA TAFEL

Date Run: UNKNOWN

File Status: NORMAL

Time Run: UNKNOWN

Cond. Time	CT	pass	s	Initial Pot.	IP	-250.0E-3	V oc
Cond. Pot.	CP	pass	V	Final Pot.	FP	250.0E-3	V oc
Initial Delay	ID	pass	s				
Scan Rate	SR	200.0E-3	mV/s	Curr. Range	CR	Auto	
Scan Incr.	SI	2.000	mV	Step Time	ST	10.00	s
No. of Points	NP	250					
Line Sync.	LS	no		GI Time Const.	TC	Off	
Rise Time	RT	high stability		IR Mode	IR	none	
Working Elec.	WE	Solid		Filter	FL	15.3Hz	
Sample Area	AR	1.000	cm ²	Ref. Elec.	RE	AgCl 197.0E-3V	
Density	DE	0.0000	g/ml	Equiv. Wt.	EW	0.0000	g
Open Circuit	OC	424.0E-3	V	AUX A/D	AU	no	

Comment: No Carbon Overcoat. D1 water O2 Saturated. Sample#2

R_p CALCULATIONS:

Corrosion Rate = N.A.

R_p = 216.2 KOHms

E(I=0) = 433.2 mV

Beta Anodic = 288.4E-3

Begin = 412.0 mV

Correlation = -993.0E-3

I_{corr}(R) = 327.7 nA/cm²

Beta Cathodic = 375.5E-3 V/decade

End = 452.0 mV

TAFEL CALCULATIONS:

Corrosion Rate = N.A.

E(I=0) = 432.9 mV

Beta Anodic = 288.4E-3

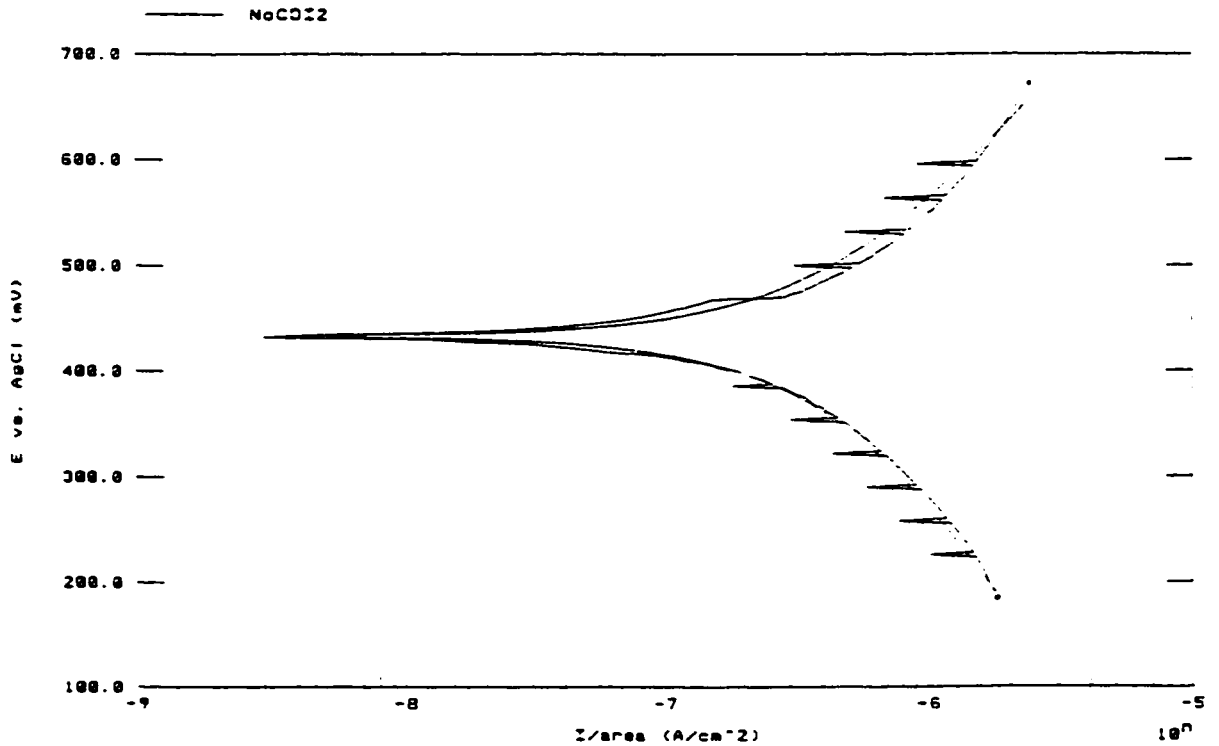
Begin = 184.0 mV

Chi² = 4.71E+001

I_{corr} = 414.6 nA/cm²

Beta Cathodic = 375.5E-3 V/decade

End = 672.0 mV



Model 352/252 Corrosion Analysis Software, v. 2.18

Filename: c:\m352\data\NocD13.t

TA TAFEL

Date Run: UNKNOWN

File Status: NORMAL

Time Run: UNKNOWN

Cond. Time	CT	pass	s	Initial Pot.	IP	-250.0E-3	V oc
Cond. Pot.	CP	pass	V	Final Pot.	FP	250.0E-3	V oc
Initial Delay	ID	pass	s				
Scan Rate	SR	500.0E-3	mV/s	Curr. Range	CR	Auto	
Scan Incr.	SI	2.000	mV	Step Time	ST	4.000	s
No. of Points	NP	250					
Line Sync.	LS	no		GI Time Const.	TC	Off	
Rise Time	RT	high stability		IR Mode	IR	none	
Working Elec.	WE	Solid		Filter	FL	15.3Hz	
Sample Area	AR	1.000	cm ²	Ref. Elec.	RE	AgCl	197.0E-3V
Density	DE	0.3000	g/ml	Equip. Wt.	EW	0.0000	g
Open Circuit	OC	287.0E-3	V	AUX A/D	AU	no	

Comment: No Carbon Overcoat, D2 water, O2 Saturated, Sample #3

R_p CALCULATIONS:

Corrosion Rate = N.A.

R_p = 262.4 KOHms

E(I=0) = 321.0 mV

Beta Anodic = 100.0E-3

Begin = 297.0 mV

Correlation = -998.4E-3

I_{corr}(R) = 82.76 nA/cm²

Beta Cathodic = 100.0E-3 V/decade

End = 335.0 mV

TAFEL CALCULATIONS:

Corrosion Rate = N.A.

E(I=0) = 321.7 mV

Beta Anodic = 1.469

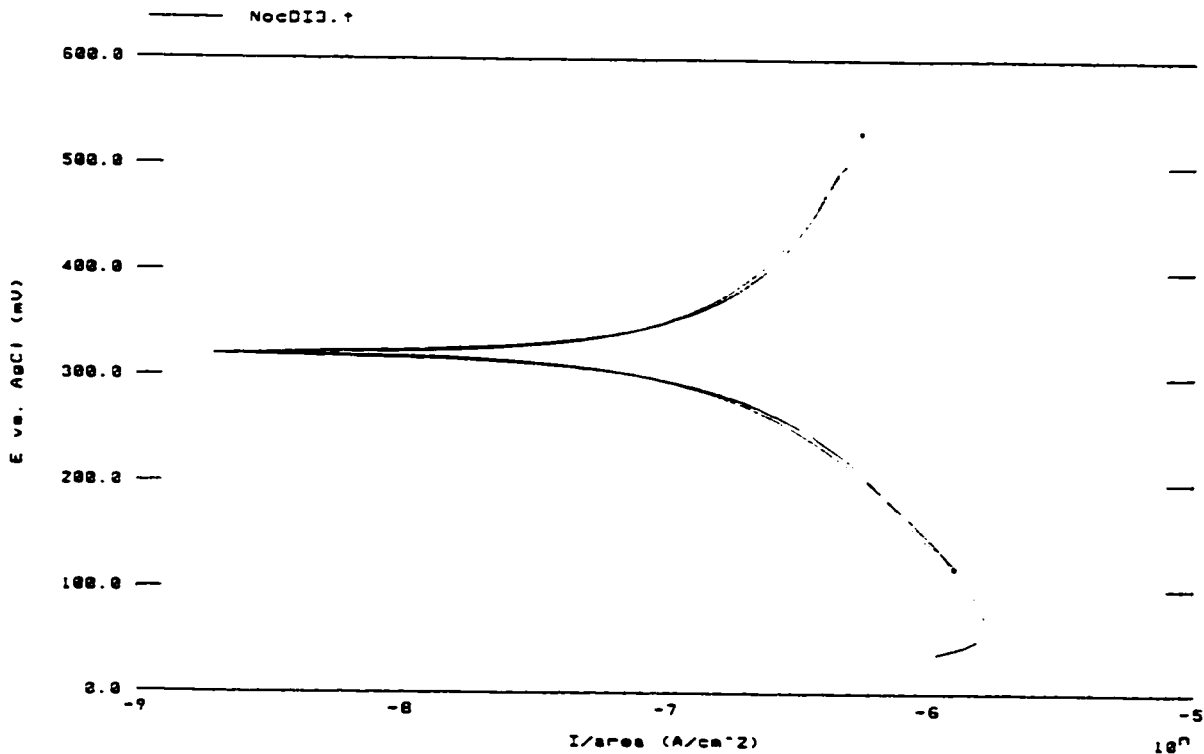
Begin = 119.0 mV

Chi² = 4.00E+000

I_{corr} = 468.5 nA/cm²

Beta Cathodic = 379.7E-3 V/decade

End = 531.0 mV



Model J52/252 Corrosion Analysis Software, v. 2.10
 Filename: c:\m352\data\acc11.t

TA TAFEL

Date Run: UNKNOWNNN

File Status: NORMAL
 Time Run: UNKNOWNNN

Cond. Time	CT	pass	s	Initial Pot.	IP	-250.0E-3	V dc
Cond. Pot.	CP	pass	s	Final Pot.	FP	250.0E-3	V dc
Initial Delay	ID	pass	s				
Scan Rate	SR	500.0E-3	mV/s	Curr. Range	CR	Auto	
Scan Incr.	SI	2.000	mV	Step Time	ST	4.000	s
No. of Points	NP	250					
Line Sync.	LS	no		GI Time Const.	TC	off	
Rise Time	RT	high stability		IR Mode	IR	none	
Working Elec.	WE	Solid		Filter	FL	2 S.3Hz	
Sample Area	AR	1.000	cm ²	Ref. Elec.	RE	AgCl	197.0E-3V
Density	DE	0.0000	g/ml	Equiv. Wt.	EW	0.0000	g
Open Circuit	OC	512.0E-3	V	AUX A/D	AU	no	

Comment: Argon Carbon, DI water, O2 saturated, Sample01

RE CALCULATIONS:

Corrosion Rate = N.A.
 Rp = 2.835 mOhas
 E(I=0) = 509.5 mV
 Beta Anodic = 100.0E-3
 Beta Cathodic = 100.0E-3
 Begin = 438.0 mV

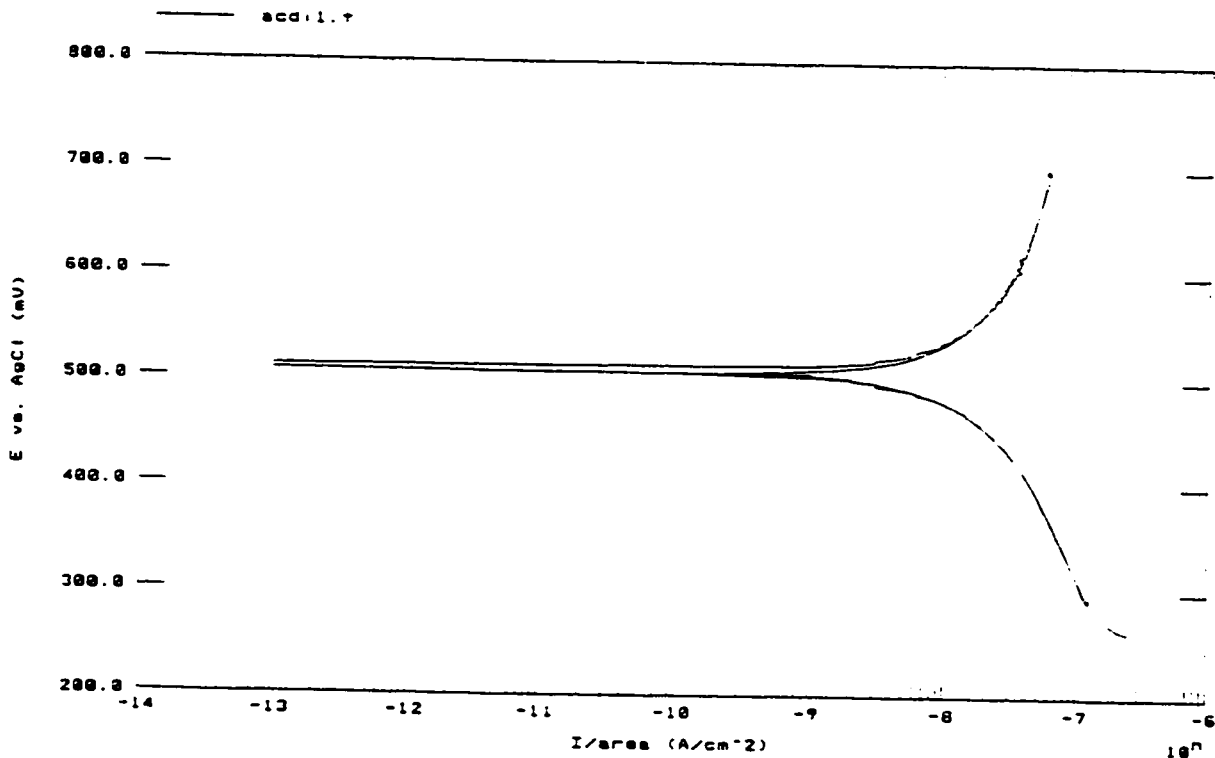
Correlation = -999.0E-3

Icorr(R) = 7.660 nA/cm²
 Beta Cathodic = 100.0E-3 V/decade
 End = 592.0 mV

TAFEL CALCULATIONS:

Corrosion Rate = N.A.
 E(I=0) = 506.4 mV
 Beta Anodic = 728.4E-3
 Beta Cathodic = 728.4E-3
 Begin = 294.0 mV

Chi² = 4.42E-001
 Icorr = 38.53 nA/cm²
 Beta Cathodic = 390.3E-3 V/decade
 End = 700.0 mV



Model 352/252 Corrosion Analysis Software, v. 2.10

Filename: c:\m352\data\ACD12.†

TA TAFEL

Date Run: UNKNOWN

File Status: NORMAL

Time Run: UNKNOWN

Cond. Time	CT	pass	s	Initial Pot.	IP	-250.0E-3	V oc
Cond. Pot.	CP	pass	V	Final Pot.	FP	250.0E-3	V oc
Initial Delay	ID	pass	s				
Scan Rate	SR	500.0E-3	mV/s	Curr. Range	CR	Auto	
Scan Incr.	SI	2.000	mV	Step Time	ST	4.000	s
No. of Points	NP	250					
Line Sync.	LS	no		GI Time Const.	TC	Off	
Rise Time	RT	high stability		IR Mode	IR	none	
Working Elec.	WE	Solid		Filter	FL	I 5.3Hz	
Sample Area	AR	1.000	cm ²	Ref. Elec.	RE	AgCl	197.2E-3V
Density	DE	0.0000	g/ml	Equiv. Wt.	EW	0.0000	g
Open Circuit	OC	418.0E-3	V	AUX A/D	AU	no	

Comment: Argon Carbon, DI water, O2 saturated, Sample02

Rp CALCULATIONS:

Corrosion Rate = N.A.

Rp = 3.885 MOhms

E(I=0) = 417.9 mV

Beta Anodic = 100.0E-3

Begin = 394.0 mV

Correlation = -993.4E-3

Icorr(R) = 5.589 nA/cm²

Beta Cathodic = 100.0E-3 V/decade

End = 516.0 mV

TAFEL CALCULATIONS:

Corrosion Rate = N.A.

E(I=0) = 416.8 mV

Beta Anodic = 1.890

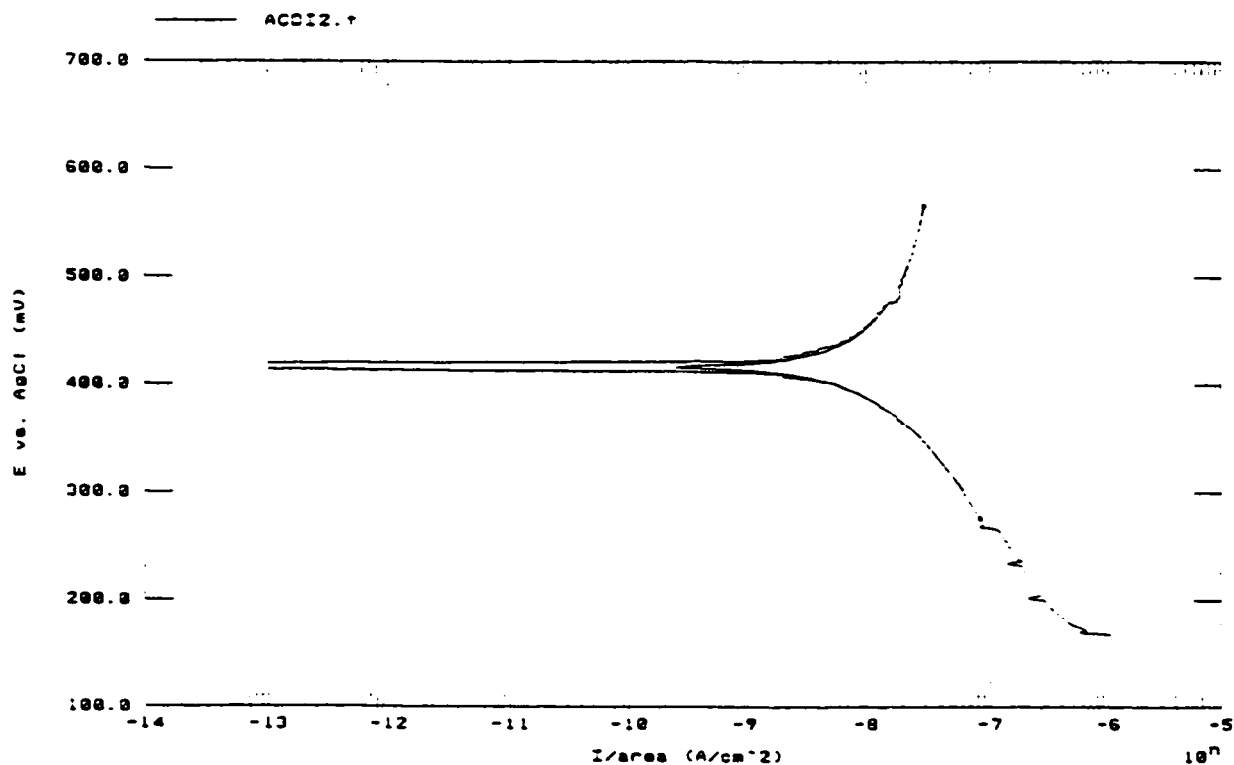
Begin = 276.0 mV

Chi² = 2.80E-001

Icorr = 31.63 nA/cm²

Beta Cathodic = 261.5E-3 V/decade

End = 566.0 mV



Model 352/252 Corrosion Analysis Software, v. 2.10

Filename: c:\m352\data\acdi3.t

TA TAFEL

Date Run: UNKNOWNN

File Status: NORMAL

Time Run: UNKNOWNN

Cond. Time	CT	pass	s	Initial Pot.	IP	-250.0E-3	V oc
Cond. Pot.	CP	pass	V	Final Pot.	FP	250.0E-3	V oc
Initial Delay	ID	pass	s				
Scan Rate	SR	500.0E-3	mV/s	Curr. Range	CR	Auto	
Scan Incr.	SI	2.000	mV	Step Time	ST	4.000	s
No. of Points	NP	250					
Line Sync.	LS	no		GI Time Const.	TC	off	
Rise Time	RT	high stability		IR Mode	IR	none	
Working Elec.	WE	Solid		Filter	FL	5.3Hz	
Sample Area	AR	1.000	cm ²	Ref. Elec.	RE	AgCl	197.0E-3V
Density	DE	0.0000	g/ml	Equiv. Wt.	EW	0.0000	g
Open Circuit	OC	250.0E-3	V	AUX A/D	AU	no	

Comment: Argon Carbon, DI water, O2 saturated, Sample#3

Rp CALCULATIONS:

Corrosion Rate = N.A.

Rp = 2.829 MOHMS

E(I=0) = 359.6 mV

Beta Anodic = 100.0E-3

Begin = 306.0 mV

Correlation = -987.4E-3

Icorr(R) = 7.676 nA/cm²

Beta Cathodic = 100.0E-3 V/decade

End = 398.0 mV

TAFEL CALCULATIONS:

Corrosion Rate = N.A.

E(I=0) = 356.0 mV

Beta Anodic = 2.064

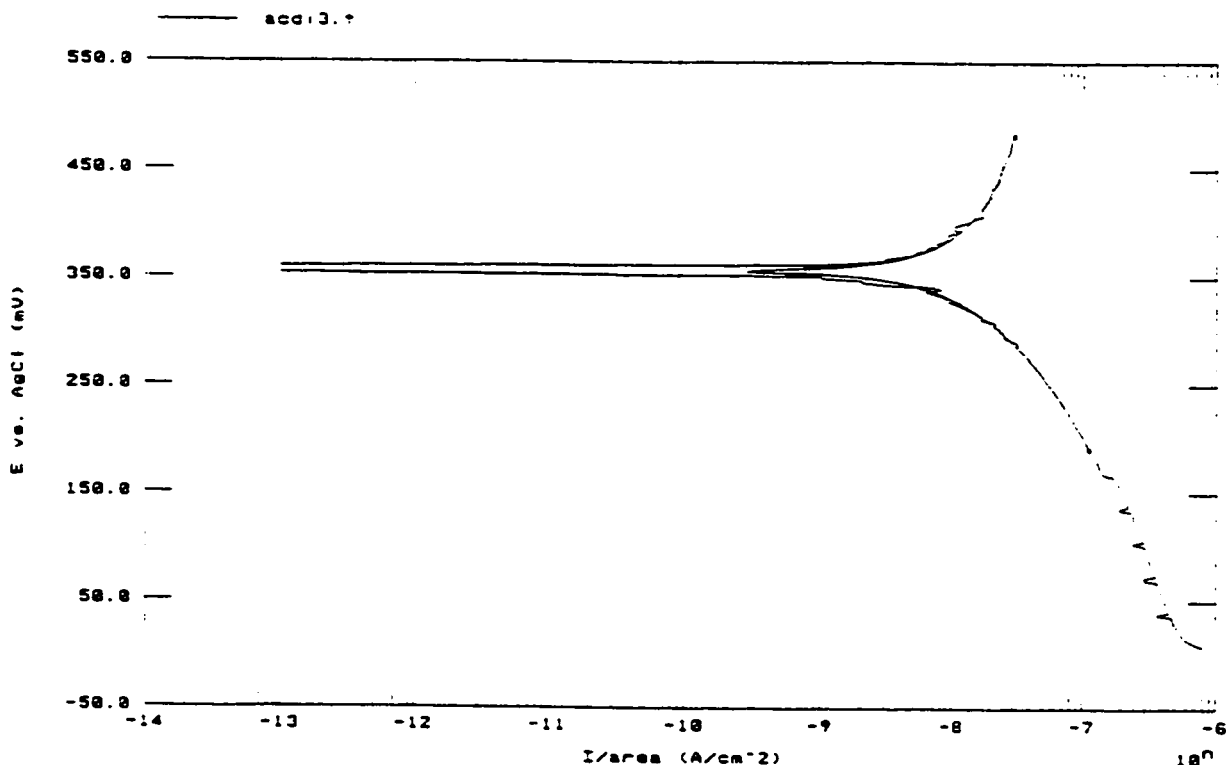
Begin = 192.0 mV

Chi² = 4.10E-001

Icorr = 37.25 nA/cm²

Beta Cathodic = 280.9E-3 V/decade

End = 482.0 mV



Model 352/252 Corrosion Analysis Software, v. 2.10

Filename: c:\a352\data\hcd11.t

TA TAFEL

Date Run: UNKNOWN

File Status: NORMAL

Time Run: UNKNOWN

Cond. Time	CT	pass	s	Initial Pot.	IP	-250.0E-3	V oc
Cond. Pot.	CP	pass	U	Final Pot.	FP	250.0E-3	V oc
Initial Delay	ID	pass	s				
Scan Rate	SR	500.0E-3	mV/s	Curr. Range	CR	Auto	
Scan Incr.	SI	2.000	mV	Step Time	ST	4.000	s
No. of Points	NP	250					
Line Sync.	LS	no		GI Time Const.	TC	off	
Rise Time	RT	high stability		IR Mode	IR	none	
Working Elec.	WE	Solid		Filter	FL	15.3Hz	
Sample Area	AR	1.000	cm ²	Ref. Elec.	RE	AgCl	197.0E-3V
Density	DE	0.0000	g/ml	Equiv. Wt.	EW	0.0000	g
Open Circuit	OC	372.0E-3	V	AUX A/D	AU	no	

Comment: Hydrogenated Carbon, DI water, O2 saturated, Sample #1

Rp CALCULATIONS:

Corrosion Rate = N.A.

Rp = 5.785 MOHMS

E(I=0) = 360.0 mV

Beta Anodic = 100.0E-3

Begin = 350.0 mV

Correlation = -995.4E-3

Icorr(R) = 3.754 nA/cm²

Beta Cathodic = 100.0E-3 V/decade

End = 450.0 mV

TAFEL CALCULATIONS:

Corrosion Rate = N.A.

E(I=0) = 379.3 mV

Beta Anodic = 1.365

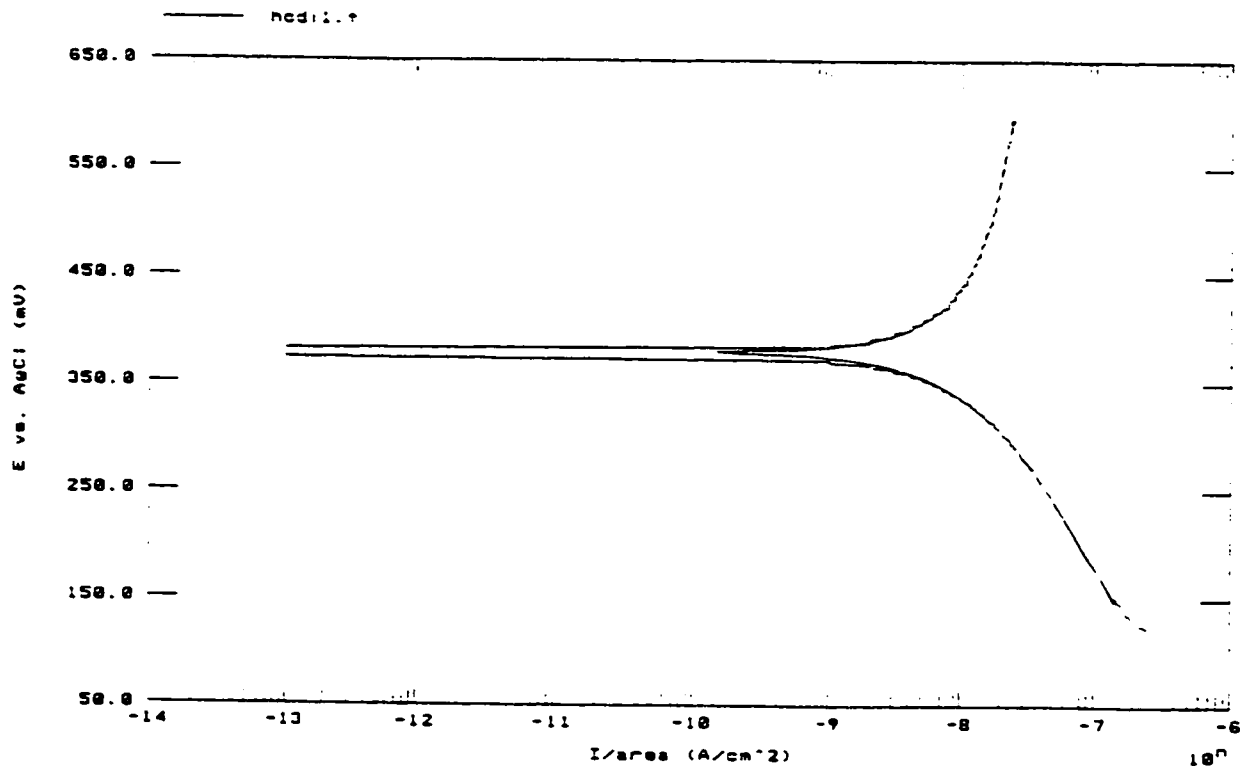
Begin = 150.0 mV

Chi² = 1.87E-001

Icorr = 18.40 nA/cm²

Beta Cathodic = 251.4E-3 V/decade

End = 594.0 mV



Model 352/252 Corrosion Analysis Software, v. 2.10

Filename: c:\m352\data\hcdi2.t

TA TAFEL

Date Run: UNKNOWNNN

File Status: NORMAL

Time Run: UNKNOWNNN

Cond. Time	CT	pass	s	Initial Pot.	IP	-250.0E-3	V oc
Cond. Pot.	CP	pass	V	Final Pot.	FP	250.0E-3	V oc
Initial Delay	ID	pass	s				
Scan Rate	SR	500.0E-3	mV/s	Curr. Range	CR	Auto	
Scan Incr.	SI	2.000	mV	Step Time	ST	4.000	s
No. of Points	NP	250					
Line Sync.	LS	no		GI Time Const.	TC	Off	
Rise Time	RT	high stability		IR Mode	IR	none	
Working Elec.	WE	Solid		Filter	FL	5.3Hz	
Sample Area	AR	1.000	cm ²	Ref. Elec.	RE	AgCl	197.0E-3V
Density	DE	0.0000	g/ml	Equiv. Wt.	EW	0.0000	g
Open Circuit	OC	404.0E-3	V	AUX A/D	AU	no	

Comment: Hydrogenated Carbon, DI water, O2 saturated, Sample #2

RP CALCULATIONS:

Corrosion Rate = N.A.

Rp = 4.221 MOhms

E(I=0) = 409.0 mV

Beta Anodic = 100.0E-3

Begin = 358.0 mV

Correlation = -993.5E-3

Icorr(R) = 5.144 nA/cm²

Beta Cathodic = 100.0E-3 V/decade

End = 474.0 mV

TAFEL CALCULATIONS:

Corrosion Rate = N.A.

E(I=0) = 405.0 mV

Beta Anodic = 1.359

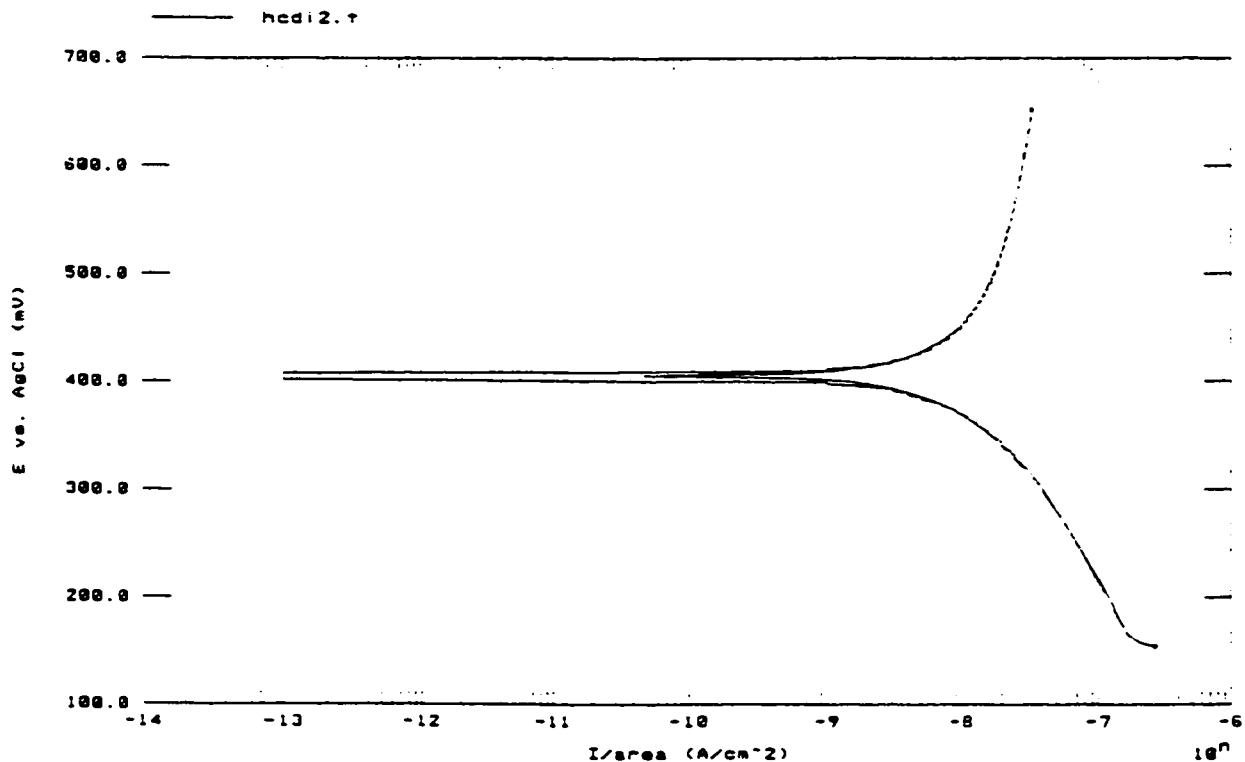
Begin = 154.0 mV

Chi² = 1.61E+000

Icorr = 23.98 nA/cm²

Beta Cathodic = 274.0E-3 V/decade

End = 652.0 mV



Model 352/252 Corrosion Analysis Software, v. 2.10

Filename: c:\m352\data\hcdi3.t

TA TAFEL

Date Run: UNKNOWNNN

File Status: NORMAL

Time Run: UNKNOWNNN

Cond. Time	CT	pass	s	Initial Pot.	IP	-250.0E-3	V oc
Cond. Pot.	CP	pass	V	Final Pot.	FP	250.0E-3	V oc
Initial Delay	ID	pass	s				
Scan Rate	SR	500.0E-3	mV/s	Curr. Range	CR	Auto	
Scan Incr.	SI	2.000	mV	Step Time	ST	4.000	s
No. of Points	NP	250					
Line Sync.	LS	no		GI Time Const.	TC	Off	
Rise Time	RT	high stability		IR Mode	IR	none	
Working Elec.	WE	Solid		Filter	FL	I 5.3Hz	
Sample Area	AR	1.000	cm ²	Ref. Elec.	RE	AgCl	197.0E-3V
Density	DE	0.0000	g/cm ³	Equiv. Wt.	EW	0.0000	g
Open Circuit	OC	396.0E-3	V	AUX A/D	AU	no	

Comment: Hydrogenated Carbon, OI water, O2 Saturated, Sample #3

RA CALCULATIONS:

Corrosion Rate = N.A.

Rp = 5.281 MOhms

E(I=0) = 411.6 mV

Beta Anodic = 581.3E-3

Begin = 298.0 mV

Correlation = -998.4E-3

Icorr(R) = 13.72 nA/cm²

Beta Cathodic = 250.1E-3 V/decade

End = 430.0 mV

TAFEL CALCULATIONS:

Corrosion Rate = N.A.

E(I=0) = 415.6 mV

Beta Anodic = 581.3E-3

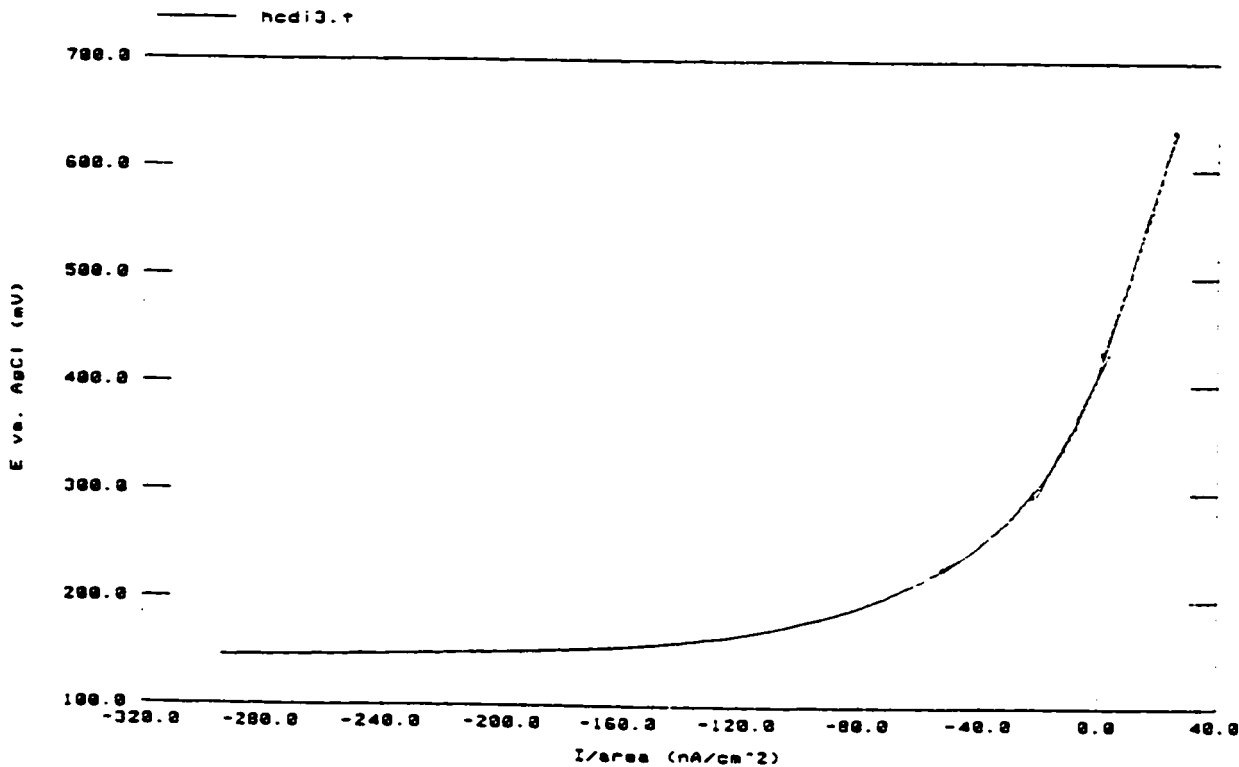
Begin = 230.0 mV

Chi² = 1.48E-001

Icorr = 9.987 nA/cm²

Beta Cathodic = 250.1E-3 V/decade

End = 636.0 mV



Model 352/252 Corrosion Analysis Software, v. 2.18

Filename: c:\m352\data\nlcd1.1

TA TAFEL

File Status: NORMAL

Date Run: UNKNOWNNN

Time Run: UNKNOWNNN

Cond. Time	CT	pass	s	Initial Pot.	IP	-250.0E-3	V oc
Cond. Pot.	CP	pass	V	Final Pot.	FP	250.0E-3	V oc
Initial Delay	ID	pass	s				
Scan Rate	SR	500.0E-3	mV/s	Curr. Range	CR	Auto	
Scan Incr.	SI	2.000	mV	Step Time	ST	4.000	s
No. of Points	NP	250					
Line Sync.	LS	no		GI Time Const.	TC	Off	
Rise Time	RT	high stability		IR Mode	IR	none	
Working Elec.	WE	Solid		Filter	FL	15.3Hz	
Sample Area	AR	1.000	cm ²	Ref. Elec.	RE	AgCl	197.0E-3V
Density	DE	0.0000	g/ml	Equiv. Wt.	EW	0.0000	
Open Circuit	OC	450.0E-3	V	AUX A/O	AU	no	

Comment: 20% Nitrogenated Carbon, O2 water, O2 saturated. Sample #1

Re CALCULATIONS:

Corrosion Rate = N.A.
 $R_p = 6.044 \text{ mOha/s}$
 $E(I=0) = 568.8 \text{ mV}$
 $\beta_{\text{Anodic}} = 211.4\text{E-3}$
 $\beta_{\text{Cathodic}} = 169.6\text{E-3 V/decade}$
 $\text{Begin} = 520.0 \text{ mV}$

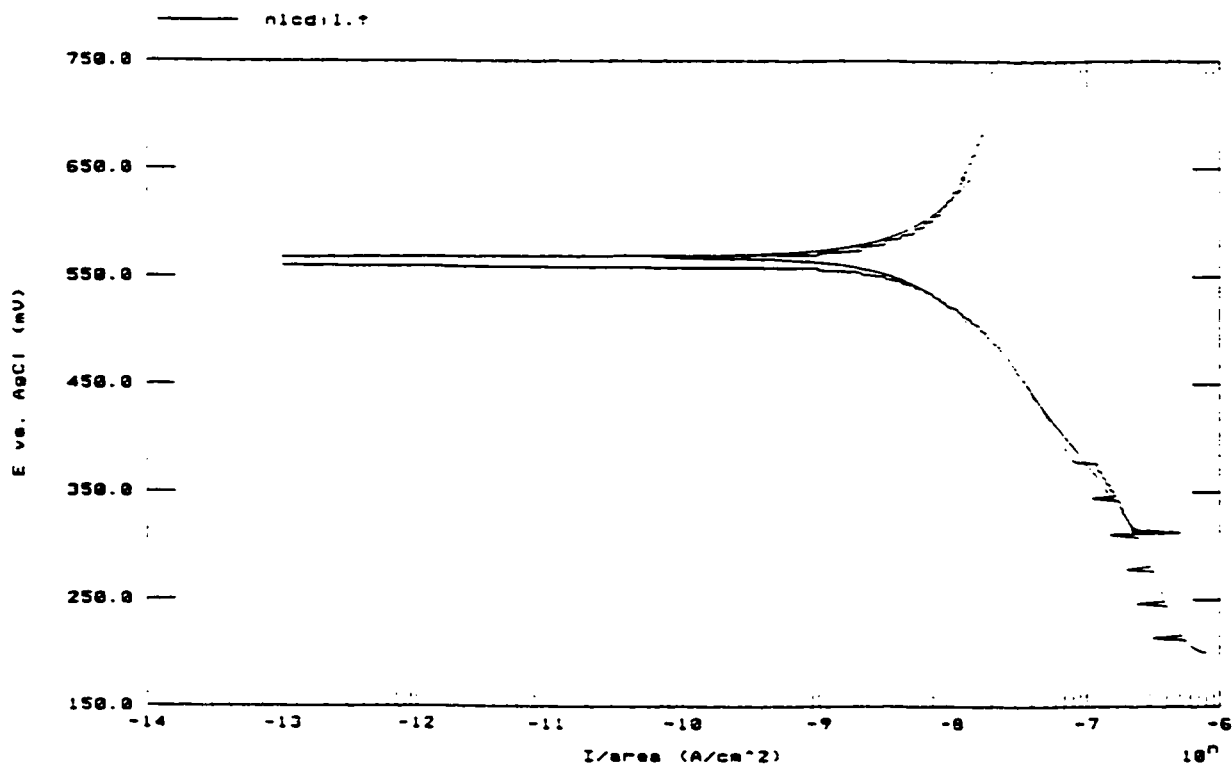
Correlation = -989.7E-3

$I_{\text{corr}}(R) = 6.762 \text{ nA/cm}^2$
 $\beta_{\text{Cathodic}} = 169.6\text{E-3 V/decade}$
 $\text{End} = 600.0 \text{ mV}$

TAFEL CALCULATIONS:

Corrosion Rate = N.A.
 $E(I=0) = 568.4 \text{ mV}$
 $\beta_{\text{Anodic}} = 211.4\text{E-3}$
 $\beta_{\text{Cathodic}} = 169.6\text{E-3 V/decade}$
 $\text{Begin} = 514.0 \text{ mV}$

$\chi^2 = 5.58\text{E+000}$
 $I_{\text{corr}} = 7.435 \text{ nA/cm}^2$
 $\beta_{\text{Cathodic}} = 169.6\text{E-3 V/decade}$
 $\text{End} = 642.0 \text{ mV}$



Model 352/252 Corrosion Analysis Software, v. 2.10
 Filename: c:\n352\data\nlcedi2.t

TA TAFEL
 Date Run: UNKNOWN File Status: NORMAL
 Time Run: UNKNOWN

Cond. Time	CT	pass	s	Initial Pot.	IP	-250.0E-3	V oc
Cond. Pot.	CP	pass	V	Final Pot.	FP	250.0E-3	V oc
Initial Delay	ID	pass	s				
Scan Rate	SR	500.0E-3	mV/s	Curr. Range	CR	Auto	
Scan Incr.	SI	2.000	mV	Step Time	ST	4.000	s
No. of Points	NP	250					
Line Sync.	LS	no		GI Time Const.	TC	off	
Rise Time	RT	high stability		IR Mode	IR	none	
Working Elec.	WE	Solid		Filter	FL	I 5.3Hz	
Sample Area	AR	1.000	cm ²	Ref. Elec.	RE	AgCl	197.0E-3V
Density	DE	0.0000	g/ml	Equiv. Wt.	EW	0.0000	g
Open Circuit	OC	206.0E-3	V	AUX A/D	AU	no	

Comment: 20% Nitrogenated Carbon, DI water, O2 saturated, Sample 02

Re CALCULATIONS:

Corrosion Rate = N.A.
 Rp = 6.403 MOhms
 E(I=0) = 272.1 mV
 Beta Anodic = 100.0E-3
 Beta Cathodic = 100.0E-3
 Begin = 212.0 mV

Correlation = -981.0E-3

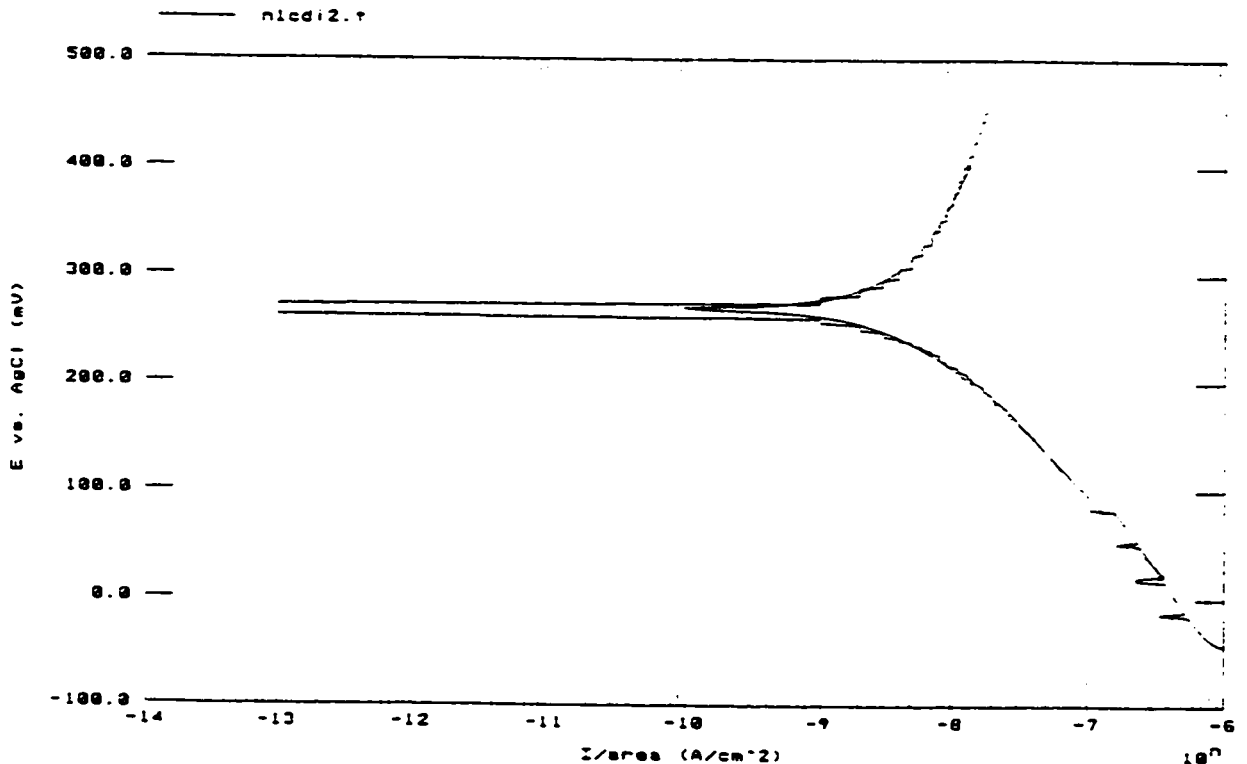
Icorr(R) = 3.391 nA/cm²
 Beta Cathodic = 100.0E-3 V/decade
 End = 316.0 mV

TAFEL CALCULATIONS:

Corrosion Rate = N.A.
 E(I=0) = 269.2 mV
 Beta Anodic = 307.4E-3
 Beta Cathodic = 132.3E-3 V/decade
 End = 402.0 mV

Chi^2 = 5.35E+000

Icorr = 5.095 nA/cm²
 Beta Cathodic = 132.3E-3 V/decade
 End = 402.0 mV



Model 352/252 Corrosion Analysis Software, v. 2.10

Filename: c:\m352\data\nicdi3.t

TA TAFEL
Date Run: UNKNOWNN

File Status: NORMAL
Time Run: UNKNOWNN

Cond. Time	CT	pass	s	Initial Pot.	IP	-250.0E-3	V oc
Cond. Pot.	CP	pass	V	Final Pot.	FP	250.0E-3	V oc
Initial Delay	ID	pass	s				
Scan Rate	SR	500.0E-3	mV/s	Curr. Range	CR	Auto	
Scan Incr.	SI	2.000	mV	Step Time	ST	4.000	s
No. of Points	NP	250					
Line Sync.	LS	no		GI Time Const.	TC	Off	
Rise Time	RT	high stability		IR Mode	IR	none	
Working Elec.	WE	Solid		Filter	FL	5.0Hz	
Sample Area	AR	1.000	cm ²	Ref. Elec.	RE	AgCl	197.0E-3V
Density	DE	0.0000	g/ml	Equiv. Wt.	EW	0.0000	g
Open Circuit	OC	166.0E-3	V	AUX A/D	AU	no	

Comment: 20% Nitrogenated Carbon, DI water, O2 saturated, Sample#3

R_p CALCULATIONS:

Corrosion Rate = N.A.
R_p = 7.311 MOHMS
E(I=0) = 294.3 mV
Beta Anodic = 100.0E-3
Beta Cathodic = 154.0 mV

Correlation = -942.0E-3

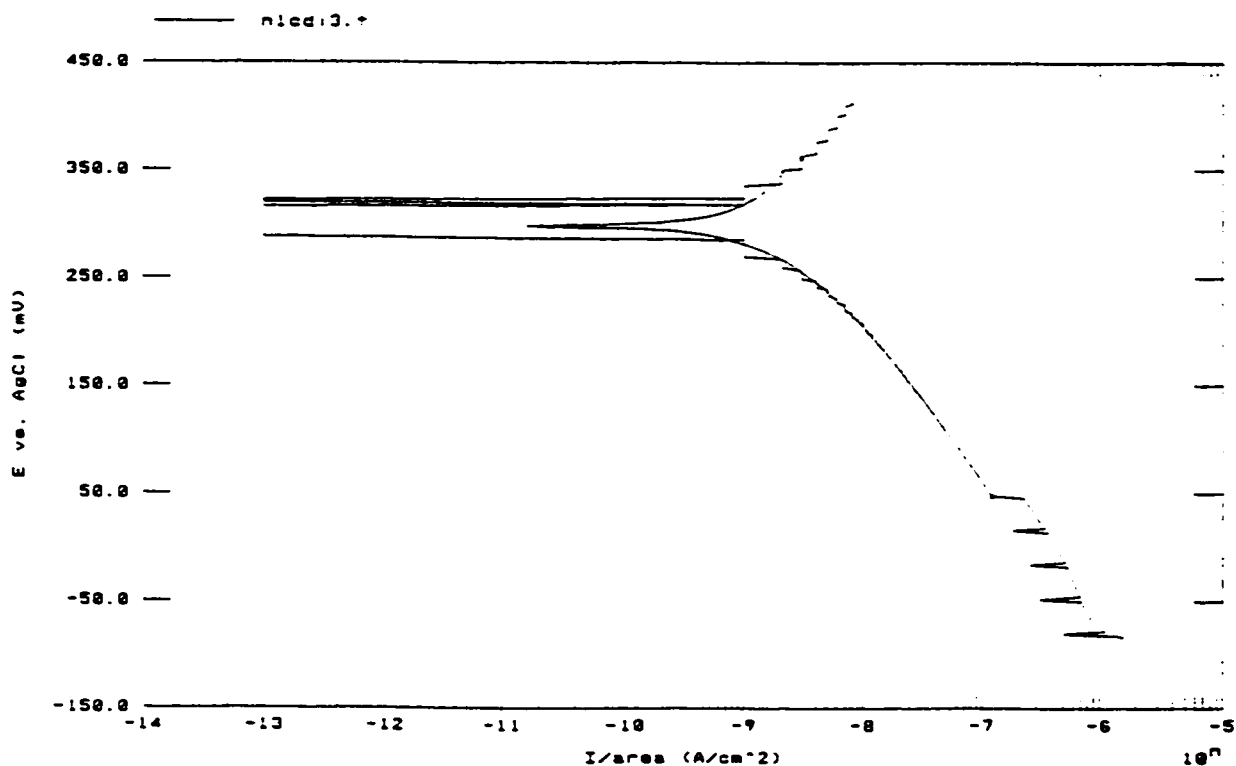
I_{corr}(R) = 2.970 nA/cm²
Beta Cathodic = 100.0E-3 V/decade
End = 346.0 mV

TAFEL CALCULATIONS:

Corrosion Rate = N.A.
E(I=0) = 298.3 mV
Beta Anodic = 991.0E-3
Beta Cathodic = 48.00 mV

Chi² = 1.14E-001

I_{corr} = 3.214 nA/cm²
Beta Cathodic = 157.8E-3 V/decade
End = 362.0 mV



Model 352/252 Corrosion Analysis Software, v. 2.10

Filename: c:\m352\data\n2dil.t

TA TAFEL

Date Run: UNKNOWNNN

File Status: NORMAL

Time Run: UNKNOWNNN

Cond. Time	CT	pass	s	Initial Pot.	IP	-250.0E-3	V oc
Cond. Pot.	CP	pass	V	Final Pot.	FP	250.0E-3	V oc
Initial Delay	ID	pass	s				
Scan Rate	SR	500.0E-3	mV/s	Curr. Range	CR	Auto	
Scan Incr.	SI	2.000	mV	Step Time	ST	4.000	s
No. of Points	NP	250					
Line Sync.	LS	no		GI Time Const.	TC	off	
Rise Time	RT	high stability		IR Mode	IR	none	
Working Elec.	WE	Solid		Filter	FL	15.3Hz	
Sample Area	AR	1.000	cm ²	Ref. Elec.	RE	AgCl	197.0E-3V
Density	DE	0.0000	g/ml	Equiv. Wt.	EW	0.0000	g
Open Circuit	OC	485.0E-3	V	AUX A/D	AU	no	

Comment: 30 x Nitrogen, DI water, 02 Saturated, Sample#1

RP CALCULATIONS:

Corrosion Rate = N.A.

Rp = 0.315 mOhms

E(I=0) = 586.3 mV

Beta Anodic = 100.0E-3

Begin = 529.0 mV

Correlation = -989.7E-3

Icorr(R) = 2.611 nA/cm²

Beta Cathodic = 100.0E-3 V/decade

End = 627.0 mV

TAFEL CALCULATIONS:

Corrosion Rate = N.A.

E(I=0) = 586.0 mV

Beta Anodic = 343.9E-3

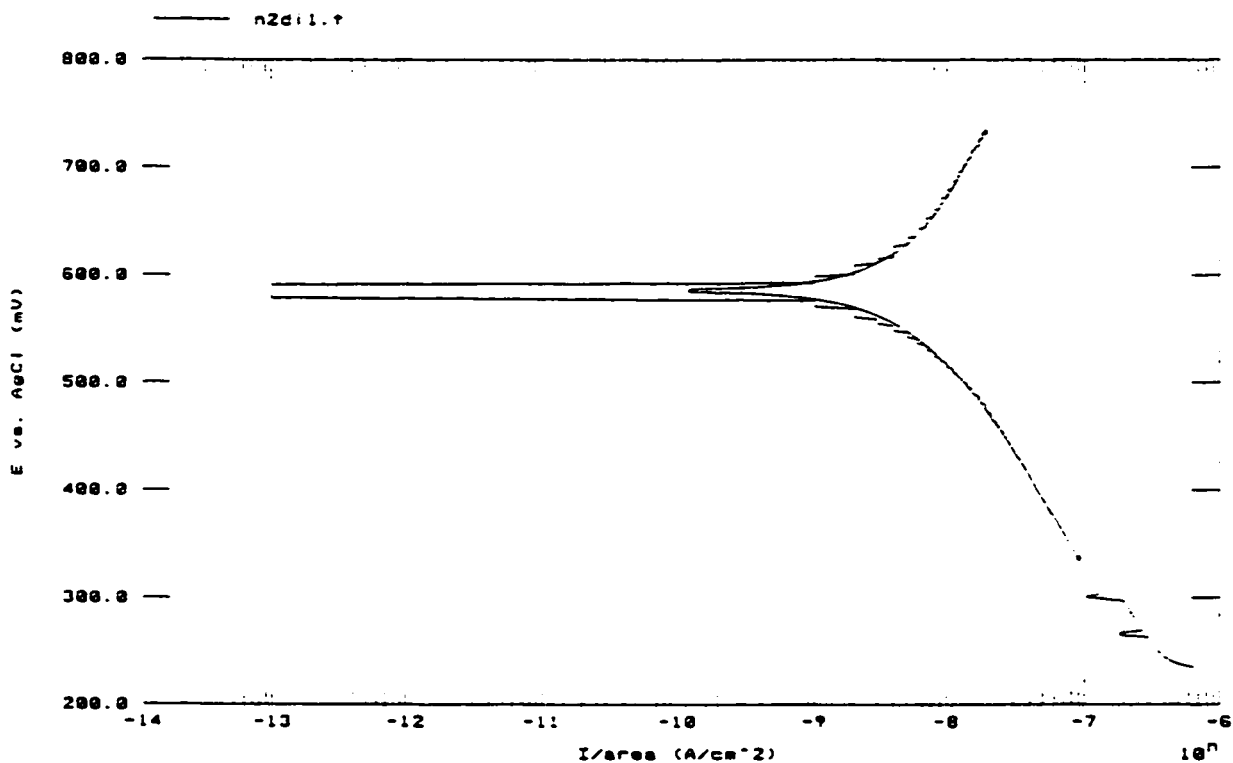
Begin = 337.0 mV

Chi² = 1.46E-001

Icorr = 7.274 nA/cm²

Beta Cathodic = 227.1E-3 V/decade

End = 733.0 mV



Model 352/252 Corrosion Analysis Software, v. 2.10

Filename: c:\m352\data\N2O12.T

TA TAFEL

Date Run: UNKNOWN

File Status: NORMAL

Time Run: UNKNOWN

Cond. Time	CT	pass	s	Initial Pot.	IP	-250.0E-3	V oc
Cond. Pot.	CP	pass	V	Final Pot.	FP	250.0E-3	V oc
Initial Delay	ID	pass	s				
Scan Rate	SR	500.0E-3	mV/s	Curr. Range	CR	Auto	
Scan Incr.	SI	2.000	mV	Step Time	ST	4.000	s
No. of Points	NP	250					
Line Sync.	LS	no		GI Time Const.	TC	Off	
Rise Time	RT	high stability		IR Mode	IR	none	
Working Elec.	WE	Solid		Filter	FL	I 5.3Hz	
Sample Area	AR	1.000	cm ²	Ref. Elec.	RE	AgCl	197.0E-3V
Density	DE	0.0000	g/ml	Equiv. Wt.	EW	0.0000	g
Open Circuit	OC	499.0E-3	V	AUX A/D	AU	no	

Comment: 30% Nitrogenated Carbon, DI water, O2 Saturated, Sample#2

R_p CALCULATIONS:

Corrosion Rate = N.A.

R_p = 8.421 MOHMS

E(I=0) = 562.0 mV

Beta Anodic = 100.0E-3

Begin = 545.0 mV

Correlation = -994.4E-3

I_{corr}(R) = 2.579 nA/cm²

Beta Cathodic = 100.0E-3 V/decade

End = 639.0 mV

TAFEL CALCULATIONS:

Corrosion Rate = N.A.

E(I=0) = 563.3 mV

Beta Anodic = 556.0E-3

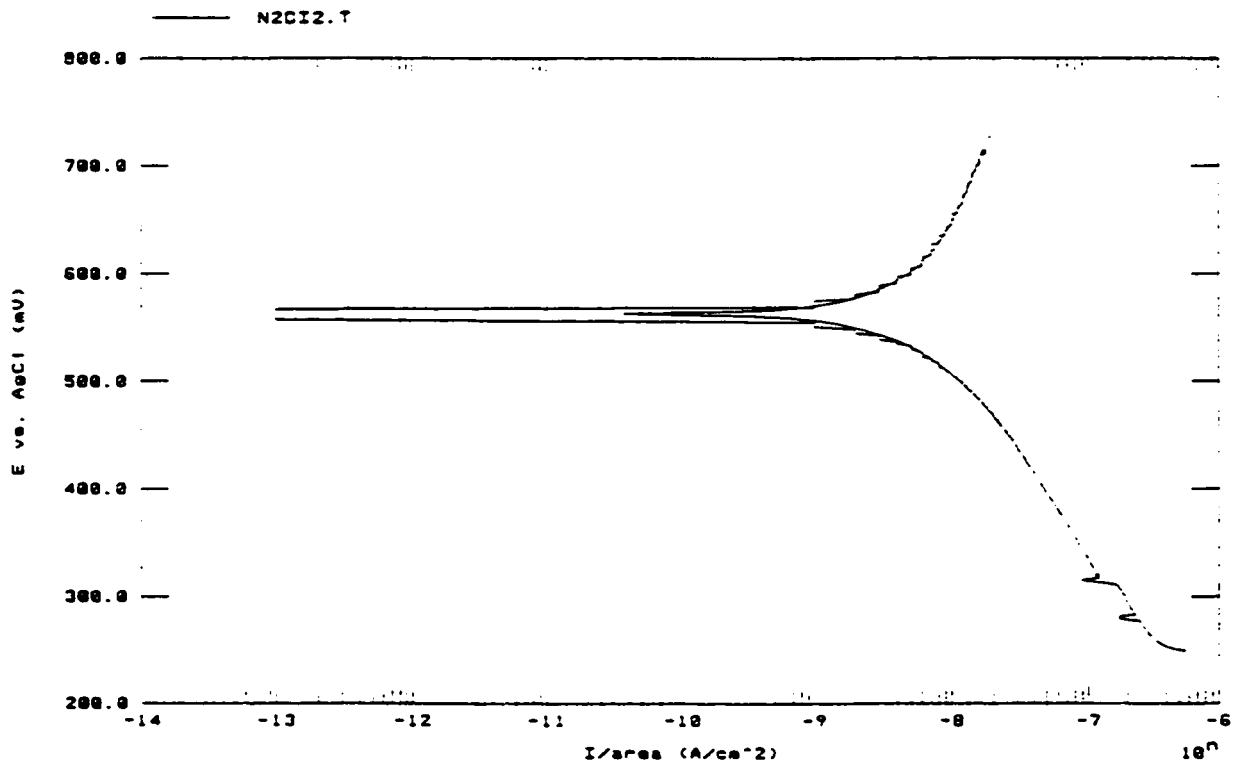
Begin = 319.0 mV

Chi² = 7.86E-002

I_{corr} = 9.983 nA/cm²

Beta Cathodic = 225.3E-3 V/decade

End = 713.0 mV



Model 352/252 Corrosion Analysis Software, v. 2.10

Filename: c:\m352\data\N2CDI3.T

TA TAFEL

Date Run: UNKNOWN

File Status: NORMAL

Time Run: UNKNOWN

Cond. Time	CT	pass	s	Initial Pot.	IP	-250.0E-3	V oc
Cond. Pot.	CP	pass	V	Final Pot.	FP	250.0E-3	V oc
Initial Delay	ID	pass	s				
Scan Rate	SR	500.0E-3	mV/s	Curr. Range	CR	Auto	
Scan Incr.	SI	2.000	mV	Step Time	ST	4.000	s
No. of Points	NP	250					
Line Sync.	LS	no		GI Time Const.	TC	off	
Rise Time	RT	high stability		IR Mode	IR	none	
Working Elec.	WE	Solid		Filter	FL	15.3Hz	
Sample Area	AR	1.000	cm ²	Ref. Elec.	RE	AgCl	197.0E-3V
Density	DE	0.0000	g/ml	Equiv. Wt.	EW	0.0000	g
Open Circuit	OC	499.0E-3	V	AUX A/D	AU	no	

Comment: 30% Nitrogenated Carbon, DI water, O2 saturated, Sample03

RA CALCULATIONS:

Corrosion Rate = N.A.

Rp = 7.981 mOhms

E(I=0) = 563.7 mV

Beta Anodic = 100.0E-3

Begin = 533.0 mV

Correlation = -992.9E-3

Icorr(R) = 2.755 nA/cm²

Beta Cathodic = 100.0E-3 V/decade

End = 627.0 mV

TAFEL CALCULATIONS:

Corrosion Rate = N.A.

E(I=0) = 564.0 mV

Beta Anodic = 489.6E-3

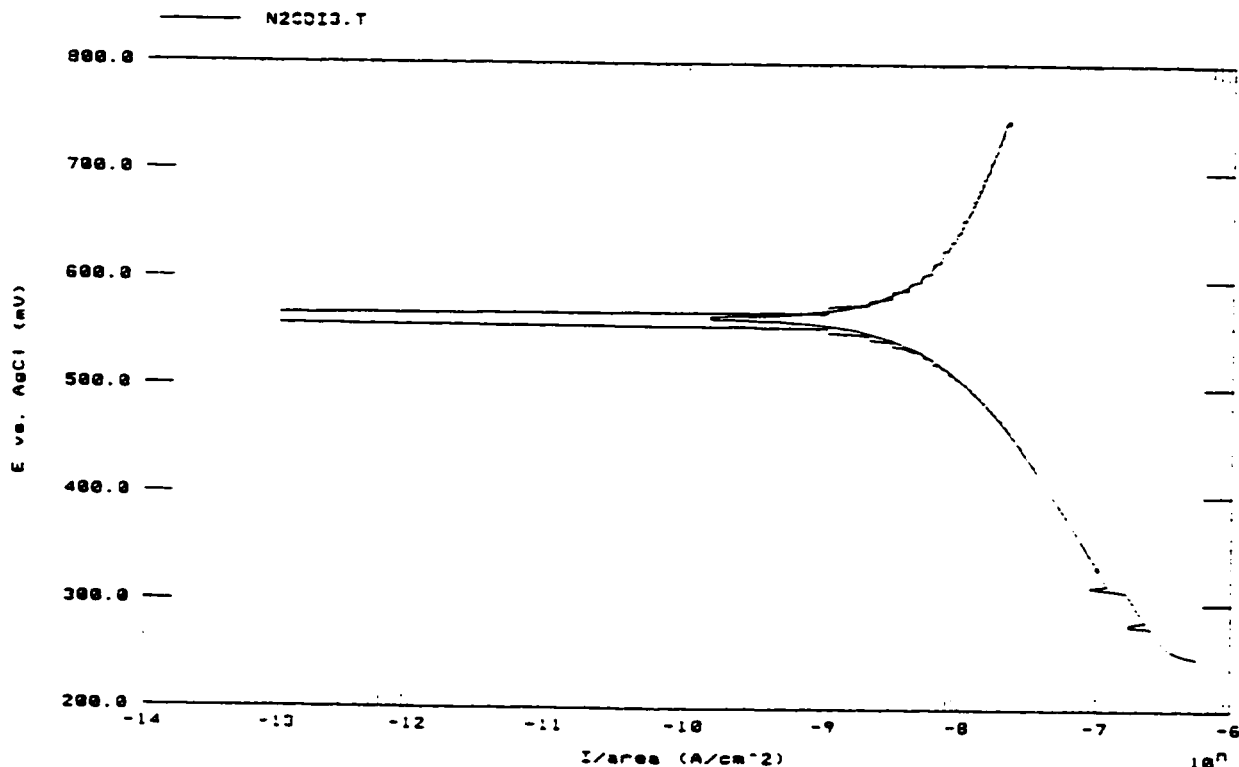
Begin = 333.0 mV

Chi² = 9.68E-002

Icorr = 9.390 nA/cm²

Beta Cathodic = 220.3E-3 V/decade

End = 747.0 mV



Model 352/252 Corrosion Analysis Software, v. 2.10

Filename: c:\a352\data\0CHCL1.t

TA TAFEL

Date Run: UNKNOWNNN

File Status: NORMAL

Time Run: UNKNOWNNN

Cond. Time	CT	pass	s	Initial Pot.	IP	-250.0E-3	V oc
Cond. Pot.	CP	pass	V	Final Pot.	FP	250.0E-3	V oc
Initial Delay	ID	pass	s				
Scan Rate	SR	500.0E-3	mV/s	Curr. Range	CR	Auto	
Scan Incr.	SI	2.000	mV	Step Time	ST	4.000	s
No. of Points	NP	250					
Line Sync.	LS	no		SI Time Const.	TC	off	
Rise Time	RT	high stability		IR Mode	IR	none	
Working Elec.	WE	Solid		Filter	FL	< 5.0Hz	
Sample Area	AR	1.000	cm ²	Ref. Elec.	RE	AgCl 197.0E-3V	
Density	DE	0.0000	g/ml	Equip. Mt.	EW	0.0000	g
Open Circuit	OC	253.0E-3	V	AUX A/D	AU	no	

Comment: No Carbon. 7.5 ppm HCl. O2 Saturated. Sample #1

Re CALCULATIONS:

Corrosion Rate = N.A.

Rp = 15.84 KOHms

E(I=0) = 294.6 mV

Beta Anodic = 100.0E-3

Begin = 285.0 mV

Correlation = -998.1E-3

Icorr(R) = 1.371 uA/cm²

Beta Cathodic = 100.0E-3 V/decade

End = 309.0 mV

TAFEL CALCULATIONS:

Corrosion Rate = N.A.

E(I=0) = 294.6 mV

Beta Anodic = 369.7E-3

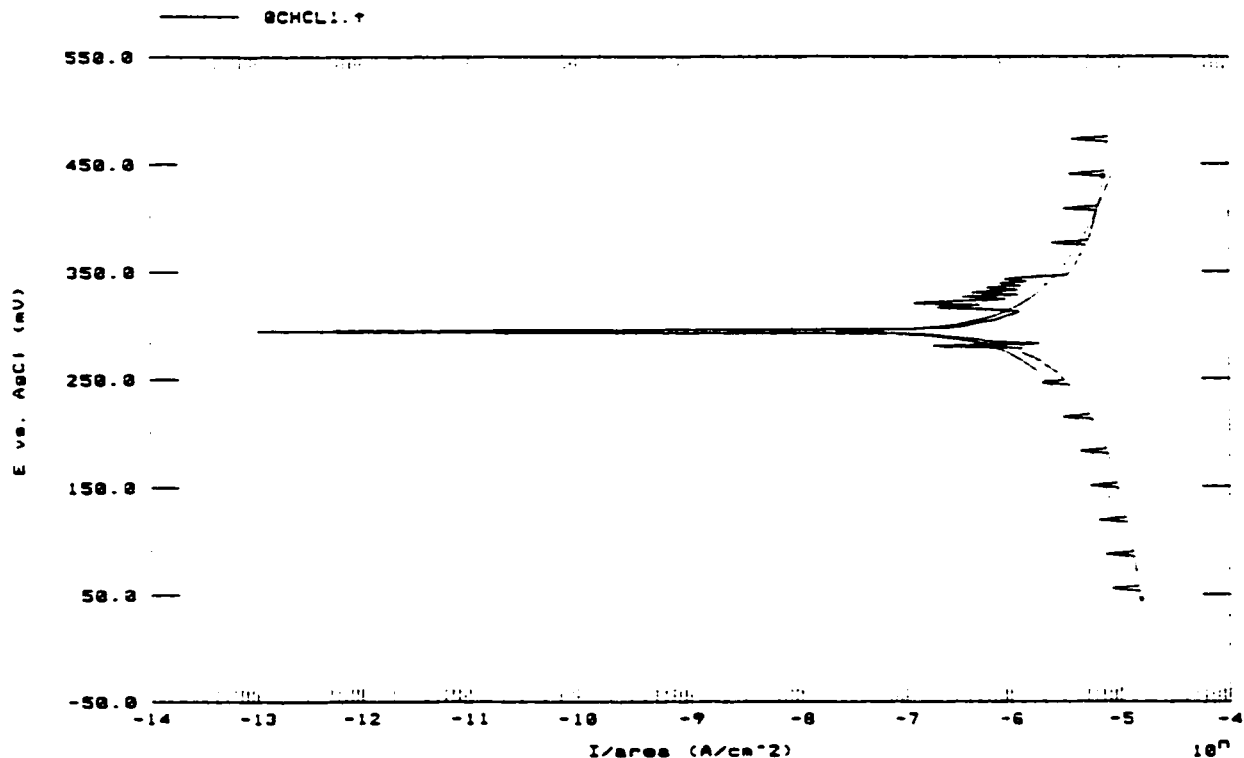
Begin = 45.00 mV

Chi² = 1.50E+003

Icorr = 4.132 uA/cm²

Beta Cathodic = 434.6E-3 V/decade

End = 439.0 mV



Model 352/252 Corrosion Analysis Software, v. 2.10

Filename: c:\a352\data\nochc12.t

TA TAFEL

Date Run: UNKNOWNN

File Status: NORMAL

Time Run: UNKNOWNN

Cond. Time	CT	pass	s	Initial Pot.	IP	-250.0E-3	V oc
Cond. Pot.	CP	pass	U	Final Pot.	FP	250.0E-3	V oc
Initial Delay	CD	pass	s				
Scan Rate	SR	500.0E-3	mV/s	Curr. Range	CR	Auto	
Scan Incr.	SI	2.000	mV	Step Time	ST	4.000	s
No. of Points	NP	250					
Line Sync.	LS	no		GI Time Const.	TC	off	
Rise Time	RT	high stability		IR Mode	IR	none	
Working Elec.	WE	Solid		Filter	FL	I 5.0Hz	
Sample Area	AR	1.000	cm ²	Ref. Elec.	RE	AgCl	197.0E-3V
Density	DE	0.0000	g/cm ³	Equiv. Wt.	EW	0.0000	g
Open Circuit	OC	482.0E-3	V	AUX A/D	AU	no	

Comment: No Carbon. 7.5 ppmv HCl. O2 saturated. Sample2

Rp CALCULATIONS:

Corrosion Rate = N.A.

Rp = 28.54 kOhms

E(I=0) = 503.6 mV

Beta Anodic = 307.8E-3

Begin = 476.0 mV

Correlation = -885.0E-3

Icorr(R) = 3.592 uA/cm²

Beta Cathodic = 1.013 V/decade

End = 518.0 mV

TAFEL CALCULATIONS:

Corrosion Rate = N.A.

E(I=0) = 503.8 mV

Beta Anodic = 307.8E-3

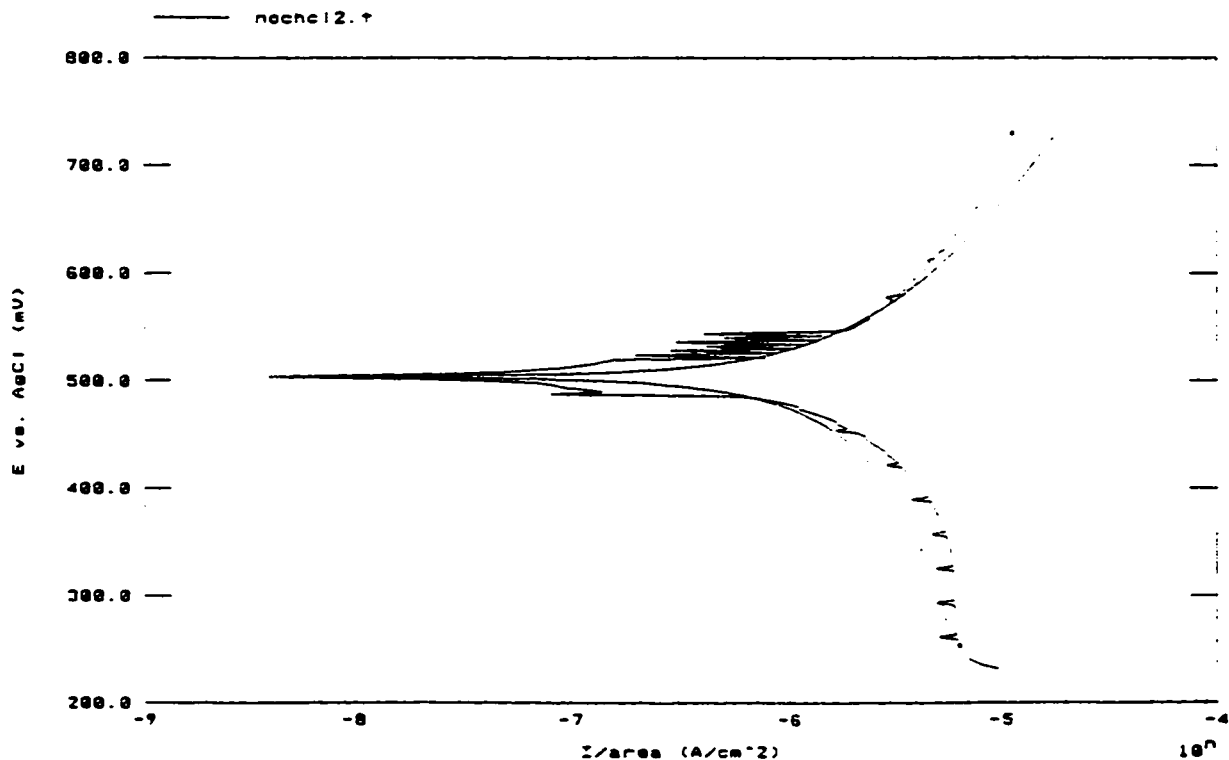
Begin = 254.0 mV

Chi² = 9.96E+002

Icorr = 3.721 uA/cm²

Beta Cathodic = 1.013 V/decade

End = 730.0 mV



Model 352/252 Corrosion Analysis Software, v. 2.10

Filename: c:\352\data\NoCHCL3.†

TA TAFEL

Date Run: UNKNOWN

File Status: NORMAL

Time Run: UNKNOWN

Cond. Time	CT	pass	s	Initial Pot.	IP	-250.0E-3	V oc
Cond. Pot.	CP	pass	s	Final Pot.	FP	250.0E-3	V oc
Initial Delay	ID	pass					
Scan Rate	SR	500.0E-3	mV/s	Curr. Range	CR	Auto	
Scan Incr.	SI	2.000	mV	Step Time	ST	4.000	s
No. of Points	NP	250					
Line Sync.	LS	no		GI Time Const.	TC	Off	
Rise Time	RT	high stability		IR Mode	IR	none	
Working Elec.	WE	Solid		Filter	FL	15.0Hz	
Sample Area	AR	1.000	cm ²	Ref. Elec.	RE	AgCl	197.0E-3V
Density	DE	0.0000	g/ml	Equiv. Wt.	EW	0.0000	g
Open Circuit	OC	254.0E-3	V	AUX A/D	AU	no	

Comment: No Carbon. 7.5 ppm HCl. O2 saturated. Sample #3

Rp CALCULATIONS:

Corrosion Rate = N.A.

Rp = 22.36 KOHms

E(I=0) = 278.6 mV

Beta Anodic = 100.0E-3

Begin = 254.0 mV

Correlation = -909.8E-3

Icorr(R) = 971.3 nA/cm²

Beta Cathodic = 100.0E-3 V/decade

End = 294.0 mV

TAFEL CALCULATIONS:

Corrosion Rate = N.A.

E(I=0) = 273.3 mV

Beta Anodic = 1.328E27

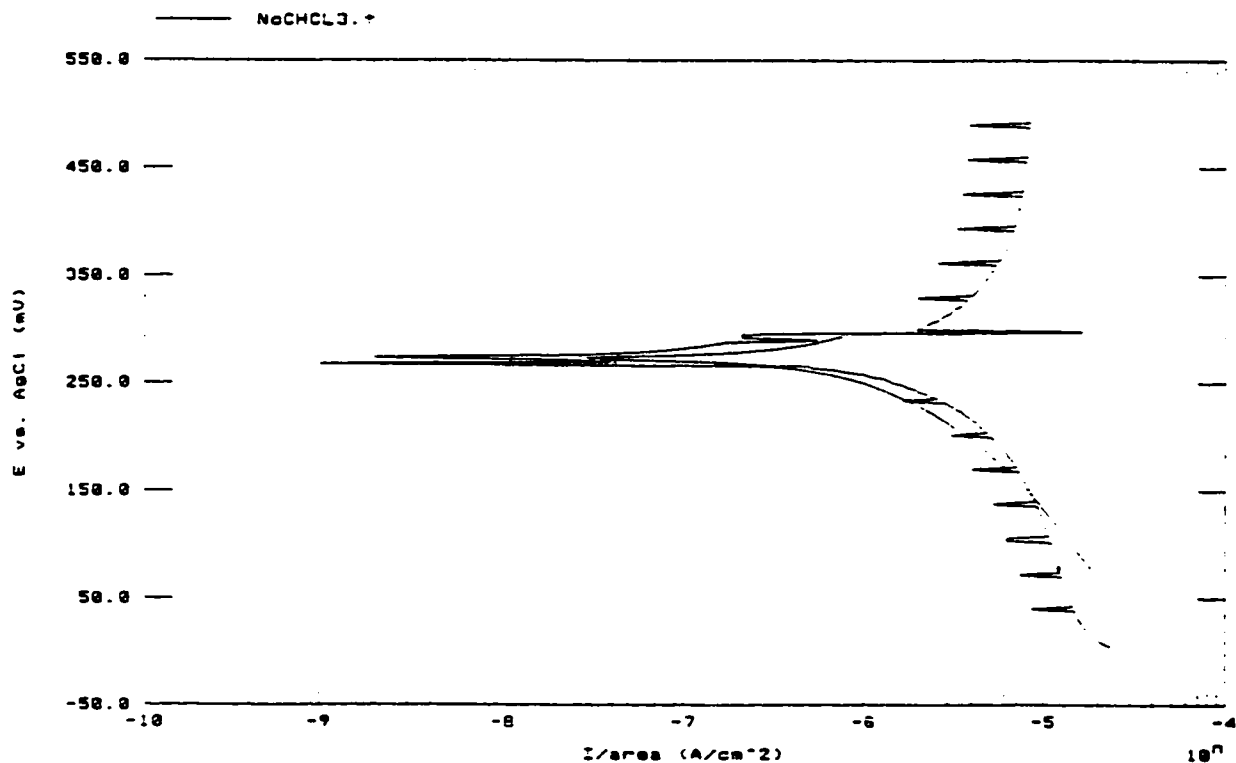
Begin = 78.00 mV

Chi² = 1.20E+003

Icorr = 4.934 uA/cm²

Beta Cathodic = 292.4E-3 V/decade

End = 294.0 mV



Model 352/252 Corrosion Analysis Software, v. 2.10

Filename: c:\m352\data\ACHCL1.t

TA TAFEL

Date Run: UNKNOWN

File Status: NORMAL

Time Run: UNKNOWN

Cond. Time	CT	pass	s	Initial Pot.	IP	300.0E-3	V
Cond. Pot.	CP	pass	V	Final Pot.	FP	900.0E-3	V
Initial Delay	ID	pass	s				
Scan Rate	SR	500.0E-3	mV/s	Curr. Range	CR	Auto	
Scan Incr.	SI	2.000	mV	Step Time	ST	4.000	s
No. of Points	NP	300					
Line Sync.	LS	no		GI Time Const.	TC	off	
Rise Time	RT	high stability		IR Mode	IR	none	
Working Elec.	WE	Solid		Filter	FL	5.0Hz	
Sample Area	AR	1.000	cm ²	Ref. Elec.	RE	AgCl	197.0E-3V
Density	DE	0.0000	g/ml	Equiv. Wt.	EW	0.0000	g
Open Circuit	OC	476.0E-3	V	AUX A/D	AU	no	

Comment: Arsen Carbon, 7.5 ppm HCl, O2 Saturated, Sample 1

Re CALCULATIONS:

Corrosion Rate = N.A.

Rp = 2.928 MOHms

E(I=0) = 718.0 mV

Beta Anodic = 100.0E-3

Begin = 658.0 mV

Correlation = -974.2E-3

Icorr(R) = 7.417 nA/cm²

Beta Cathodic = 100.0E-3 V/decade

End = 754.0 mV

TAFEL CALCULATIONS:

Corrosion Rate = N.A.

E(I=0) = 723.6 mV

Beta Anodic = 121.4E-3

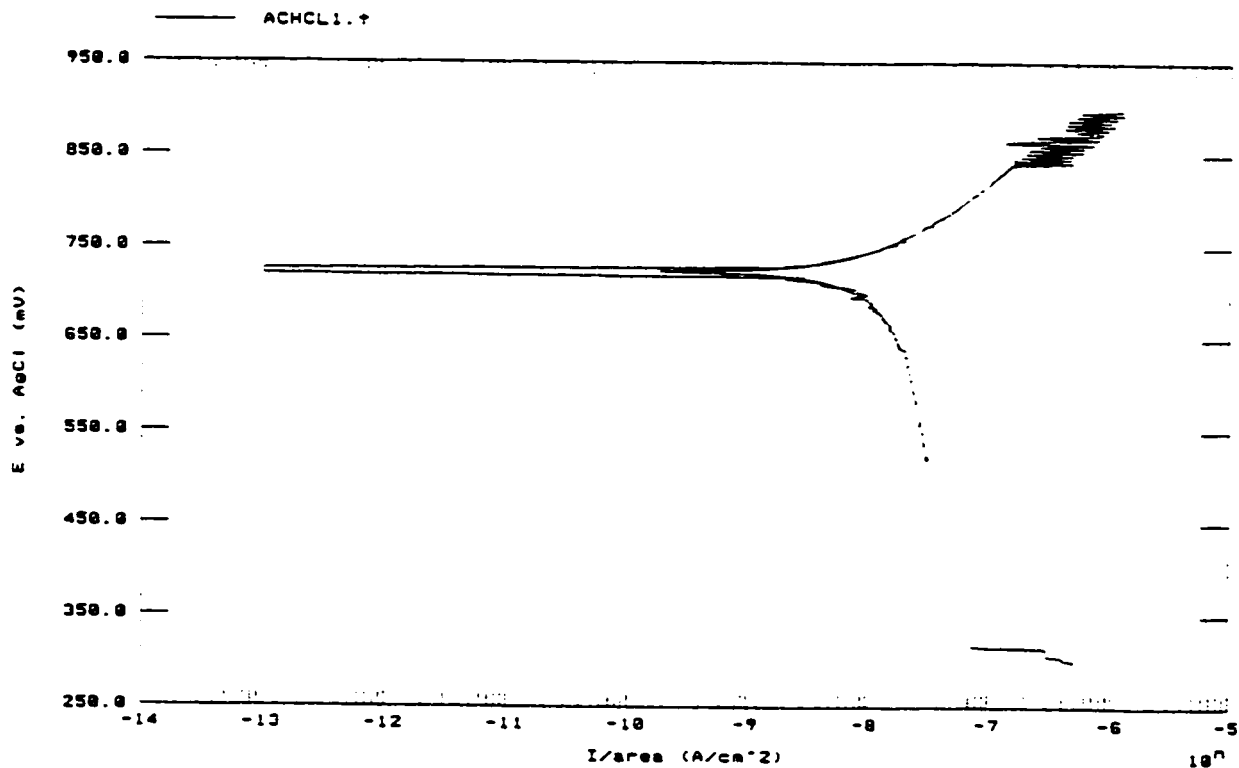
Begin = 522.0 mV

Chi² = 5.76E+000

Icorr = 18.73 nA/cm²

Beta Cathodic = 901.3E-3 V/decade

End = 844.0 mV



Model 352/252 Corrosion Analysis Software, v. 2.10

Filename: c:\a352\data\ACHCL2.†

TA TAFEL

Date Run: UNKNOWN

File Status: NORMAL

Time Run: UNKNOWN

Cond. Time	CT	pass	s	Initial Pot.	IP	300.0E-3	V
Cond. Pot.	CP	pass	U	Final Pot.	FP	850.0E-3	V
Initial Delay	CD	pass	s				
Scan Rate	SR	500.0E-3	mV/s	Curr. Range	CR	Auto	
Scan Incr.	SI	2.000	mV	Step Time	ST	4.000	s
No. of Points	NP	275					
Line Sync.	LS	no		GI Time Const.	TC	Off	
Rise Time	RT	high stability		IR Mode	IR	none	
Working Elec.	WE	Solid		Filter	FL	I 5.3Hz	
Sample Area	AR	1.000	cm ²	Ref. Elec.	RE	AgCl	197.0E-3V
Density	DE	0.0000	g/ml	Equiv. Wt.	EW	0.0000	g
Open Circuit	OC	495.0E-3	V	AUX A/D	AU	no	

Comment: Argon Carbon, 7.5 ppmu HCl, O2 Saturated, Sample #2

Re CALCULATIONS:

Corrosion Rate = N.A.

R_s = 2.803 MOhms

E(I=0) = 789.4 mV

Beta Anodic = 100.0E-3

Begin = 674.0 mV

Correlation = -951.3E-3

I_{corr}(R) = 7.748 nA/cm²

Beta Cathodic = 100.0E-3 V/decade

End = 740.0 mV

TAFEL CALCULATIONS:

Corrosion Rate = N.A.

E(I=0) = 712.7 mV

Beta Anodic = 110.6E-3

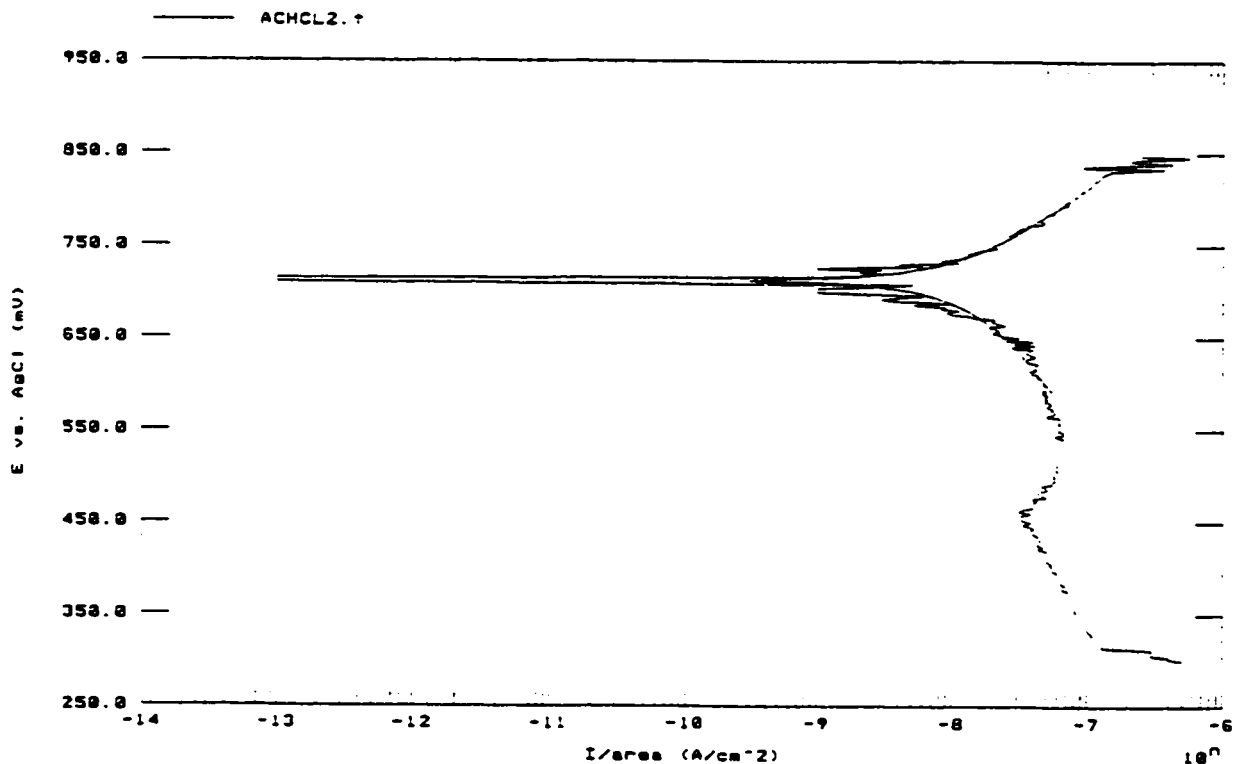
Begin = 592.0 mV

Chi² = 5.83E+000

I_{corr} = 12.80 nA/cm²

Beta Cathodic = 180.2E-3 V/decade

End = 796.0 mV



Model 352/252 Corrosion Analysis Software, v. 2.10

Filename: c:\m352\data\schc13.t

TA TAFEL

Date Run: UNKNOWN

File Status: NORMAL

Time Run: UNKNOWN

Cond. Time	CT	pass	s	Initial Pot.	IP	-150.0E-3	V oc
Cond. Pot.	CP	pass	V	Final Pot.	FP	300.0E-3	V oc
Initial Delay	ID	pass	s				
Scan Rate	SR	500.0E-3	mV/s	Curr. Range	CR	Auto	
Scan Incr.	SI	2.000	mV	Step Time	ST	4.000	s
No. of Points	NP	225					
Line Sync.	LS	no		GI Time Const.	TC	Off	
Rise Time	RT	high stability		IR Mode	IR	none	
Working Elec.	WE	Solid		Filter	FL	1 3.3Hz	
Sample Area	AR	1.000	cm ²	Ref. Elec.	RE	AgCl	197.0E-3V
Density	DE	0.0000	g/ml	Equiv. Wt.	EW	0.0000	g
Open Circuit	OC	507.0E-3	V	AUX A/D	AU	no	

R_p CALCULATIONS:

Corrosion Rate = N.A.

R_p = 5.474 MOHMS

E(I=0) = 716.0 mV

Beta Anodic = 130.1E-3

Begin = 675.0 mV

Correlation = -989.6E-3

I_{corr}(R) = 7.960 nA/cm²

Beta Cathodic = 438.4E-3 V/decade

End = 749.0 mV

TAFEL CALCULATIONS:

Corrosion Rate = N.A.

E(I=0) = 718.9 mV

Beta Anodic = 130.1E-3

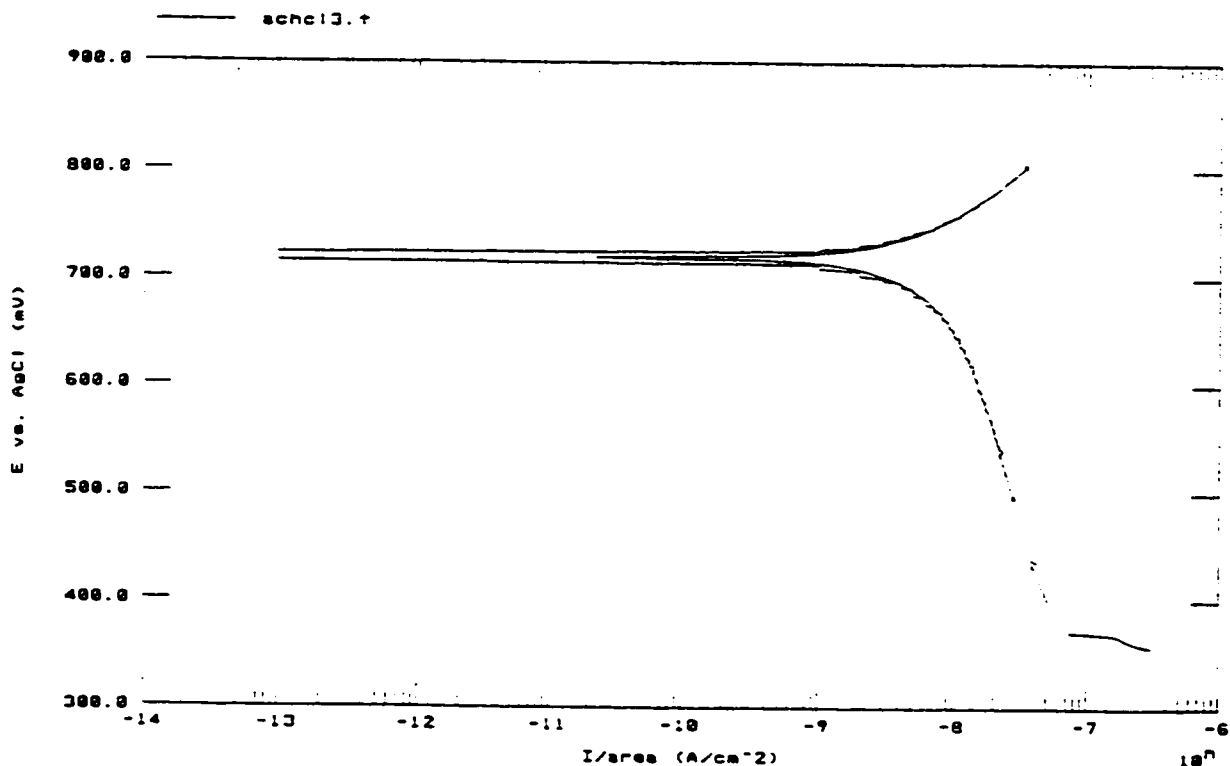
Begin = 497.0 mV

Chi² = 1.05E-001

I_{corr} = 8.700 nA/cm²

Beta Cathodic = 438.4E-3 V/decade

End = 885.0 mV



Model 352/252 Corrosion Analysis Software, v. 2.10

Filename: C:\m352\data\MCHCL1.†

TA TAFEL

Date Run: UNKNOWN

File Status: NORMAL

Time Run: UNKNOWN

Cond. Time	CT	pass	s	Initial Pot.	IP	500.0E-3	V
Cond. Pot.	CP	pass	V	Final Pot.	FP	1.000	V
Initial Delay	ID	pass	s				
Scan Rate	SR	500.0E-3	mV/s	Curr. Range	CR	Auto	
Scan Incr.	SI	2.000	mV	Step Time	ST	4.000	s
No. of Points	NP	250					
Line Sync.	LS	no		GI Time Const.	TC	Off	
Rise Time	RT	high stability		IR Mode	IR	none	
Working Elec.	WE	Solid		Filter	FL	5.3Hz	
Sample Area	AR	1.000	cm ²	Ref. Elec.	RE	AgCl	197.0E-3V
Density	DE	0.0000	g/ml	Equiv. Wt.	EW	0.0000	g
Open Circuit	OC	467.0E-3	V	AUX A/D	AU	no	

Comment: Hydrogenated Carbon, 7.5 ppm HCl, O2 saturated, Sample#1

Re CALCULATIONS:

Corrosion Rate = N.A.

Rp = 1.679 MOHms

E(I=0) = 833.9 mV

Beta Anodic = 100.0E-3

Begin = 794.0 mV

Correlation = -982.0E-3

Icorr(R) = 12.74 nA/cm²

Beta Cathodic = 100.0E-3 V/decade

End = 882.0 mV

TAFEL CALCULATIONS:

Corrosion Rate = N.A.

E(I=0) = 839.3 mV

Beta Anodic = 140.5E-3

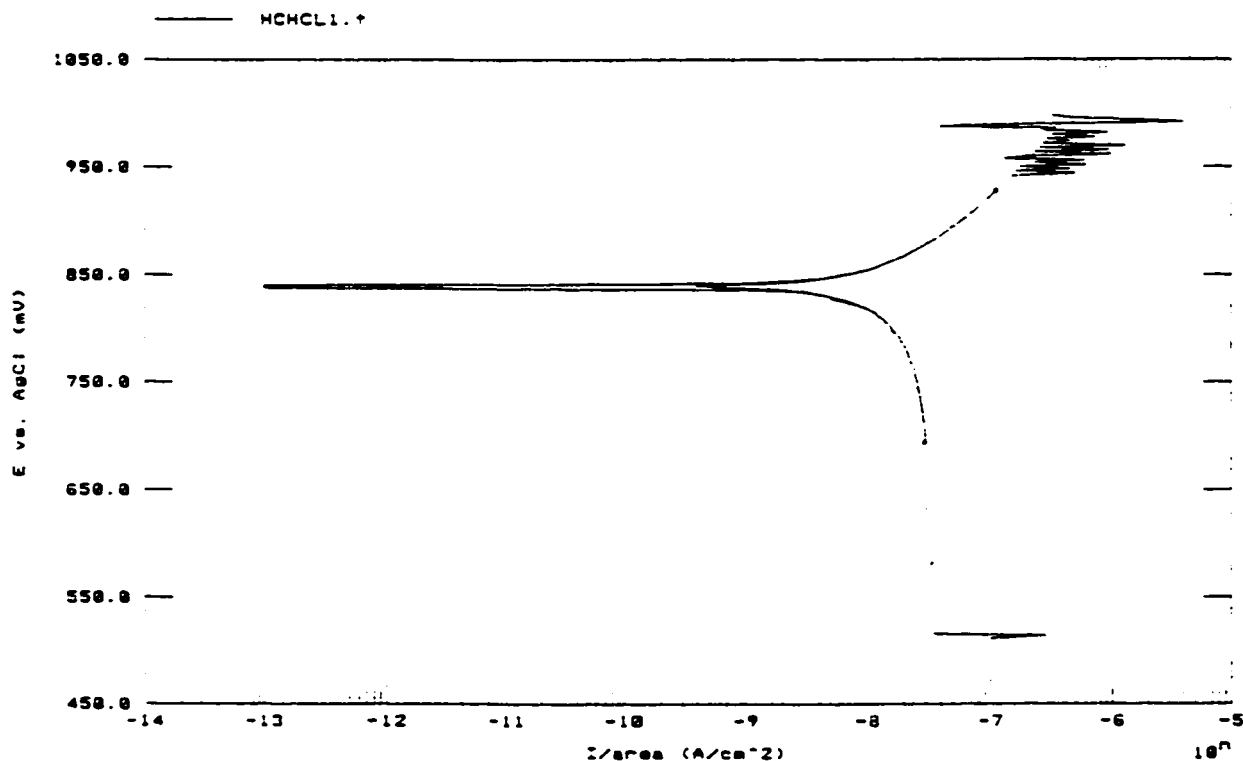
Begin = 694.0 mV

Chi² = 1.34E-001

Icorr = 34.32 nA/cm²

Beta Cathodic = 98.62E6 V/decade

End = 928.0 mV



Model 352/252 Corrosion Analysis Software, v. 2.10

Filename: c:\m352\data\HCHCL2.t

TA TAFEL

Date Run: UNKNOWN

File Status: NORMAL

Time Run: UNKNOWN

Cond. Time	CT	pass	s	Initial Pot.	IP	400.0E-3	V
Cond. Pot.	CP	pass	U	Final Pot.	FP	950.0E-3	V
Initial Delay	ID	pass	s				
Scan Rate	SR	500.0E-3	mV/s	Curr. Range	CR	Auto	
Scan Incr.	SI	2.000	mV	Step Time	ST	4.000	s
No. of Points	NP	275					
Line Sync.	LS	no		GI Time Const.	TC	Off	
Rise Time	RT	high stability		IR Mode	IR	none	
Working Elec.	WE	Solid		Filter	FL	5.3Hz	
Sample Area	AR	1.000	cm ²	Ref. Elec.	RE	AgCl 197.0E-3V	
Density	DE	0.0000	g/ml	Equip. Wt.	EW	0.0000	g
Open Circuit	OC	421.0E-3	V	AUX A/D	AU	no	

Comment: Hydrogenated Carbon, 7.5 ppm HCl, O2 Saturated, Sample #2

R_p CALCULATIONS:

Corrosion Rate = N.A.

R_p = 1.368 MOHMS

E(I=0) = 756.9 mV

Beta Anodic = 100.0E-3

Beta Cathodic = 714.0 mV

Correlation = -970.0E-3

I_{corr}(R) = 15.88 nA/cm²

Beta Cathodic = 100.0E-3 V/decade

End = 814.0 mV

TAFEL CALCULATIONS:

Corrosion Rate = N.A.

E(I=0) = 754.3 mV

Beta Anodic = 116.5E-3

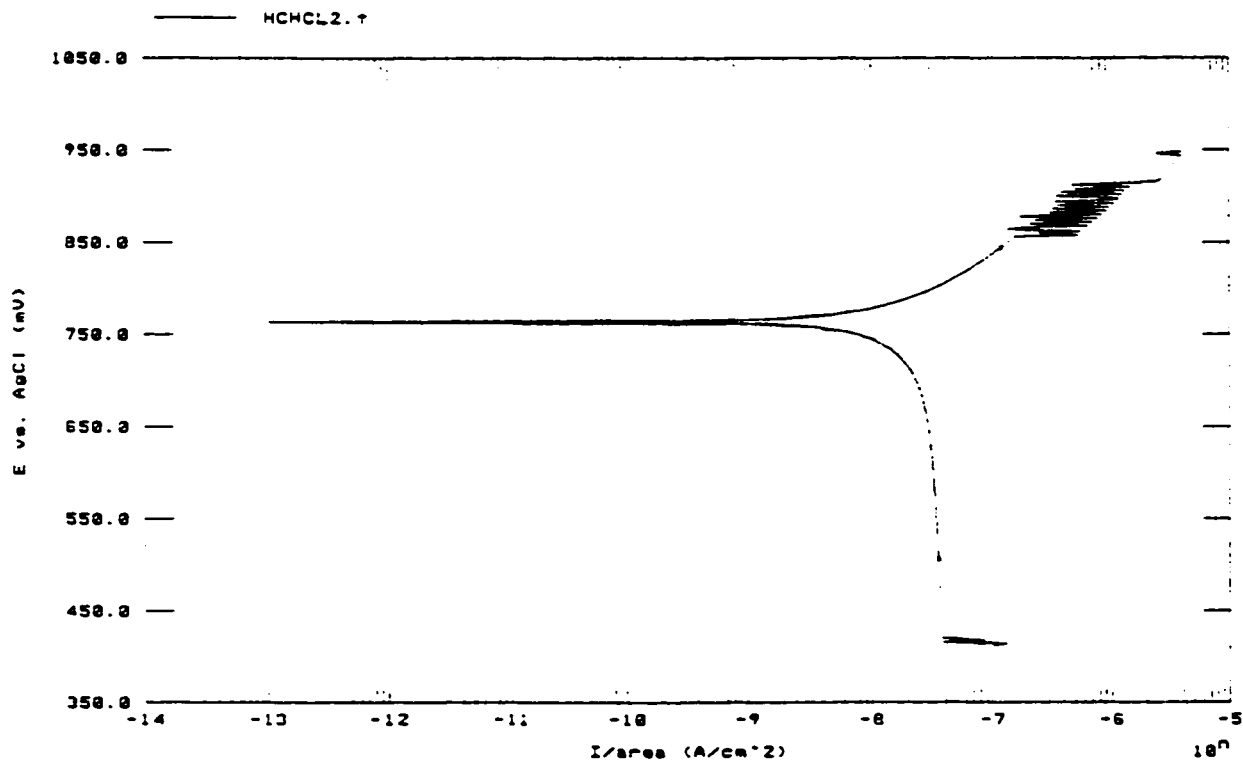
Beta Cathodic = 506.0 mV

Chi² = 6.99E-002

I_{corr} = 30.68 nA/cm²

Beta Cathodic = 4.995 V/decade

End = 844.0 mV



Model 352/252 Corrosion Analysis Software, v. 2.10

Filename: c:\352\data\MCHCL3.†

TA TAFEL

Date Run: UNKNOWN

File Status: NORMAL

Time Run: UNKNOWN

Cond. Time	CT	pass	s	Initial Pot.	IP	480.0E-3	V
Cond. Pot.	CP	pass	V	Final Pot.	FP	950.0E-3	V
Initial Delay	ID	pass	s				
Scan Rate	SR	500.0E-3	mV/s	Curr. Range	CR	Auto	
Scan Incr.	SI	2.000	mV	Step Time	ST	4.000	s
No. of Points	NP	275					
Line Sync.	LS	no		GI Time Const.	TC	Off	
Rise Time	RT	high stability		IR Mode	IR	none	
Working Elec.	WE	Solid		Filter	FL	I 5.3Hz	
Sample Area	AR	1.000	cm ²	Ref. Elec.	RE	AgCl 197.0E-3V	
Density	DE	0.0000	g/ml	Equiv. Wt.	EW	0.0000	g
Open Circuit	OC	437.0E-3	V	AUX A/D	AU	no	

Comment: Hydrogenated Carbon, 7.5 ppm HCl, O2 saturated, Sampled3

R_p CALCULATIONS:

Corrosion Rate = N.A.

R_p = 1.519 MOhm

E(I=0) = 819.2 mV

Beta Anodic = 100.0E-3

Begin = 774.0 mV

Correlation = -976.7E-3

I_{corr}(R) = 14.29 nA/cm²

Beta Cathodic = 100.0E-3 V/decade

End = 866.0 mV

TAFEL CALCULATIONS:

Corrosion Rate = N.A.

E(I=0) = 826.2 mV

Beta Anodic = 113.4E-3

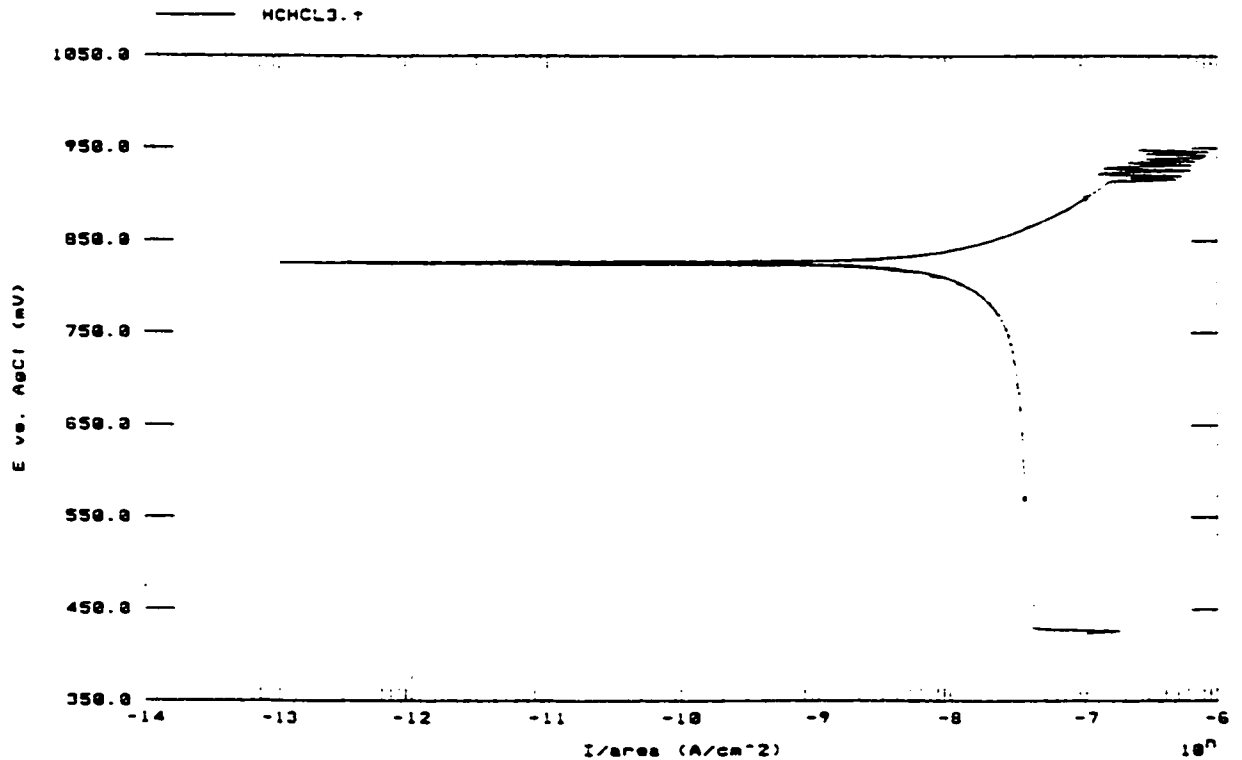
Begin = 570.0 mV

Chi² = 1.09E-001

I_{corr} = 31.60 nA/cm²

Beta Cathodic = 5.335 V/decade

End = 896.0 mV



Model 352/252 Corrosion Analysis Software, v. 2.18

Filename: c:\a352\data\nihcl1.t

TA TAFEL

Date Run: UNKNOWNNN

File Status: NORMAL

Time Run: UNKNOWNNN

Cond. Time	CT	pass	s	Initial Pot.	IP	500.0E-3	V
Cond. Pot.	CP	pass	V	Final Pot.	FP	1.000	V
Initial Delay	ID	pass	s				
Scan Rate	SR	500.0E-3	mV/s	Curr. Range	CR	Auto	
Scan Incr.	SI	2.000	mV	Step Time	ST	4.000	s
No. of Points	NP	250					
Line Sync.	LS	no		GI Time Const.	TC	Off	
Rise Time	RT	high stability		IR Mode	IR	none	
Working Elec.	WE	Solid		Filter	FL	15.3Hz	
Sample Area	AR	1.000	cm ²	Ref. Elec.	RE	AgCl	197.0E-3V
Density	DE	0.0000	g/ml	Equiv. Wt.	EW	0.0000	
Open Circuit	OC	447.0E-3	V	AUX A/D	AU	no	

Comment: 20x Nitrogenated Carbon, 7.5 ppm HCl, O2 Saturated, Sampled

RP CALCULATIONS:

Corrosion Rate = N.A.

Rp = 3.628 MOHMS

E(I=0) = 701.9 mV

Beta Anodic = 123.7E-3

Begin = 548.0 mV

Correlation = -940.3E-3

Icorr(R) = 13.66 nA/cm²

Beta Cathodic = 1.465 V/decade

End = 748.0 mV

TAFEL CALCULATIONS:

Corrosion Rate = N.A.

E(I=0) = 711.8 mV

Beta Anodic = 123.7E-3

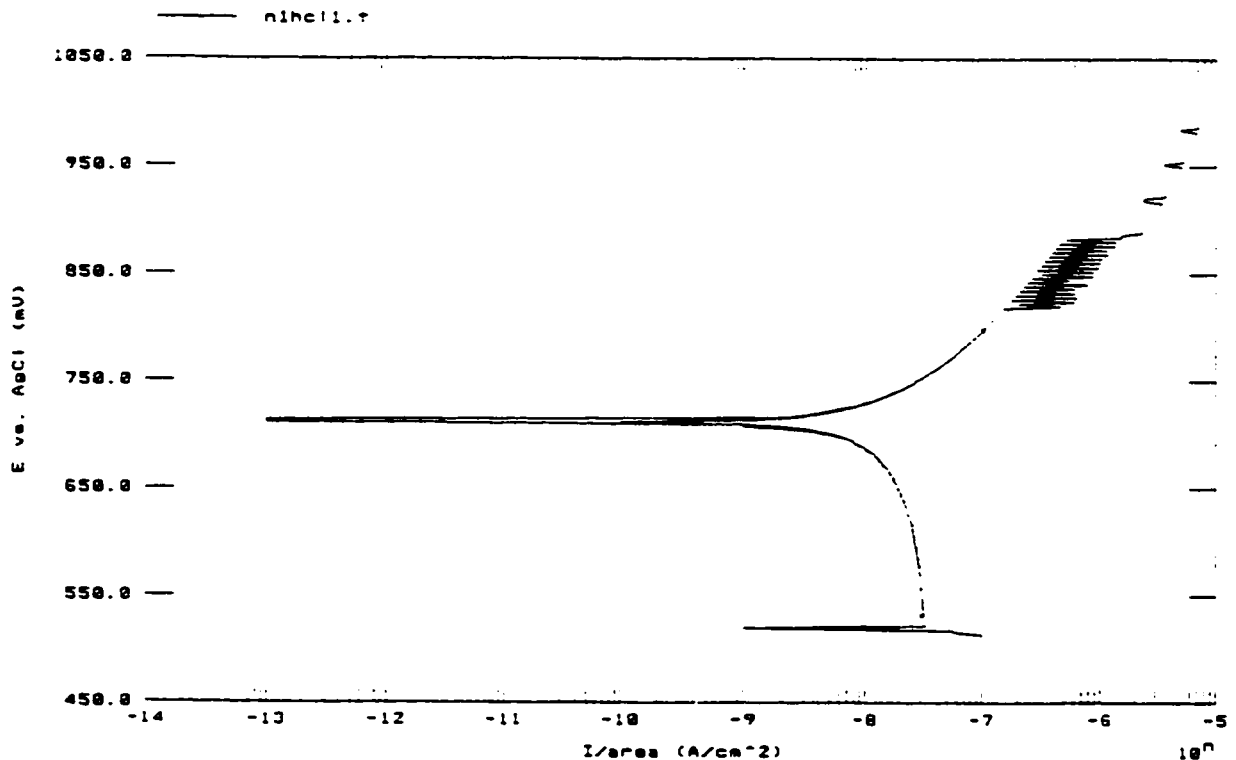
Begin = 532.0 mV

Chi² = 1.45E-001

Icorr = 25.03 nA/cm²

Beta Cathodic = 1.465 V/decade

End = 798.0 mV



Model 352/252 Corrosion Analysis Software, v. 2.10

Filename: c:\m352\data\N1HCL2.t

TA TAFEL

Date Run: UNKNOWN

File Status: NORMAL

Time Run: UNKNOWN

Cond. Time	CT	pass	s	Initial Pot.	IP	400.0E-3	V
Cond. Pot.	CP	pass	V	Final Pot.	FP	950.0E-3	V
Initial Delay	ID	pass	s				
Scan Rate	SR	500.0E-3	mV/s	Curr. Range	CR	Auto	
Scan Incr.	SI	2.000	mV	Step Time	ST	4.000	s
No. of Points	NP	275					
Line Sync.	LS	no		GI Time Const.	TC	Off	
Rise Time	RT	high stability		IR Mode	IR	none	
Working Elec.	WE	Solid		Filter	FL	15.3Hz	
Sample Area	AR	1.000	cm ²	Ref. Elec.	RE	AgCl 197.0E-3V	
Density	DE	0.0000	g/ml	Equip. Wt.	EW	0.0000	g
Open Circuit	OC	468.0E-3	V	AUX A/D	AU	no	

Comment: 20 x Nitrogenated Carbon, 7.5ppm HCl, O2 saturated, Sample 02

Rp CALCULATIONS:

Corrosion Rate = N.A.

Rp = 1.864 MOhms

E(I=0) = 777.8 mV

Beta Anodic = 100.0E-3

Begin = 726.0 mV

Correlation = -970.2E-3

Icorr(R) = 11.65 nA/cm²

Beta Cathodic = 100.0E-3 V/decade

End = 830.0 mV

TAFEL CALCULATIONS:

Corrosion Rate = N.A.

E(I=0) = 785.9 mV

Beta Anodic = 118.9E-3

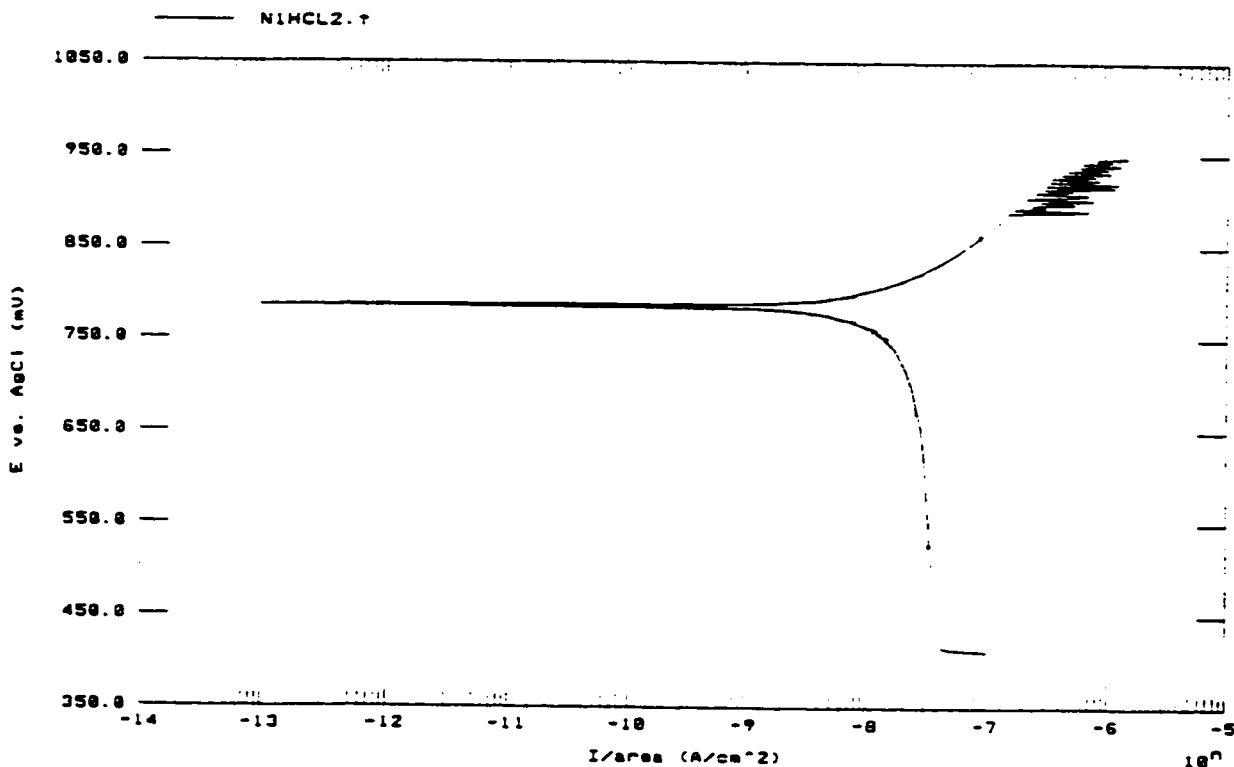
Begin = 528.0 mV

Chi² = 1.33E-001

Icorr = 25.47 nA/cm²

Beta Cathodic = 2.128 V/decade

End = 862.0 mV



Model 352/252 Corrosion Analysis Software, v. 2.10

Filename: c:\m352\data\NIHCL3.1

TA TAFEL
Date Run: UNKNOWN

File Status: NORMAL
Time Run: UNKNOWN

Cond. Time	CT	pass	s	Initial Pot.	IP	400.0E-3	V
Cond. Pot.	CP	pass	V	Final Pot.	FP	950.0E-3	V
Initial Delay	ID	pass	s				
Scan Rate	SR	500.0E-3	mV/s	Curr. Range	CR	Auto	
Scan Incr.	SI	2.000	mV	Step Time	ST	4.000	s
No. of Points	NP	275					
Line Sync.	LS	no		GI Time Const.	TC	off	
Rise Time	RT	high stability		IR Mode	IR	none	
Working Elec.	WE	Solid		Filter	FL	15.3Hz	
Sample Area	AR	1.000	cm ²	Ref. Elec.	RE	AgCl	197.0E-3V
Density	DE	0.0000	g/ml	Equiv. Wt.	EW	0.0000	g
Open Circuit	OC	468.0E-3	V	AUX A/D	AU	no	

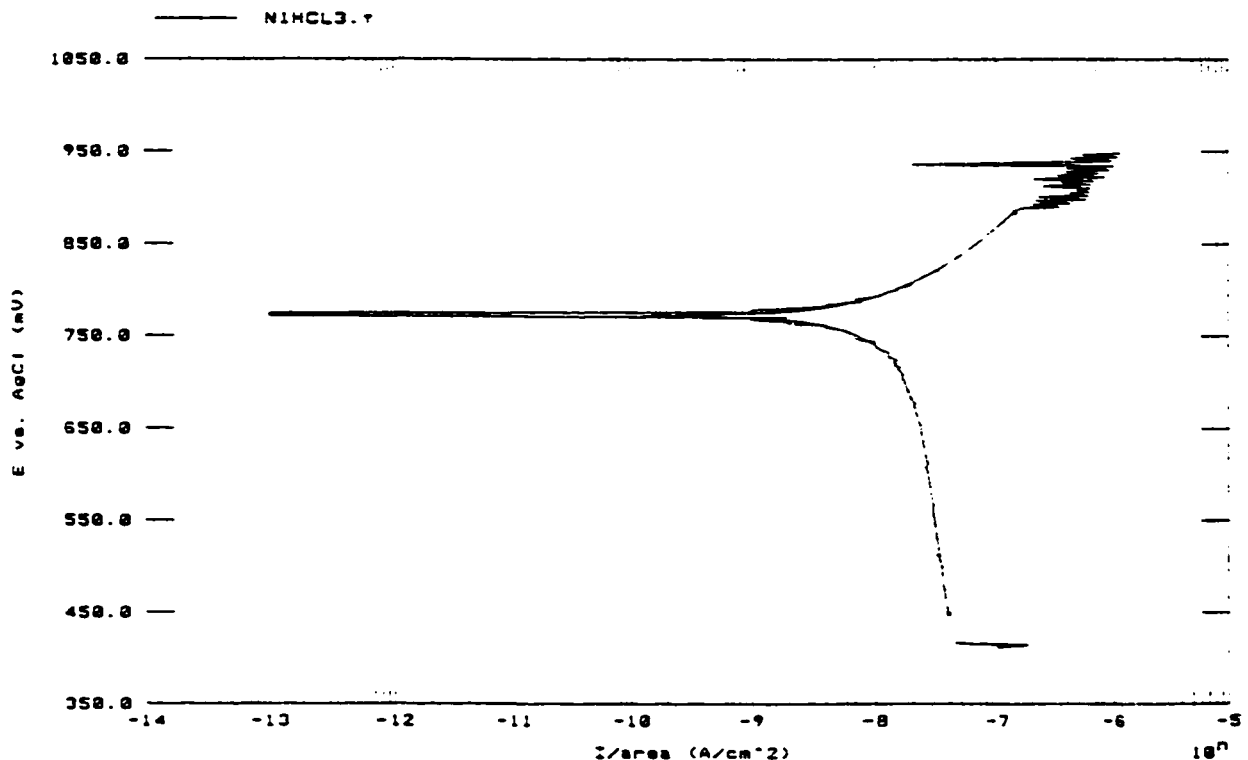
Comment: 20X Nitrogenated Carbon, 7.5ppm HCl, O2 saturated, Sample03

RE CALCULATIONS:
Corrosion Rate = N.A.
R_s = 2.420 MOHMS
E(I=0) = 767.3 mV
Beta Anodic = 122.7E-3
Beta Cathodic = 724.0 mV

Correlation = -980.7E-3
I_{corr}(R) = 19.80 nA/cm²
Beta Cathodic = 1.093 V/decade
End = 810.0 mV

TAFEL CALCULATIONS:
Corrosion Rate = N.A.
E(I=0) = 772.3 mV
Beta Anodic = 122.7E-3
Beta Cathodic = 448.0 mV

Chi² = 2.03E-001
I_{corr} = 19.26 nA/cm²
Beta Cathodic = 1.093 V/decade
End = 884.0 mV



Model 352/252 Corrosion Analysis Software, v. 2.10

Filename: C:\m352\data\NZHCL1.t

TA TAFEL

Date Run: UNKNOWN

File Status: NORMAL
Time Run: UNKNOWN

Cond. Time	CT	pass	s	Initial Pot.	IP	450.0E-3	V
Cond. Pot.	CP	pass	V	Final Pot.	FP	1.000	V
Initial Delay	ID	pass	s				
Scan Rate	SR	500.0E-3	mV/s	Curr. Range	CR	Auto	
Scan Incr.	SI	2.000	mV	Step Time	ST	4.000	s
No. of Points	NP	275					
Line Sync.	LS	no		GI Time Const.	TC	off	
Rise Time	RT	high stability		IR Mode	IR	none	
Working Elec.	WE	Solid		Filter	FL	15.3Hz	
Sample Area	AR	1.000	cm ²	Ref. Elec.	RE	AgCl	197.0E-3V
Density	DE	0.0000	g/ml	Equiv. Wt.	EW	0.0000	g
Open Circuit	OC	543.0E-3	V	AUX A/D	AU	no	

Comment: 30% Nitrogenated Carbon, 7.5 ppm HCl, O2 saturated, Sample1

Rp CALCULATIONS:

Corrosion Rate = N.A.

Rp = 2.560 MOhm

E(I=0) = 892.9 mV

Beta Anodic = 107.0E-3

Begin = 822.0 mV

Correlation = -975.1E-3

Icorr(R) = 17.51 nA/cm²

Beta Cathodic = 2.853 V/decade

End = 916.0 mV

TAFEL CALCULATIONS:

Corrosion Rate = N.A.

E(I=0) = 895.8 mV

Beta Anodic = 107.0E-3

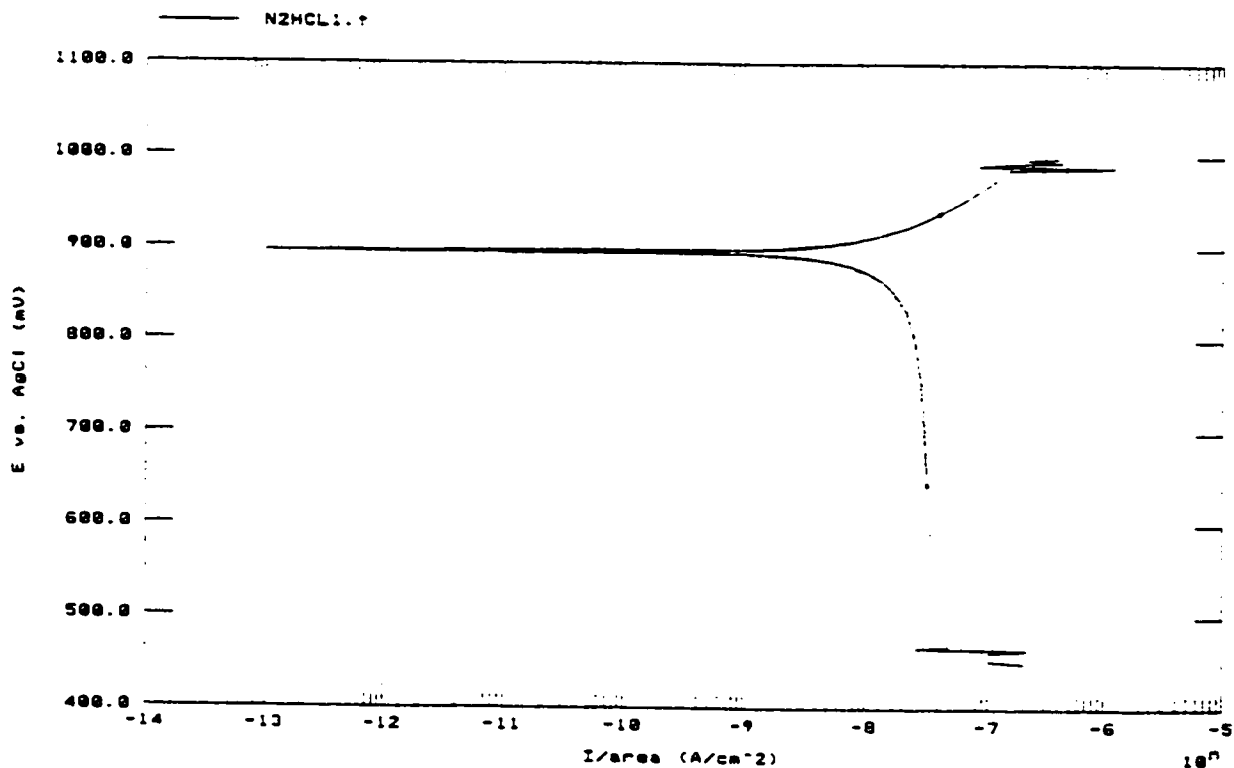
Begin = 644.0 mV

Chi² = 8.65E-002

Icorr = 26.31 nA/cm²

Beta Cathodic = 2.853 V/decade

End = 938.0 mV



Model 352/252 Corrosion Analysis Software, v. 2.10

Filename: c:\m352\data\N2HCL2.t

TA TAFEL

Date Run: UNKNOWN

File Status: NORMAL

Time Run: UNKNOWN

Cond. Time	CT	pass	s	Initial Pot.	IP	400.0E-3	V
Cond. Pot.	CP	pass	V	Final Pot.	FP	950.0E-3	V
Initial Delay	ID	pass	s				
Scan Rate	SR	500.0E-3	mV/s	Curr. Range	CR	Auto	
Scan Incr.	SI	2.000	mV	Step Time	ST	4.000	s
No. of Points	NP	275					
Line Sync.	LS	no		GI Time Const.	TC	Off	
Rise Time	RT	high stability		IR Mode	IR	none	
Working Elec.	WE	Solid		Filter	FL	5.3Hz	
Sample Area	AR	1.000	cm ²	Ref. Elec.	RE	AgCl	197.0E-3V
Density	DE	0.0000	g/ml	Equiv. Wt.	EW	0.0000	g
Open Circuit	OC	505.0E-3	V	AUX A/D	AU	no	

Comment: 30% Nitrogenated Carbon, 7.5 ppm HCl, O2 saturated, Sample02

Rp CALCULATIONS:

Corrosion Rate = N.A.

Rp = 2.447 MOHMS

E(I=0) = 865.3 mV

Beta Anodic = 108.4E-3

Beta Cathodic = 822.0 mV

Correlation = -986.7E-3

Icorr(R) = 18.30 nA/cm²

Beta Cathodic = 2.133 V/decade

End = 888.0 mV

TAFEL CALCULATIONS:

Corrosion Rate = N.A.

E(I=0) = 867.9 mV

Beta Anodic = 108.4E-3

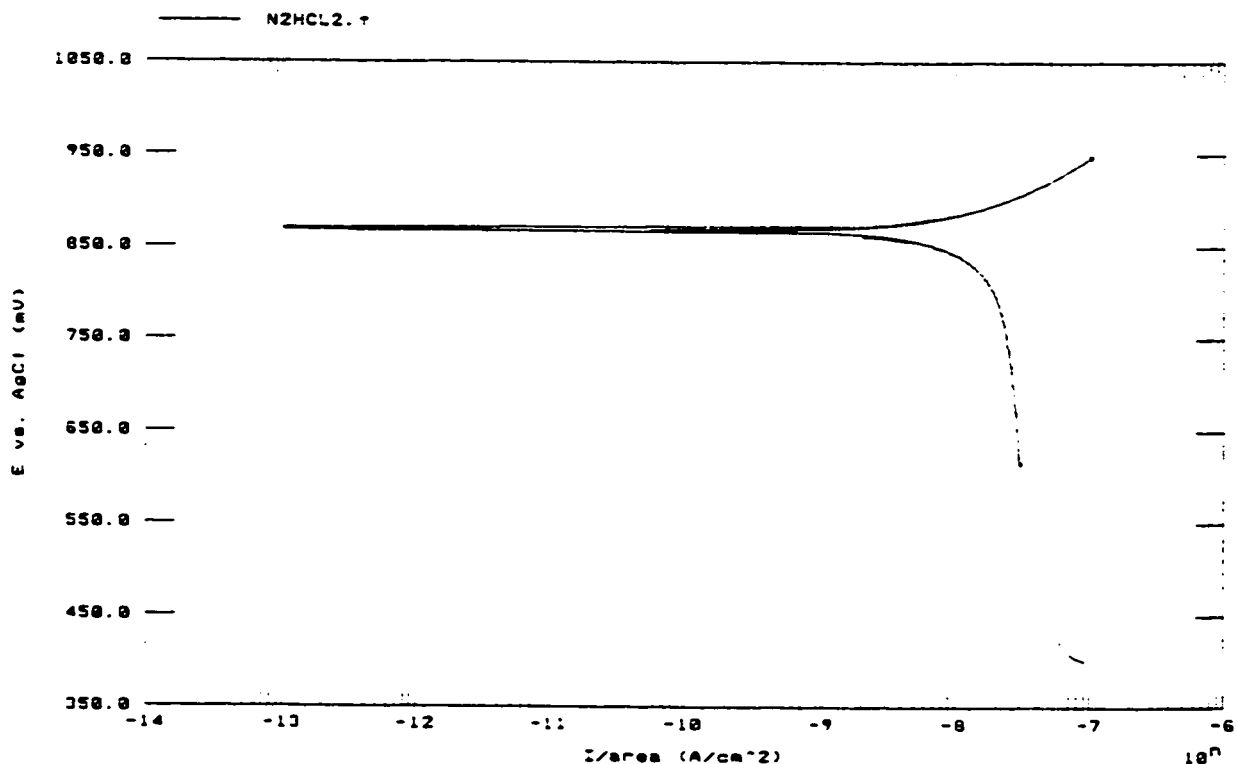
Beta Cathodic = 616.0 mV

Chi² = 6.99E-002

Icorr = 22.63 nA/cm²

Beta Cathodic = 2.133 V/decade

End = 948.0 mV



Model 352/252 Corrosion Analysis Software, v. 2.10

Filename: c:\a352\data\N2HCL3.†

TA TAFEL

Date Run: UNKNOWN

File Status: NORMAL

Time Run: UNKNOWN

Cond. Time	CT	pass	s	Initial Pot.	IP	400.0E-3	V
Cond. Pot.	CP	pass	V	Final Pot.	FP	950.0E-3	V
Initial Delay	ID	pass	s				
Scan Rate	SR	500.0E-3	mV/s	Curr. Range	CR	Auto	
Scan Incr.	SI	2.000	mV	Step Time	ST	4.000	s
No. of Points	NP	275					
Line Sync.	LS	no		GI Time Const.	TC	Off	
Rise Time	RT	high stability		IR Mode	IR	none	
Working Elec.	WE	Solid		Filter	FL	1 5.3Hz	
Sample Area	AR	1.000	cm ²	Ref. Elec.	RE	AgCl 197.0E-3V	
Density	DE	0.0000	g/ml	Equiv. Wt.	EW	0.0000	
Open Circuit	OC	560.0E-3	V	AUX A/D	AU	no	

Comment: 30x Nitrogenated Carbon, 7.5ppm HCl, O2 saturated, Sample03

RE CALCULATIONS:

Corrosion Rate = N.A.

Rp = 2.955 MOHMS

E(I=0) = 873.3 mV

Beta Anodic = 100.0E-3

Begin = 830.0 mV

Correlation = -989.5E-3

Icorr(R) = 14.79 nA/cm²

Beta Cathodic = 1.338 V/decade

End = 880.0 mV

TAFEL CALCULATIONS:

Corrosion Rate = N.A.

E(I=0) = 874.2 mV

Beta Anodic = 100.0E-3

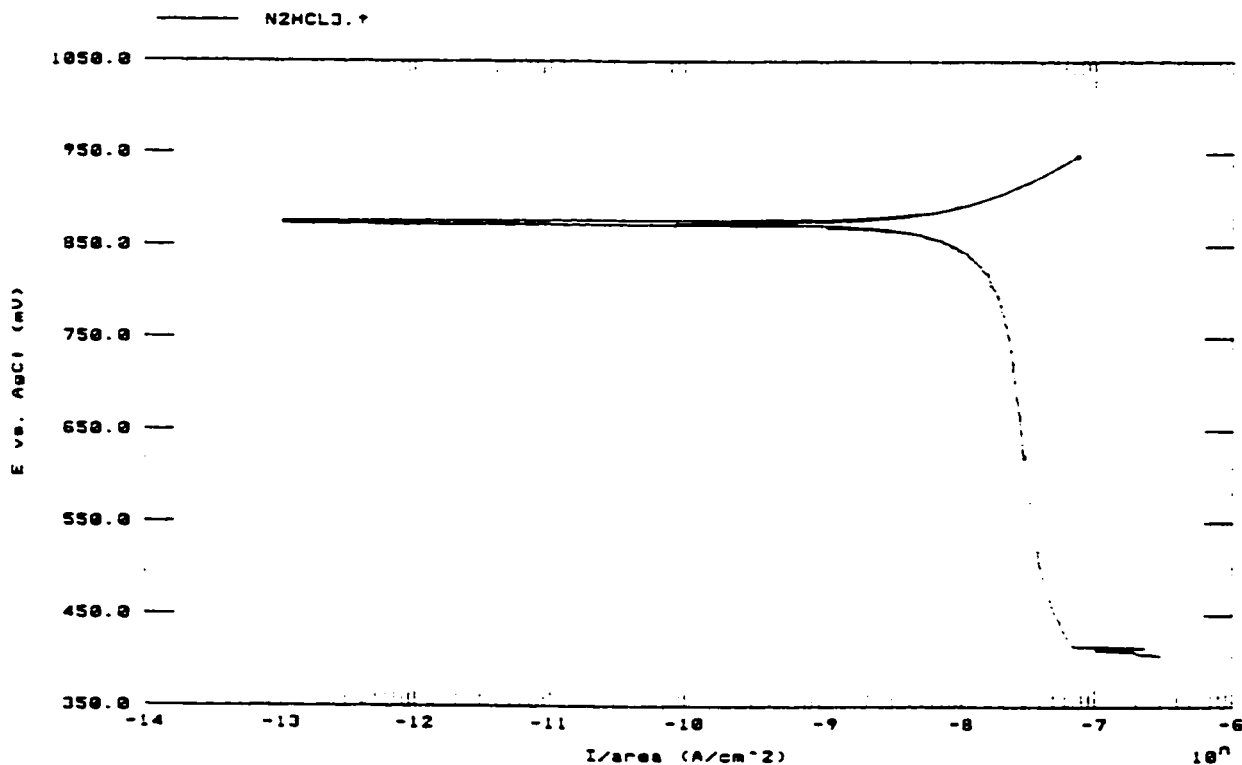
Begin = 622.0 mV

Chi² = 0.50E-002

Icorr = 19.38 nA/cm²

Beta Cathodic = 1.338 V/decade

End = 940.0 mV



Vivares, Valerie

From: Vivares, Valerie
Sent: Monday, June 29, 1998 8:31 AM
To: 'grchwski@almaden.ibm.com'
Subject: Authorization to use Figure in thesis

Sir,

I called you the first week of April to solicit the authorization to use one of your figures in my thesis. You did authorize me on the phone and I would appreciate if you could confirm your authorization by replying favorably to this email.

I attached the page of my thesis where I used the illustration in order for you to be able to judge of the context in which it is used.

The thesis this page belong to is my Master's thesis from San Jose State University's Material Engineering program.

Thanks you for your help



Page1thesis.doc

Regards

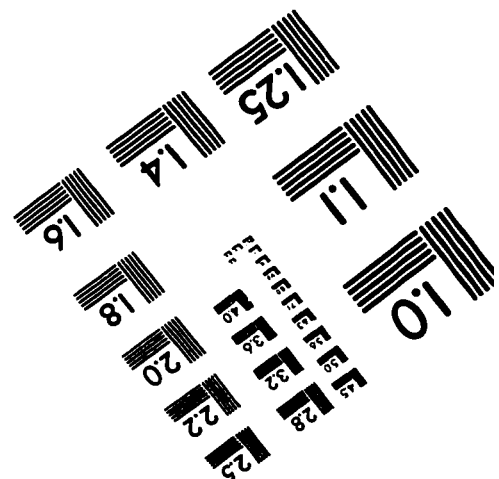
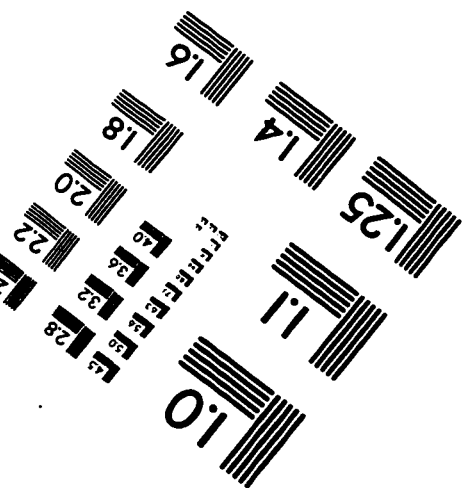
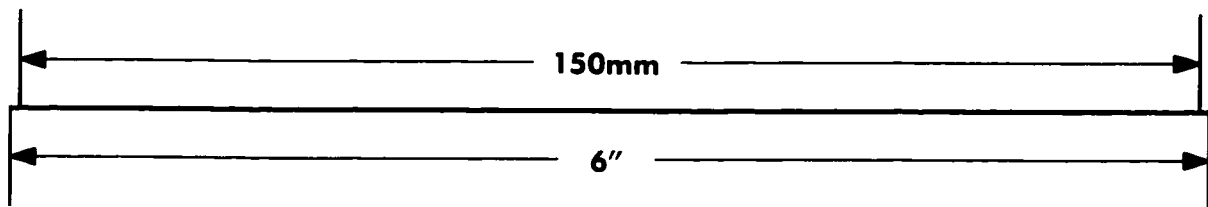
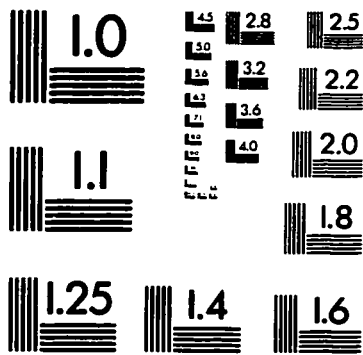
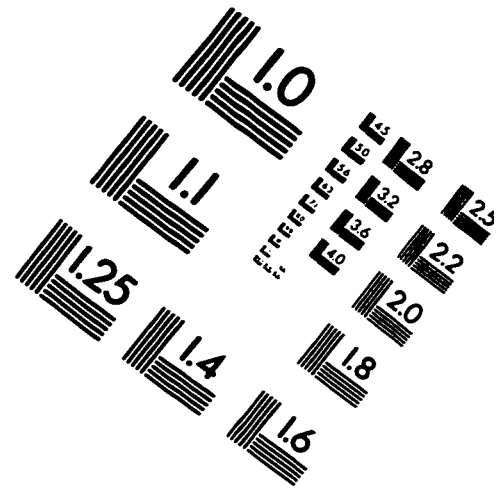
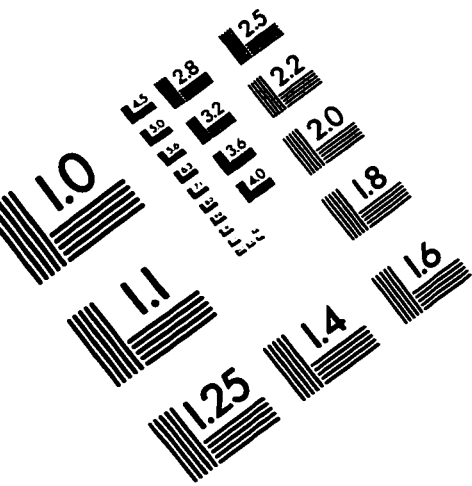
Valerie Vivares
Package engineer
AMD Inc.
(408) 982-6027

Vivares, Valerie

From: grchwski@almaden.ibm.com
Sent: Monday, June 29, 1998 8:41 AM
To: Vivares, Valerie
Subject: Re: Authorization to use Figure in thesis

Val: You are authorized to use the figure we discussed. Good luck. Ed

IMAGE EVALUATION TEST TARGET (QA-3)



APPLIED IMAGE, Inc
1653 East Main Street
Rochester, NY 14609 USA
Phone: 716/482-0300
Fax: 716/288-5989

© 1993, Applied Image, Inc., All Rights Reserved